

UNIVERSITY OF SOUTHAMPTON
SCHOOL OF OCEAN AND EARTH SCIENCE

**The Behaviour of Manganese and Cobalt in
a Hypoxic Fjord (Loch Etive, Scotland)**

A dissertation submitted by
Emily Bulukin
in candidature for the degree of Master of Philosophy

October 2001

Table of contents

Abstract	4
Acknowledgements.....	5
List of figures	6
List of tables	6
Chapter 1. Introduction	7
1.1. Characteristics of hypoxic environments	7
1.2. Distribution of Mn and Co in marine waters.....	11
1.2.1. <i>Distribution in the open ocean</i>	11
1.2.2. <i>Distribution in anoxic environments</i>	12
1.2.3. <i>Distribution in hypoxic environments</i>	14
1.3. Mechanisms of Mn and Co oxidation	15
1.4. Cobalt and manganese interactions	19
1.5. Research objectives	20
Chapter 2. Sampling and analytical procedures	21
2.1. Study area	21
2.2. Sampling.....	22
2.2.1. <i>Autosub</i>	24
2.2.2. <i>Aqua monitor</i>	25
2.2.3. <i>CTD</i>	27
2.3. Dissolved trace metal analysis.....	27
2.3.1. <i>Introduction</i>	27
2.3.2. <i>Preparation of equipment</i>	28
2.3.3. <i>Sample manipulation and storage</i>	28
2.3.4. <i>Preparation of chemicals</i>	29
2.3.5. <i>Preconcentration and back-extraction</i>	30
2.3.6. <i>Determination of total dissolved trace metals by GFAAS</i>	32
2.3.7. <i>Calculation of dissolved sample concentration</i>	33
2.4. Use and development of an in-situ detection technique.....	34
2.4.1. <i>Introduction</i>	34
2.4.2. <i>Chemical manifold</i>	35
2.4.3. <i>Optimisation of the surfactant concentration</i>	37
2.4.4. <i>Test of the iron interference</i>	38
2.4.5. <i>Choice of mixing coil design</i>	38
2.4.6. <i>Analytical method</i>	39
2.4.7. <i>In-situ housing</i>	39
2.5. Particulate trace metal analysis	40
2.5.1. <i>Sample preparation and analysis</i>	40
2.5.2. <i>Calculation of particulate sample concentration</i>	40
Chapter 3. Results and discussion.....	41
3.1. Data processing	41
3.2. Hydrographic data	42

3.2.1. <i>General overview</i>	42
3.2.2. <i>Comparison of two depth-transects</i>	45
3.3. Dissolved manganese	48
3.3.1. <i>General overview</i>	48
3.3.2. <i>Surface water</i>	49
3.3.3. <i>Deep water</i>	51
3.4. Particulate Mn	55
3.4.1. <i>General overview</i>	55
3.4.2. <i>Surface water</i>	56
3.4.3. <i>Deep water</i>	57
3.5. Manganese oxidation rates	59
3.6. Dissolved and particulate Co.....	60
3.6.1. <i>General overview</i>	60
3.6.2. <i>Surface water</i>	62
3.6.3. <i>Deep water</i>	63
3.7. Manganese and cobalt correlations	66
3.8. In-situ measurements.....	67
Chapter 4. Conclusions	69
4.1. Dissolved and particulate Mn and Co	69
4.2. Recommendations for further work	72
References	74
Appendix	88

UNIVERSITY OF SOUTHAMPTON

ABSTRACT

FACULTY OF SCIENCE

OCEAN AND EARTH SCIENCES

Master of Philosophy

THE BEHAVIOUR OF MANGANESE AND COBALT IN
A HYPOXIC FJORD (LOCH ETIVE, SCOTLAND)

by Emily Bulukin

Measurements of dissolved and particulate manganese (Mn) and cobalt (Co) were made on samples collected during two seasons (November 1999 and April 2000) in the oxidising and hypoxic waters of Loch Etive, Scotland. Collection of samples was made using an Aqua Monitor that was mounted on Autosub, an autonomous underwater vehicle. In addition, an in-situ chemical analyser was developed and tested for the determination of dissolved Mn (Mn_d). Analysis of collected water samples were undertaken in a clean room Class-100 laminar flow hood, and the data subjected to rigorous quality control. Due to the unique sampling technique the study presents high-resolution data not previously obtained. The results give evidence for the presence of localised variations within the general depth trend for Mn and Co. During both seasons the Mn_d concentrations in the oxidising surface waters (44.5 nM in November and 79.8 nM in April, respectively) were significantly lower than those recorded in the hypoxic bottom waters (120 nM in November and 358 nM in April, respectively). Results indicate that the high concentrations in deep-water were produced by a sedimentary source of Mn_d . Pronounced seasonal variability was observed in the Mn_d concentration, this being the result of increasing reducing conditions that favour Mn reduction. Particulate manganese concentrations (M_p) followed the same trend as that observed for Mn_d , i.e. increasing concentrations in deep waters. This trend is suggested to be the result of scavenging of Mn_d . The dissolved Co (Co_d) concentrations were higher than those recorded in the open ocean. Highest Co_d concentrations were recorded in surface waters (81 – 288 pM in November and 71 – 246 pM in April, respectively), values decreasing with depth. In deep-water, low, stable concentrations were observed during both seasons. In surface waters, riverine inputs are expected to influence the concentrations while in deep-water the controlling mechanisms are suggested to be desorption from Mn-oxides and microbial oxidation. The study investigates the correlation between Co and Mn, arguing that in a hypoxic environment biogeochemical processes affect Mn and Co differently, resulting in a geochemical separation of these two elements.

Acknowledgements

I am extremely thankful to Dr. Peter Statham (School of Ocean and Earth Science) and Dr. Chris German (Southampton Oceanography Centre, Challenger Division) for their invaluable guidance and friendly supervision. I am also grateful to Dr. D. Connelly, Dr. J. Overnell and T. Brand for their assistance and many advises. I also wish to thank the Autosub team, and the captain and crew members of the vessels Terscelling and Calanus, for without their very generous support this study would not have been possible.

Finally, I wish to thank Francesco and those friends, especially Laura, who supported me as circumstances changed and I decided for a different path. I am grateful to them all.

List of figures

Chapter 1:	
Figure 1. Sequence of redox reactions at different pE in the marine environment.	8
Figure 2. Schematic representation of deep water stagnation.	10
Figure 3. Typical depth profile of dissolved manganese in the open ocean.	11
Figure 4. Reactions and processes contributing to manganese cycling in shallow marine ecosystems.	16
Figure 5. Schematic representation of the internal and external sedimentary cycling of manganese.	18
Chapter 2:	
Figure 6. Map of the study area: Loch Etive.	22
Figure 7. Bathymetric map of Loch Etive.	24
Figure 8. Schematic layout of Autosub.	25
Figure 9. Schematic layout of Aqua Monitor.	26
Figure 10. Flow diagram of the extraction procedure.	31
Figure 11. Photograph and schematic layout of the manifold.	36
Chapter 3:	
Figure 12. Oxygen, temperature and salinity data, Loch Etive November 1999.	43
Figure 13. Oxygen, temperature and salinity data, Loch Etive April 2000.	44
Figure 14. The geographical sampling positions of M212 (November 1999) and M227 (April 2000), Loch Etive.	47
Figure 15. Oxygen data (ml l^{-1}) vs depth (m) for missions M212 (November 1999) and M227 (April 2000), Loch Etive.	47
Figure 16. Dissolved Mn (nM) vs depth (m) Loch Etive November 1999 (total CTD casts and Autosub M212).	48
Figure 17. Dissolved Mn (nM) vs depth (m) Loch Etive April 2000 (M226-231).	49
Figure 18. Total Mn (nM) vs depth (m), Loch Etive Nov 1999.	52
Figure 19. Total Mn (nM) vs depth (m), Loch Etive April 2000.	52
Figure 20. Dissolved Mn (nM) vs depth (m) for M212 (3 rd November 1999) and M227 (6 th April 2000), Loch Etive.	53
Figure 21. Particulate Mn (nM) vs depth (m) Loch Etive November 1999.	55
Figure 22. Particulate Mn (nM) vs depth (m) Loch Etive April 2000.	56
Figure 23. SPM (mg l^{-1}) vs depth (m) for collected CTD data November 1999 and Autosub data M226-M231, April 2000, Loch Etive.	58
Figure 24. Dissolved Co (pM) vs depth (m) Loch Etive, November 1999.	61
Figure 25. Dissolved Co (pM) vs depth (m) Loch Etive, April 2000.	61
Figure 26. Results from the in-situ chemical Mn-analyser for M225 Loch Etive, April 2000.	68

List of tables

Table 1. Standard reduction potentials for Mn(II) and Co(II).	19
Table 2. Autosub missions November 1999 and April 2000.	23
Table 3. Coordinates of positions for CTD casts, November 1999.	24
Table 4. GFAAS conditions for analysis of back extracts.	32
Table 5. Average blanks, detection limits and recovery data for Mn and Co.	33
Table 6. Optimised %Triton X-100 in the PAN solution.	37
Table 7-14. Lists of all data represented in figures.	87

Chapter 1. Introduction

1.1. Characteristics of hypoxic environments

Redox processes in the marine environment regulate the distribution and biogeochemical behaviour of many trace metals by affecting their phase transformations between insoluble and more soluble forms (Whitfield and Turner, 1987). These redox processes are strongly influenced by the presence of dissolved oxygen, which acts as the primary electron acceptor in the breakdown of organic matter (Froehlich *et al.*, 1979; Stumm and Morgan, 1981).

In marine systems, the distribution of dissolved oxygen in the water column is, beyond simple exchange with the atmosphere, the result of the balance between production, through photosynthesis in the photic zone, and consumption, principally through the oxidation of organic matter. In most areas of the world's oceans the exchange between surface and deep water is such that dissolved oxygen is transferred to water below the photic zone through advection and diffusion processes (Wyrski, 1962). Hence, the dissolved oxygen concentration remains close to saturation throughout the water column. In certain regions, however, where respiration rates are high or in areas where water circulation is restricted, the rate of oxygen consumption exceeds the rate of circulatory renewal and areas of oxygen depletion arise (Richards, 1965; Breck, 1974). As the oxygen is used up, alternative terminal electron acceptors are required in the oxidation of organic matter (Froehlich *et al.*, 1979). The sequence of these is determined by the pE (electron activity), which in an aquatic environment is controlled in turn by the oxygen supply and by the presence of organic matter (Stumm and Morgan, 1996). As illustrated schematically in Figure 1, when available dissolved oxygen is exhausted, nitrate acts as the primary alternative terminal electron acceptor in the oxidation process (Cline and Richards, 1972; Froehlich *et al.*, 1979). Under such conditions the water becomes *hypoxic* (Sillén, 1965). Hypoxic water is characterised by low (generally $< 5 \mu\text{M}$), but not zero concentrations of dissolved oxygen (Murray *et al.*, 1989) and evidence of denitrification from the presence of a negative anomaly within the dissolved nitrate profile (Brandhorst, 1958; Cline and Richards, 1972; Codispoti and Richards, 1976). Prolonged periods during which utilisation exceeds renewal will cause the dissolved oxygen to eventually become completely absent from intermediate and deep

waters, resulting in fully *anoxic* conditions (Deuser, 1975). Anoxic waters are strongly reducing and a pronounced O_2/H_2S interface is often typically established, marking the boundary between oxic and anoxic regions (Richards, 1965). Flushing events, where the stagnant oxygen-poor water is replaced by more oxygenated water, induces a switch back to fully *oxic* conditions.

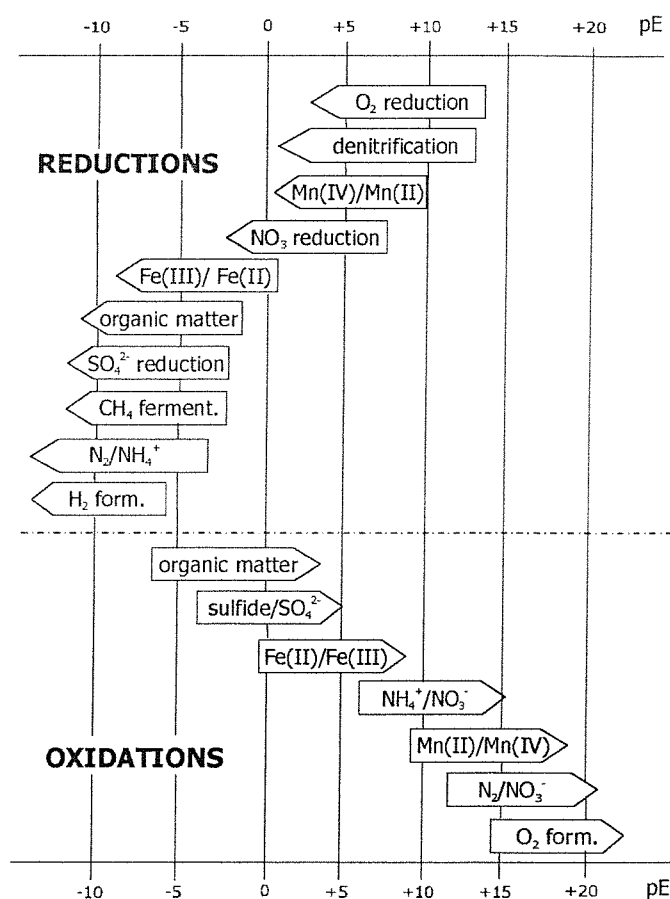


Figure 1. Sequence of redox reactions at different pE in the marine environment (from Stumm and Morgan, 1996).

For redox sensitive elements, such as manganese (Mn) and cobalt (Co), improved understanding of their behaviour under hypoxic conditions is of particular interest. Manganese is a transition element (Group VII in the periodic table) that in dissolved form mainly occurs in seawater as Mn(II). In this form Mn exists as free hydrated Mn(II) or as $MnCl^+$ (Bruland, 1983). In oxygenated seawater the thermodynamically stable form of Mn is as particulate Mn(IV) (MnO_x , $x = 1.5-2$, Yeats and Strain, 1990). Despite Mn(IV) being thermodynamically more stable, both forms can be measured in seawater due to the slow reaction kinetics of the oxidation process

(Yeats and Strain, 1990). The particulate Mn-oxides have large specific surface areas ($10^2 \text{ m}^2 \text{ g}^{-1}$) (Santschi *et al.*, 1990) and a high capacity for cation exchange (Balistrieri and Murray, 1986). Hence, the redox cycling of Mn in marine waters can greatly affect the fate of many other trace metals (*e.g.* Aller, 1980; Balzer, 1982; Balistrieri and Murray, 1986).

Cobalt (Group VIII) is another trace metal sensitive to redox changes, which is of both biological and environmental importance. In oxygenated waters the scarcely soluble trivalent Co(III) is the thermodynamically stable form, while Co(II) dominates under anoxic conditions (Stone and Morgan, 1987). As the central metal cofactor in vitamin B₁₂ (cobalamine) Co is an essential micronutrient for organisms (Carlucci and Cuhel, 1977; Swift, 1981). Cobalt is also of environmental interest since the ⁶⁰Co isotope is an activation product of radioactive waste (Robertson, 1970). At high concentrations (approximately greater than 17 μM), Co is toxic to living organisms (Lienemann *et al.*, 1997). Despite the fact that concentrations in this range are rarely observed in aquatic systems, Co like other metals can be bioaccumulated through the food web. Furthermore, Co plays an important role in the biomethylation of *e.g.* mercury (Hg) (Fergusson, 1990). An understanding of processes controlling the distribution of Co in the water column therefore assumes particular importance in evaluating any anthropogenic impact.

The area chosen for this study was Loch Etive, a fjord (loch¹) system located on the west coast of Scotland. Due to the presence of a sill, loch systems exhibit restricted deep-water exchange with the open ocean and this can result in the formation of stagnant bottom water (Grasshoff, 1975). As such, loch systems are delicately balanced and small inputs of organic matter can have a strong effect on the prevailing oxygen concentrations, often resulting in reducing conditions. These systems therefore, represent an ideal natural environment in which the biogeochemical behaviour of redox sensitive trace metals can be investigated.

Loch Etive has a rainwater catchment area of 1400 km², larger than any other Scottish loch (Edwards and Edelsten, 1977). Thus, during periods of high freshwater runoff, mixing occurs between freshwater flowing out of the loch and the more saline water below it. Consequently, the density of the saline water is reduced preventing it to flow across the sill and displace the deeper waters. This causes stagnation of the water

¹ The word loch will be used to denote a Scottish fjord.

in the deep basins, with slowly falling oxygen concentrations and with the development of a secondary pycnocline below sill depth (Figure 2). On the contrary, during periods of low freshwater runoff, the salinity of the sill water is raised. The waters of the Firth of Lorne are then sufficiently saline and dense to flow across the sill into the bottom of the basins whereby partial or complete renewal of the bottom water takes place (Edwards and Grantham, 1986). (For a more detailed discussion on the process of deep water renewal see Gade and Edwards, 1980). The periods of stagnation of the deep water in Loch Etive may extend up to 30 months with a mean of 16 months between overturning events (Edwards and Edelsten, 1977). During these periods the secondary pycnocline hinders mixing of surface waters with the deep stagnant water and the dissolved oxygen concentration slowly falls (Edwards and Grantham, 1986). Compared to other Scottish lochs that display similarly long periods of deep water stagnation (notably Loch Obisary, Edwards, 1989), Loch Etive is unusual in that deep-water remains hypoxic during these periods of stagnation without becoming fully anoxic. This has wide-reaching implications for the solubility and resulting distribution of redox sensitive trace metals.

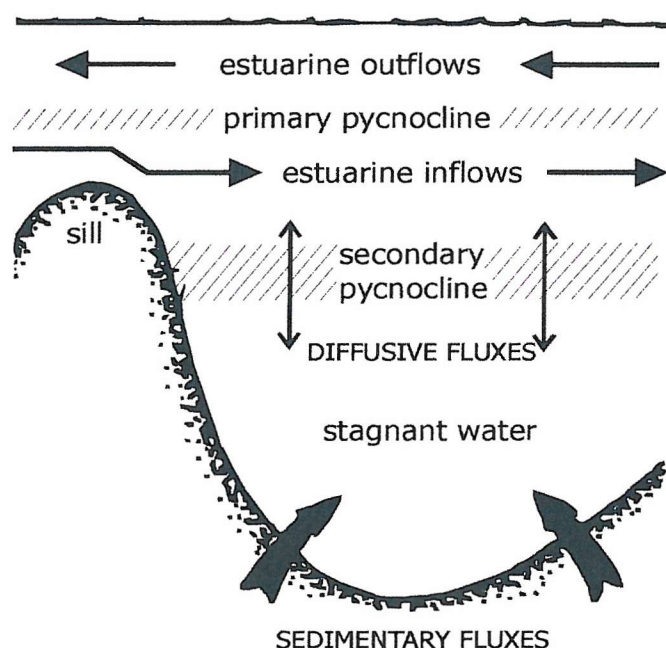


Figure 2. Schematic representation of deep water stagnation, where the secondary pycnocline (oxycline) hinders estuarine water from mixing with the deep stagnant water (from Edwards and Grantham, 1986).

1.2. Distribution of Mn and Co in marine waters

1.2.1. Distribution in the open ocean

The distribution of Mn in the water column has been well documented (see reviews by Bruland (1983) and Burton and Statham (1990)). The general vertical distribution in open ocean regions is characterised by high surface concentrations (typically in the range of 1 - 3 nM), a sub surface maximum within the mixed layer and uniformly low concentrations in deep water, as illustrated by Figure 3. (Klinkhammer and Bender, 1980; Landing and Bruland, 1980; 1987; Burton and Statham, 1990). In areas close to the ocean margins high surface concentrations have been related to river and sedimentary sources (Bender *et al.*, 1977), whereas, in more remote sites, atmospheric inputs have been shown to be dominant (Klinkhammer and Bender, 1980; Statham and Chester, 1988; Guieu *et al.*, 1998; Statham *et al.*, 1998).

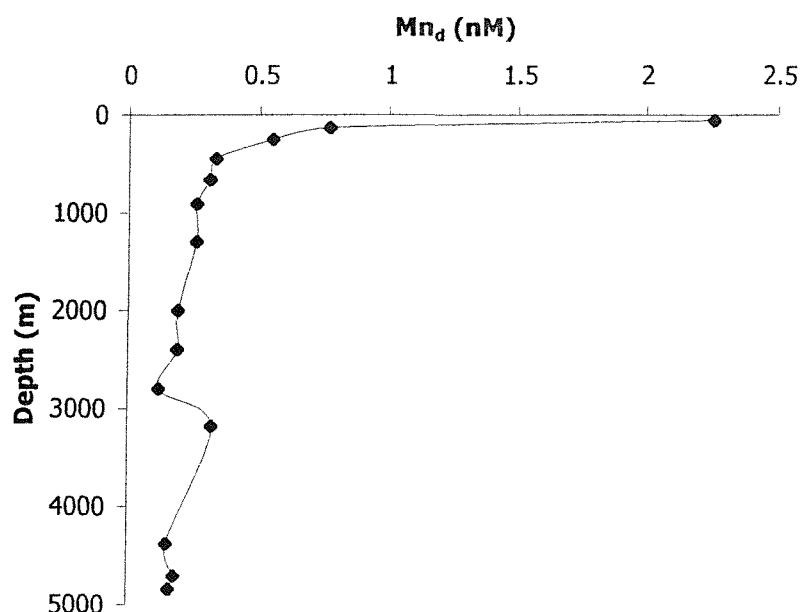


Figure 3. Typical depth profile of dissolved Mn in the open ocean (from Statham *et al.*, 1998, data from the eastern Atlantic Ocean).



In the northwestern Atlantic Ocean, Yeats and Bowers (1985) recorded Mn concentrations in the range of 0.4 - 0.6 nM. The measured surface concentrations of Mn in the northeastern Atlantic Ocean are higher, (1 - 3 nM) with a rapid decrease to < 0.5 nM in deep waters (Statham and Burton, 1986). Landing and Bruland (1980) measured dissolved Mn in the North Pacific and found concentrations ranging from 1 nM in surface waters decreasing to 0.6 nM in deep water.

Although deep-ocean concentrations are generally low, deep water Mn enrichments have been observed in vicinity to the ocean-ridge spreading centres (see Lilley *et al.* (1995) for a review). This source does not have a direct influence on the Mn concentration in the studied area and hence, will not be discussed further in this work.

Cobalt exists in the open ocean at concentrations of generally less than 100 pM (Knauer *et al.*, 1982; Martin, 1985). Due to these low concentrations it is only recently, with the development of clean extraction techniques, that it has become possible to obtain reliable Co data. Previous studies reported Co as undetectable in some cases (Bowers *et al.*, 1976; Danielsson, 1980) or highly elevated in others (Robertson, 1970). It is now generally recognised that Co displays an open ocean vertical depth profile comparable to that of Mn (Knauer *et al.*, 1982; Martin, 1985; Jickells and Burton, 1988; Westerlund and Öhman, 1991; Wong *et al.*, 1995). Like Mn, Co may be added to surface waters by both riverine and atmospheric inputs (Pacyna, 1984; Arimoto *et al.*, 1989; Donat and Bruland, 1995).

Martin (1985) reported values for Co in northeast Pacific surface waters in the range 60 - 100 pM, decreasing in deep water to < 50 pM. Jickells and Burton (1988) measured Co in the Sargasso sea and found concentrations of *ca.* 20 - 40 pM in surface waters decreasing rapidly with depth to less than 15 - 20 pM. Recorded concentrations in the Mediterranean are higher, with surface values ranging from 80 - 250 pM decreasing to 30 - 50 pM in deep waters (Huynh-Ngoc and Whitehead, 1986). More recently, Wong *et al.* (1995) measured Co concentrations in the western Philippine Sea and reported surface concentrations of 95 pM decreasing to less than 25 pM in waters below 1000 m.

1.2.2. Distribution in anoxic environments

Anoxic waters are found in areas with extremely restricted water circulation like in the deep water of the Black Sea (Spencer and Brewer, 1971; Deuser, 1975; Murray *et al.*,

1989), the Cariaco Trench (Richards and Vaccaro, 1956; Fanning and Pilson, 1972; Deuser, 1973; Bacon *et al.*, 1980; Jacobs *et al.*, 1987) and the Framvaren Fjord (Jacobs *et al.*, 1985; Haraldsson and Westerlund, 1988). In addition, anoxic waters are found in the Drømmensfjord (Öztürk, 1995), in the hyper-saline Tyro and Bannock basins in the eastern Mediterranean (Jongsma *et al.*, 1983; Van der Sloot *et al.*, 1990) and in the Baltic Sea (Grasshoff, 1975; Dyrssen and Kremling, 1990).

Haraldsson and Westerlund (1988) measured Mn and Co in the Black Sea and Framvaren fjord (Norway). Their findings showed a maximum in the dissolved Mn concentration just below the O₂/H₂S interface of 15 µM in the Black Sea and 8 µM in Framvaren. The dissolved Co concentrations in the same regions indicated a maximum of 4.2 and 9 nM respectively, *i.e.* approximately two orders of magnitude higher than in open ocean settings. Dyrssen and Kremling (1990) recorded dissolved Mn and Co concentrations in association with the O₂/H₂S boundary in anoxic Baltic waters. For both elements, dissolved concentrations increased markedly below the oxycline to a maximum of 12 µM (Mn) and 2 nM (Co). Particulate Mn and Co were measured in the Framvaren fjord (Jacobs *et al.*, 1985). The highest concentrations were recorded just above the O₂/H₂S interface and were found to be of the order of 20 µM for Mn and 15 nM for Co.

The general depth profiles of Mn and Co in anoxic waters can be explained by the influence of two controlling processes (a) redox cycling of dissolved phases and oxide particles at the O₂/H₂S interface and (b) the formation of metal sulfides (Jacobs *et al.*, 1985). The solubility of Mn increases as it is reduced from Mn(IV) to Mn(II). Likewise, the reduced species of Co (Co(II)) is more soluble than the oxidised form (Co(III)). Thus dissolved concentrations of both Mn and Co show a characteristic increase just below the O₂/H₂S interface (Jacobs and Emerson, 1982). The formation of metal sulfides is dependant on the total sulfur (ΣH₂S) concentration. In areas with highly pronounced anoxia such as the Framvaren, where the total sulfur (ΣH₂S) concentration in bottom waters reaches mM concentrations, the solubility of both Mn and Co has been observed to decrease due to the precipitation of particulate metal sulfides (Jacobs *et al.*, 1985). In areas where the sulfide concentration is lower, however, such as the Black Sea (bottom water sulfide concentration *ca.* 300 µM), Mn-sulfide formation does not appear to take place, although evidence of Fe-sulfide precipitation has been observed (Lewis and Landing, 1992). The presence of an

enriched Mn particulate layer above the O_2/H_2S boundary has been related to biologically enhanced oxidation of dissolved Mn(II) diffusing out from the anoxic zone (Emerson *et al.*, 1982; Tebo *et al.*, 1984).

1.2.3. Distribution in hypoxic environments

As an intermediate between anoxic and oxic (oxygen saturated waters), few regions in the modern ocean can be classified as truly hypoxic. In open ocean areas, hypoxic zones can be found at the eastern boundaries of both the South and North Pacific (Cline and Richards, 1972; Martin and Knauer, 1984; Hong and Kester, 1986; Landing and Bruland, 1987; Rue *et al.*, 1997) and the northern Indian Ocean (Sen Gupta and Naqvi, 1984; Saager *et al.*, 1989; Warren, 1994). In areas such as the Arabian Sea (northwest Indian Ocean), oxygen depletion is initiated as a result of the high rate of oxygen consumption brought about from the microbial oxidation of large quantities of organic matter (Sen Gupta and Naqvi, 1984; Slater and Kroopnick, 1984).

In addition to the open ocean, hypoxic waters can be found as transient features during flushing events of many anoxic areas. An example of this is Saanich Inlet, British Columbia, Canada, where deep water becomes isolated behind a shallow sill causing oxygen depletion and anoxia for long time periods (Richards, 1965; Anderson and Devol, 1973). Periodically, the inlet is flushed and anoxic deep water is refreshed with highly oxygenated water, resulting in intermittently hypoxic conditions becoming established (Emerson *et al.*, 1979; Jacobs and Emerson, 1982). Hypoxic conditions have also been observed as a specific event in the Black Sea (Murray and Izdar, 1989; Murray *et al.*, 1989; Codispoti *et al.*, 1991).

Furthermore, hypoxic conditions can be produced as a result of restricted water circulation in several fjord systems along the Norwegian and Scottish west coasts *e.g.* the Drammesfjord (Öztürk, 1995), Loch Fyne (Tett *et al.*, 1986), Loch Goil (Mackay and Halcow, 1976; Edwards *et al.*, 1986) and Loch Etive (Edwards and Grantham, 1986). Although these areas represent interesting and particular sites for the study of trace metals, few studies have focused on the influence of these hypoxic conditions upon the distribution of Mn and Co.

In 1984, Martin and Knauer investigated changes in dissolved and particulate Mn concentrations with depth, through a zone with low oxygen content in the eastern tropical Pacific. Their findings indicated that Mn was released from particles as they sank through the oxygen minimum, this producing an observable increase in the

dissolved Mn concentration. Landing and Bruland (1987) studied the redox behaviour of Mn in the same area and found further evidence of *in situ* reduction of particulate Mn within the hypoxic zone. Saager *et al.* (1989) presented the first vertical depth profiles for dissolved Mn in the northwest Indian Ocean. Their results indicated a strong similarity to the depth profiles of Mn observed in the eastern Pacific, with a dissolved Mn maximum in the hypoxic zone. More recently, a study by Rue *et al.* (1997) carried out in the eastern boundary of the tropical North Pacific indicated that particulate Mn was completely reduced to dissolved Mn in the hypoxic zone. Hence, sinking particulate Mn can be solubilised within the thermocline. The resultant water mass containing high concentrations of dissolved Mn can then mix along isopycnals into oxygenated regions, where eventually the metals will become oxidatively scavenged and removed to the underlying sediments. As such, hypoxic areas can act as a source of dissolved metals to oxic oceanic regions.

In intermittently hypoxic areas such as the Saanich Inlet, the dissolved Mn concentration increases in the oxygen minimum zone, followed by a decrease as the hydrogen sulfide concentration increases (Jacobs and Emerson, 1982).

The Black Sea generally shows a distinct O_2/H_2S interface. During the spring and summer of 1988, however, shoaling of this interface was observed with the development of a distinct hypoxic, sulfide free zone overlying the anoxic waters (Murray and Izdar, 1989; Murray *et al.*, 1989). Lewis and Landing (1991) investigated the redox behaviour of Mn in this zone and found further evidence of Mn reduction within the hypoxic zone. Tankéré *et al.* (submitted) measured dissolved Co in the northwestern Black Sea. The measured Co concentrations were generally in the range of 200 to 1700 pM with higher concentrations found at depth. Simultaneous oxygen measurements indicated low (1.8 ml l^{-1}), but not zero dissolved oxygen concentrations. High particulate and dissolved Co concentrations were recorded in surface waters influenced by the freshwater inflow from the Danube river. Moreover, the authors found that the dissolved Co concentration was limited by the presence of Mn-oxides.

1.3. Mechanisms of Mn and Co oxidation

The redox cycling of Mn in the marine environment is a complex process, influenced by a range of chemical, physical and biological factors (Figure 4). In particular, for a relatively shallow system such as a loch, the concentration of Mn in the water column is

influenced by continuous interactions between the water and bottom sediments. As illustrated by Figure 4, this interaction is multidirectional.

Dissolved Mn is particle reactive and will therefore undergo oxidation to form Mn(IV). This oxidation process of Mn(II) was first shown by Morgan (1967) to include a homogenous oxidation and a heterogeneous autocatalytic step as illustrated in Equation (1).

$$\frac{-d[\text{Mn(II)}]}{dt} = k_1[\text{Mn(II)}] + k_2[\text{Mn(II)}][\text{MnO}_x] \quad (1)$$

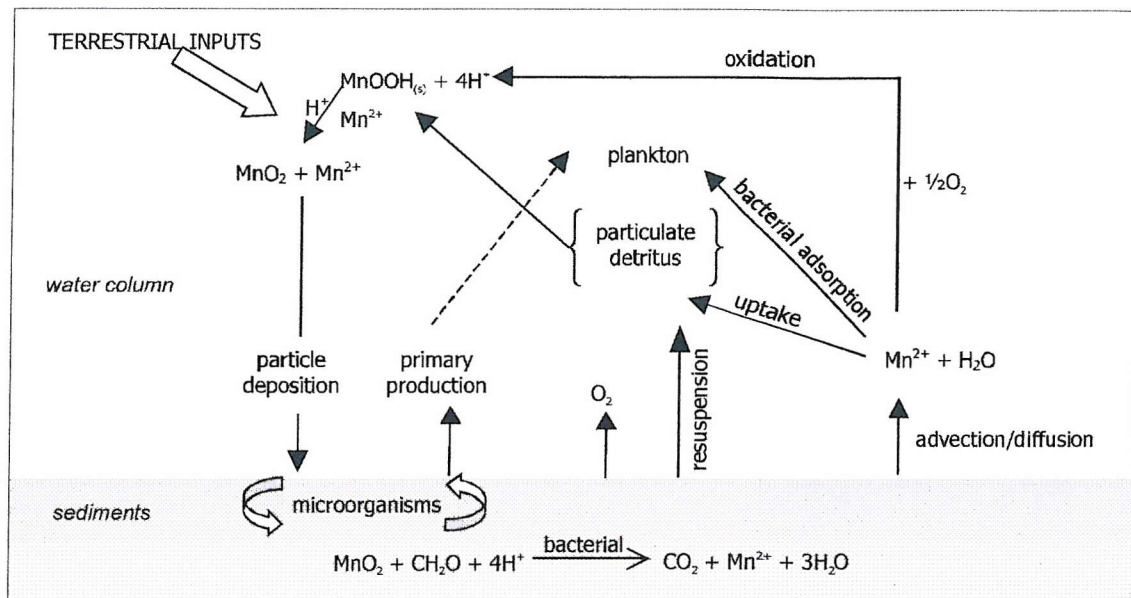


Figure 4. Reaction and processes contributing to Mn cycling in shallow marine ecosystems (from Hunt and Kelly, 1988).

More recently, the kinetics of the Mn oxidation has been proposed to be dependent on the oxygen concentration and the square of the hydroxyl concentration (Murray and Brewer, 1975), as illustrated in equation (2). Since in aquatic systems there is a marked presence of potential catalytic surfaces, the use of this form of the rate equation has been suggested to be more appropriate (Yeats and Strain, 1990).

$$\frac{-d[\text{Mn(II)}]}{dt} = k[\text{Mn(II)}][\text{MnO}_2][\text{O}_2][\text{OH}^-]^2 \quad (2)$$

In addition, several studies have concluded that the Mn-oxidation is driven by microbial catalysis (Emerson *et al.*, 1979; Wollast *et al.*, 1979; Emerson *et al.*, 1982). Thus, even though Mn(II) can be autocatalytically oxidised, microbial catalysis may act as the driving force (Tebo *et al.*, 1984).

Once oxidised, the particulate Mn can be deposited by passive (gravitational settling) or active (*e.g.* via filter feeding microorganisms) transport to the sediments (Santschi *et al.*, 1983; Hunt, 1983a). In the sediments, particulate Mn-oxides can undergo reduction during the decomposition of organic matter to form the more soluble Mn(II). This reduction can be chemically mediated by organic compounds, for example chinones and catecholes (Stone and Morgan, 1984a). Other organic compounds such as puruvates and oxalates have also been shown to increase the Mn reduction rate. By contrast, the oxidation rate is reduced by adsorption of Mn onto humics (Stone and Morgan, 1984b). In its reduced form Mn(II), manganese can cycle internally in the sediments as illustrated by route [A] in Figure 5. Alternatively, dissolved Mn(II) can be remobilised and returned to the water column (route [B] Figure 5) by advective sediment-water exchange, by bioturbation or by diffusive processes (Hunt and Kelly, 1988). These processes are, in turn, influenced by a range of factors including oxygen, pH, temperature, tidal and benthic activity (Aller, 1978, 1980; Morris *et al.*, 1982; Hunt, 1983b).

Given that many of the processes shaping the Mn distribution are influenced by oxygen concentrations, it is of interest to further investigate how low oxygen concentrations might, as a direct consequence, affect the cycling and concentration of Mn in a hypoxic loch system.

By contrast, little is known about the redox processes of Co. The low seawater concentration of Co (see Section 1.2.1) has made the collection of information about its speciation and cycling in the marine environment difficult and at present the controlling processes and redox behaviour of Co are poorly understood. Investigations of Co speciation in seawater have shown that up to 60 % of the total dissolved Co in seawater exists as the free ion Co(II) (Pan and Susak, 1991; see also Čosović *et al.*, 1982). In oxic waters, however, due to the thermodynamic instability of Co(II), low concentrations of dissolved Co would be expected. Furthermore, it has been suggested that in surface waters a significant fraction of Co exists as organic complexes, but the exact contribution of this fraction has not been established (Lewis and Landing, 1992).

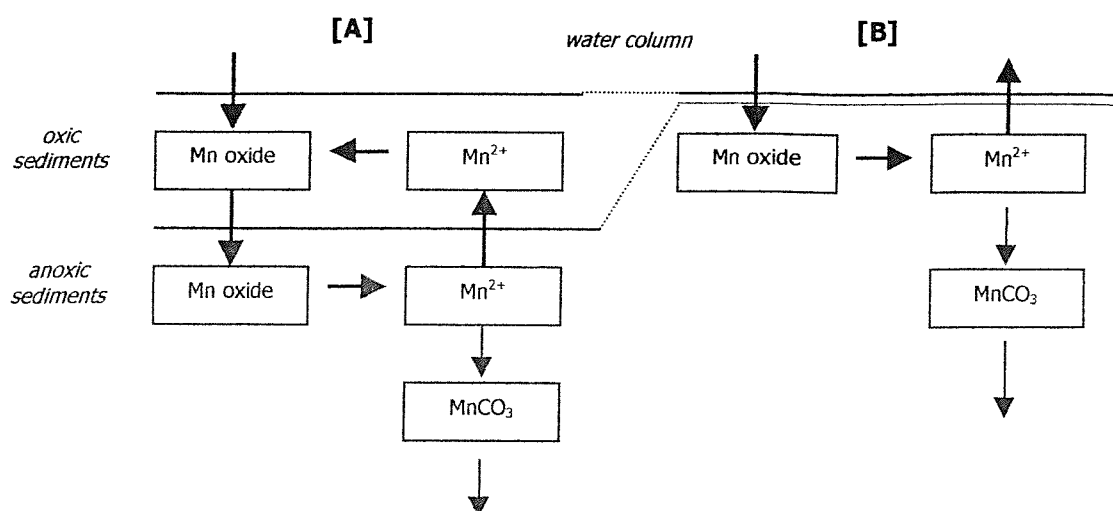


Figure 5. Schematic representation of the internal and external sedimentary cycling of Mn (redrawn from Slomp *et al.*, 1997). The precipitation of Mn as reduced authigenic minerals has for simplicity been denoted as Mn-carbonates although other phases may also occur (see Slomp *et al.*, 1997 and references therein).

Under reduced oxygen concentrations Co exists mainly as free cationic species. In anoxic waters the fraction of free Co ion decreases suggesting the presence of a dissolved Co metal-sulfide complex, possibly as $CoS(HS)^-$. On thermodynamical grounds, however, it would be suggested that the precipitation of a discrete Co-sulfide phase is unlikely (Landing and Lewis, 1991). Instead, it has been suggested that the precipitation of sulfidic Co may take place by co-precipitation with Fe-sulfides.

In marine sediments the cycling of Co has been linked to that of Mn. Indeed, under oxic conditions Co has shown a strong adsorption affinity for Mn-oxides (Murray, 1975). Under hypoxic conditions Co can be released into porewaters during Mn-oxide dissolution, diffuse upwards and, upon reaching oxic sediments, be removed from the dissolved phase as particulate Co(III) (Heggie and Lewis, 1984; Lewis and Landing, 1992). This leads to the hypothesis that a similar cycling of Co in hypoxic waters may occur, whereby dissolved Co(II) may diffuse into the hypoxic zone, be scavenged onto Mn(IV)-oxides (and/or Fe(III) oxyhydroxides), and only released when the Mn-oxides are subsequently reduced under hypoxic and/or anoxic conditions.

1.4. Cobalt and manganese interactions

Several authors (Murray, 1975; Murray and Dillard, 1979; Kremling *et al.*, 1987; Tappin, 1988; Kremling and Hydes, 1988; Lienemann *et al.*, 1997) have suggested a correlation between the distribution of Co and Mn, which would indicate similarities in the geochemical cycling of these two elements.

This has been suggested firstly on the basis of analysis of ferromanganese crust and Mn nodules showing high Co enrichments (Burns, 1976; Baturin, 1988; Manheim, 1991). The observed enrichment has been inferred as a result of Co(II) adsorption and subsequent oxidation on the surface of Mn oxides, a process that has also been suggested to take place in the water column (Moffet and Ho, 1996). Thermodynamically, the oxidation of Co(II) by MnO_x should be a spontaneous process at the pH of seawater (Burns, 1976); this could, therefore, be a significant mechanism for removing dissolved Co from the water column.

Secondly, the correlation between Co and Mn has been suggested from recent studies of Mn oxidising bacteria (Lee and Fisher, 1993; Lee and Tebo, 1994; Moffet and Ho, 1996). Spores of marine *Bacillus* spp., which oxidise Mn(II), have also been shown to oxidise Co(II) to Co(III)-oxide, even in the absence of Mn (Lee and Tebo, 1994). This common microbial pathway for the oxidation of Co and Mn would also be supported by thermodynamics, considering the similar reduction potentials of Co(III) and Mn(III) (Table 1). The similarities in potential between the reduction half reactions for these two elements indicate that both reactions could occur under similar environmental conditions.

The exact mechanism of the oxidation, however, is not yet understood. Lee and Tebo (1994) suggest that the oxidation of Co on Mn-oxides might occur via some indirect mechanism, in which surface catalysis reduces the activation energy for the oxidation of Co(II) (see also Diem and Stumm, 1984). Alternatively, the reaction could be directly mediated by microbial activity.

Table 1. Standard reduction potentials for Mn(II) and Co(II) (Moffet and Ho, 1996).

Half reaction	E^0 (volts)
$\text{MnOOH}_{(s)} + 3\text{H}^+ + \text{e}^- \longleftrightarrow \text{Mn}^{2+} + 2\text{H}_2\text{O}$	+1.50
$\text{CoOOH}_{(s)} + 3\text{H}^+ + \text{e}^- \longleftrightarrow \text{Co}^{2+} + 2\text{H}_2\text{O}$	+1.48

Although a detailed investigation of the association between Co and Mn is outside the scope of this study, quantification of these trace metals in the particulate and dissolved phase will give an indication of any covariance and hence provide a background for further investigations.

1.5. Research objectives

The principal aim of this study is to improve our understanding of the distribution and behaviour of two redox sensitive trace metals, Mn and Co, in a hypoxic environment (Loch Etive, Scotland).

Specifically:

1. To investigate seasonal variation in the dissolved and particulate concentrations of Co and Mn.
2. To investigate the correlation, if any, between Co and Mn under different redox conditions.
3. To apply a new sampling and measurement technology to the determination of Mn. The development work was done in collaboration with Dr. P. Statham and Dr. D. Connelly at the School of Ocean and Earth Science, University of Southampton.

Chapter 2. Sampling and analytical procedures

2.1. Study area

Loch Etive is situated on the west coast of Scotland, 5 km north of Oban (Figure 6). It extends for about 28 km in an eastward, followed by a north-eastward, direction and is connected to the coastal waters of the Firth of Lorne via a sill at Connel which measures 300 m wide, 5 km long and 10 m deep (Ridgway and Price, 1987). Loch Etive is divided into two main basins: the inner basin (furthest northeast) is the deeper of the two with a maximum depth of about 150 m, the shallower outer basin has a maximum depth of 60 m. The two basins are separated by a shallow sill (13 m) at Bonawe (Edwards and Edelsten, 1977). The loch has a large catchment area (1400 km²), with two main freshwater inputs, the River Etive, entering at the northeast end and the River Awe entering at Bonawe. Smaller additional freshwater sources are the rivers Noe, Lover and Kinglass, flowing into the loch from the south. In addition, the loch receives a high annual rainfall (*ca.* 200 cm a⁻¹, Williams *et al.*, 1988). These high freshwater inputs produce an intense halocline leading to the formation of stagnant bottom water. (The process of deep-water renewal in Loch Etive was outlined in Section 1.1). During these periods of deepwater stagnation the dissolved oxygen concentration falls to about 3 ml l⁻¹ (Edwards and Grantham, 1986).

Price and Calvert (1973) investigated the characteristics of the sediments in the two deep basins in Loch Etive. The sediments are dominated by organic-rich (3 to 8% w/w organic carbon), principally non-carbonate, fine grained silts and muds, turning more sandy towards the northeast part of the loch. A difference in the characteristics was noted between the two basins, with the organic matter from the inner basin indicating a higher carbon content, characteristic of a higher contribution of terrigenous material (Price and Calvert, 1973). As a consequence, the sediment surface in the inner basin has been described as having a thin (1 cm) oxidising surface below which grey/black reducing sediments occur. For the outer basin this oxidising layer is deeper, extending to approximately 5 cm (Williams *et al.*, 1988). In this oxidising layer of the outer basin there is an abundant macrofaunal presence, which is dominated by the two worm species, *Capitella capitata* and *Nephtys hombergi*. In the inner basin, however,

the faunal activity is more restricted with only the tube worm *Spirochaetopterus typicus* being prevalent (Ridgway and Price, 1987).

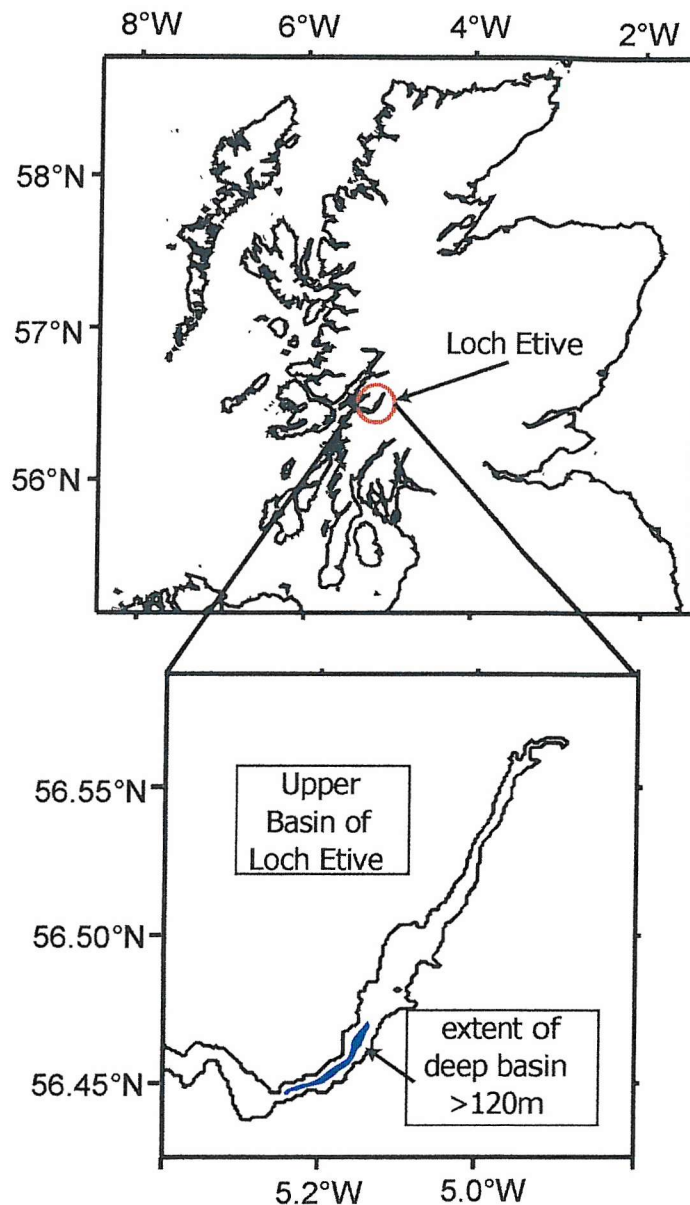


Figure 6. Map of the study area: Loch Etive.

2.2. Sampling

Water samples were collected on two cruises in Loch Etive: the first aboard R.V. Calanus in November 1999 (21st October to 8th November) and the second aboard the Terschelling in April 2000 (4-8th April). The bottom water in Loch Etive is known to turn over without a fixed periodicity but the mean repetition rate is about 16 months

(Edwards and Edelsten, 1977). The sampling periods were chosen so as to obtain samples from within a long period of stagnation where the bottom waters on both occasions would be hypoxic with a decrease in oxygen concentration.

Samples for dissolved metal analysis were collected using an Aqua Monitor mounted on Autosub (see below). A range of missions were run including some in bottom hugging mode (constant altitude over bottom) and a greater number in constant depth mode, following tracks based on given way-points (WP) along the centre of the loch. In addition, the Autosub performed *lawnmower pattern*, a square wave pattern track along the loch providing a full two dimensional coverage. The performed missions and their track routes are listed in Table 2, and illustrated graphically in Figure 7.

Table 2. Autosub missions in Loch Etive November 1999 and April 2000 (WP = way point, see text).

Cruise date	Mission no	Depth/altitude	Description
03-11-99	212	Variable starting at 100 m	Depth transect, upper basin
06-04-00	226	Constant altitude 25, 10 m	WP1-19 at 25m, WP19-36 at 10 m
06-04-00	227	Constant depth 100, 80 m	WP15-7 at 100m, WP7-25 at 80 m
06-04-00	228	Constant depth 70, 50 m	WP26-7 at 70m, WP7-26 at 50 m
07-04-00	229	Constant depth 50 m	Lawnmower pattern, WP50-70
07-04-00	230	Constant depth 80 m	Lawnmower pattern, WP50-77
07-04-00	231	Constant depth 20 m	WP26-6

During the November cruise several vertical CTD profiles were obtained in addition to the Autosub missions. The locations of these are listed in Table 3. In relation to the WP used by Autosub, station AT05 and AT06 were positioned on a transect-line from the river Kinglass, closest waypoint being WP24. AT07 were located further down the loch, at WP21, and AT9-12 were on a transect-line from the river Glen Liver (with WP09 closest to the river mouths on the east shore of the Loch) in close vicinity to WP17. During both cruises, continuous CTD measurements were made using the Autosub CTD system, that in addition to conductivity, salinity and pressure measured the dissolved oxygen concentration. Furthermore, during the April cruise, dissolved Mn data were also obtained in-situ using a spectrophotometric chemical analyser mounted on Autosub.

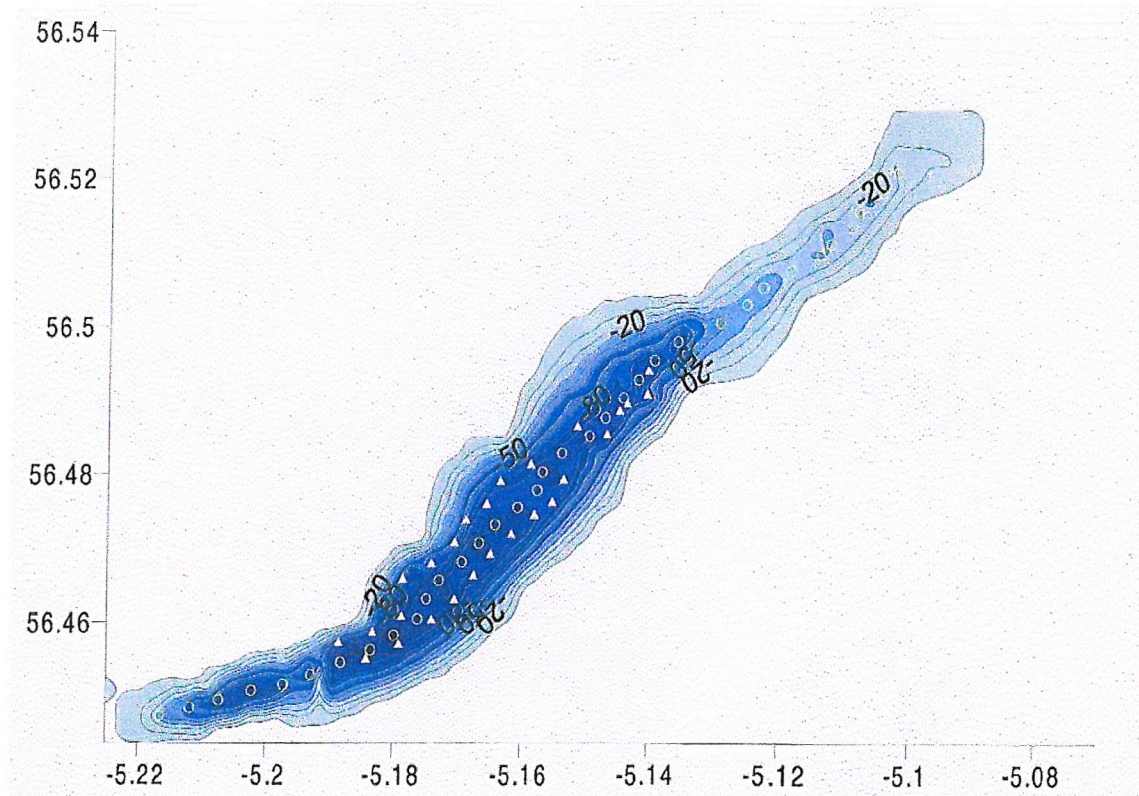


Figure 7. Bathymetric map of Loch Etive, waypoints are indicated by circles for straight depth transects (waypoint numbers starting from 1) and by triangles for lawnmower transects (waypoint numbers starting from 50), respectively, increasing further northeast (from D. Connelly, unpublished data).

Table 3. Coordinates of positions for CTD casts, Loch Etive November 1999.

Station	Lat.	Long.
AT05	56 29.82'N	5 08.65'W
AT06	56 29.84'	5 08.69'
AT07	56 29.24'	5 08.79'
AT08	56 28.64'	5 08.68'
AT09	56 28.62'	5 09.18'
AT10	56 28.71'	5 09.32'
AT11	56 28.71'	5 09.33'
AT12	56 28.84'	5 10.03'

2.2.1. Autosub

Autosub (Figure 8) is an AUV (Autonomous Underwater Vehicle) developed by the Ocean Technology Division at the Southampton Oceanography Centre. The 6.8 m long and 0.9 m diameter vehicle travels with an average speed of 4 knots (2 ms^{-1}) through the water and is designed to carry a wide variety of scientific instruments depending on its mission (Griffiths *et al.*, 1997; 1998).

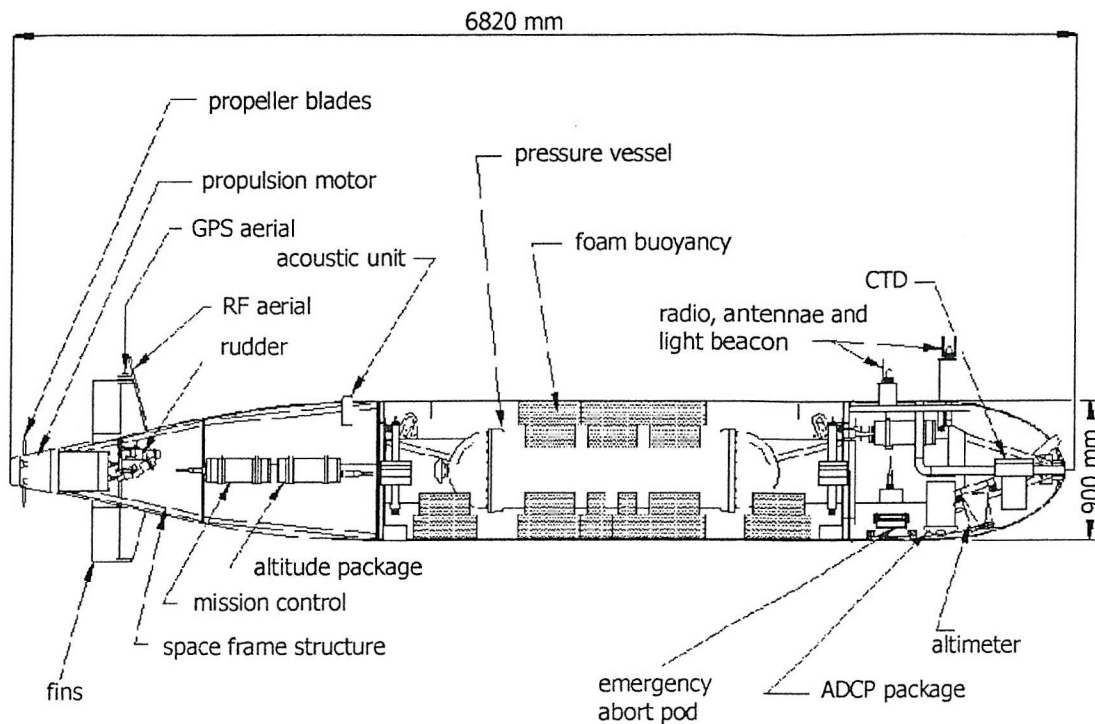


Figure 8. Schematic layout of Autosub (from Griffiths *et al.*, 1998).

The autonomous nature of Autosub enables each sampling run to be programmed based on given positions (way points, WP) and the desired water depth or altitude over the sea-bed using a ship based mission control. As a result, the vehicle is able to travel in complex three-dimensional pathways carrying its instrument load and continuously recording measurements in areas of the water column that would not be accessible using traditional CTD-hydrocast techniques. When equipped with the appropriate sensor instruments, therefore, Autosub provides a powerful tool with which to obtain a detailed spatial distribution of the elements under investigation.

During the November and April cruises in Loch Etive, in addition to navigational sensors for position, depth, speed and altitude above the sea-bed, Autosub carried a CTD system together with an oxygen probe, an Aqua Monitor and an in-situ chemical analyser for measuring dissolved Mn (April sampling cruise only).

2.2.2. Aqua monitor

Water samples for trace metal analysis were collected using an Aqua Monitor (AqM) Model WMS-1 (W.S. Ocean Systems Ltd) (Figure 9). The AqM is able to collect water

samples in-situ using a pre-programmed and automated time series mode. The AqM was mounted on board Autosub and the sampling sequence was controlled using the Autosub onboard mission control.

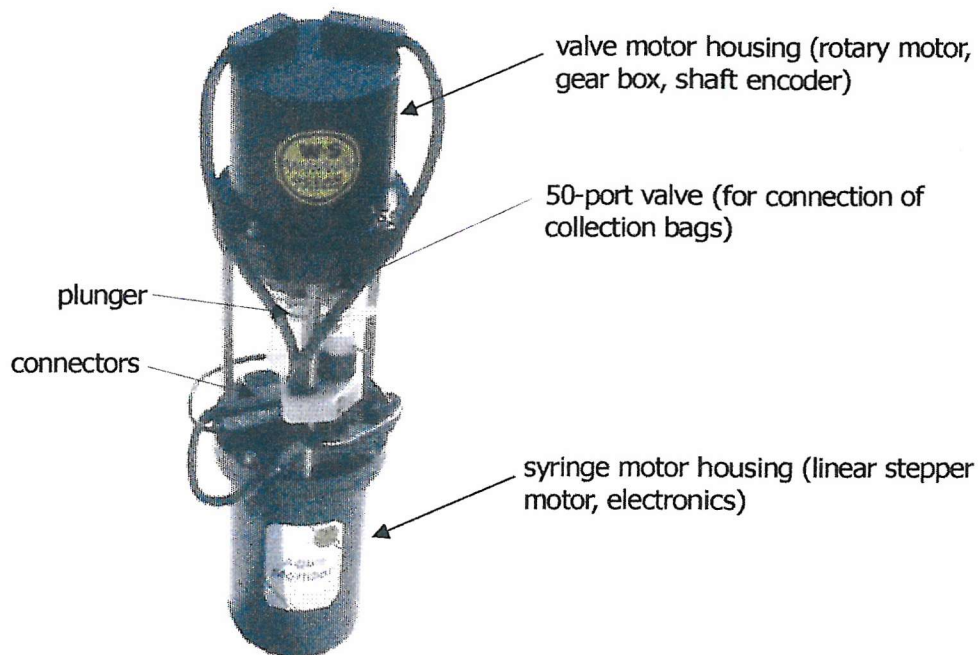


Figure 9. Schematic layout of Aqua Monitor (from AqM Model WMS-1 Operating Manual, W.S. Ocean System Ltd. 1999).

The monitor consists of two main components (Figure 9): i) the syringe and valve motor pressure housings and ii) the valve/syringe assembly. To the valve ports, 50 pre-cleaned bags (transfusion bags, 500 ml) were attached. The cleaning procedure involved an initial soak in detergent (Micro) followed by consecutive cleaning steps in strong acids, see Section 2.3.2. The rotary valve and syringe were both controlled by a stepper motor powered from a battery pack on the Autosub. Each water sample (400 ml) was obtained through an inlet at the hull of Autosub, as the syringe plunger was driven back at the current sample port. The sample entered the syringe chamber via a one-way valve and was then transferred to the sample bag as the syringe plunger was driven forward. After each cycle (4 min) the rotary valve was turned clockwise to the next sample port. After each sample run, the sample bags from the AqM were recovered and immediately filtered on board [April] or in the laboratory [November] (see Section 2.3.3).

2.2.3. CTD

During the November cruise CTD profiles were taken prior to the Autosub sampling run. The CTD (Sea-bird 9/11 + and rosette (12 x 51) Niskin bottles) was operated using direct reading mode, allowing the operation of supplementary sensors measuring dissolved oxygen (Beckman polarographic oxygen sensor), transmission (Sea-Tech 25 cm beam transmissiometer) and chlorophyll (Sea-Tech fluorometer). Data received during the cast were logged onto a personal computer using the Sea-bird SEASAVE v1.15 acquisition software program and post processing was made using the Sea-bird software v4.244.

2.3. Dissolved trace metal analysis

2.3.1. Introduction

Successful analysis of low (nano- to pico-molar range) dissolved metal concentrations in a complex matrix such as seawater requires the use of extraction techniques (Donat and Bruland, 1995). These techniques allow the concentration of the analyte and removal of the salt matrix before analysis.

Several pre-concentration techniques have been used in the past including; (i) ion-exchange (*e.g.* Pai *et al.*, 1988), (ii) co-precipitation, for example using cobalt pyrrolidine dithiocarbamate (Boyle and Edmond, 1977) and (iii) liquid-liquid extractions employing a variety of different chelation-solvent combinations (Donat and Bruland, 1995). Commonly used chelating agents include dithiocarbamates mainly because of their non-selective complexing properties over a broad pH range (Bruland *et al.*, 1979; Danielsson *et al.*, 1978; Bruland *et al.*, 1985; Sturgeon *et al.*, 1980) and dithizone (Armannsson, 1979; Smith and Windon, 1980). Alternatively, ion-exchange resins such as Chelex-100 (Kingston *et al.*, 1978; Bruland *et al.*, 1985) and 8-hydroxyquinoline (Klinkhammer, 1980; Landing and Bruland, 1980) have been employed. For a more in-depth review of analytical considerations concerning trace metal analysis see Donat and Bruland (1995).

In this study, a chelation-solvent extraction procedure was employed to pre-concentrate the cobalt (Co) and manganese (Mn) prior to analysis by Graphite Furnace Atomic Absorption Spectrophotometry (GFAAS). The method is based on the work of Danielsson *et al.* (1978), as modified by Statham (1985) and Tappin (1988). In the method by Statham (1985), a metal-carbamate complex is formed using ammonium

pyrrolidine dithiocarbamate (APDC) and diethylammonium diethyldithiocarbamate (DDDC). The formed metal-carbamate complex is then extracted into Freon TF and subsequently back-extracted into nitric acid prior to analysis by GFAAS. However, due to the known damaging effects that chlorofluorocarbon and similar compounds have on the ozone layer, the use of an alternative solvent phase was preferred. Chloroform has shown to be an effective solvent phase for this purpose (Bruland *et al.*, 1979; Magnusson and Westerlund, 1981; Jickells and Knap, 1984) and hence in the APDC/DDDC-Freon system, the Freon TF was replaced by chloroform.

2.3.2. Preparation of equipment

To minimise the risk of sample contamination, all equipment used in the procedure was rigorously cleaned prior to use. This involved an initial soak in detergent (Micro, 2% v/v) followed by consecutive cleaning steps in strong acids (HCl and HNO₃).

All bottles and vials used for the analytical procedure were cleaned according to the following protocol:

- a) Initial rinse with R.O. (reverse osmosis) water followed by a soak in a non-phosphate detergent (Micro, 2% v/v) for 1 week.
- b) Rinse with Milli-Q water (Millipore) followed by soak in 50% HCl for 1 week.
- c) Rinse with Milli-Q water followed by soak in 50% HNO₃ for 1 week.
- d) Final rinse with Milli-Q water.

The bottles and vials were transferred to a clean room Class-100 laminar flow hood and rinsed with SBD-H₂O (see below) and allowed to dry. Cleaned bottles were stored in individual resealable plastic bags.

2.3.3. Sample manipulation and storage

Samples were filtered immediately upon collection using pre-weighed and pre-cleaned 0.4µm Nuclepore filters. The filters were handled at all times using plastic tweezers. The filters were rinsed with SBD-H₂O to remove salt residues before storage in cleaned polyethylene dishes at -20 °C. To minimise any contamination, the filtration was performed using a closed system, whereby the sample bags from the Aqua Monitor were connected to a specially designed vacuum filtration unit. The filtrates were collected in ultra clean bottles (cleaned by the procedure outlined in 2.3.2.) and, after transport to the laboratory, they were acidified by addition of SBD- HNO₃ (1µl/1ml

SW) to a final pH of < 2 . Acidified water samples were stored in resealable plastic bags in a clean room environment.

2.3.4. Preparation of chemicals

The preparation of all chemicals used in the procedure took place in a clean room environment within a Class-100 laminar flow hood.

a) Sub-Boiled Distilled Water (SBD-H₂O)

Sub-boiled Distilled Water (SBDW) was produced by the use of a Quartz system. This system is based on heating of water by silica-sheathed elements in a closed system to create vapour that is allowed to condense on a quartz cold finger which leads the condensate to a collection vessel outside the still (see Howard and Statham, 1993). Milli-Q water was sub-boiled distilled and collected in an ultra clean FEP (Fluorinated Ethylene Propylene) bottle (1000 ml).

b) SBD-HNO₃

SBD-HNO₃ was prepared through sub-boiling distillation of 16N analytical grade nitric acid using a Quartz system as described in (a).

c) Isothermally Distilled Ammonia (ID-NH₄OH)

Isothermally Distilled Ammonia (ID-NH₄OH) was prepared from analytical grade ammonia in a clean room. A PTFE (polytetrafluoroethylene) beaker (500 ml) containing analytical grade ammonia (NH₄OH) was placed together with a beaker with SBD-H₂O in a sealed, airtight, container and left for one week. During this time the ammonia gas (NH_{3(g)}) equilibrated with the SBD-H₂O to form ID-NH₄OH. The formed ID-NH₄OH was decanted and stored in a bagged FEP (fluorinated ethylene propylene) bottle.

d) Chloroform (HPLC grade CHCl₃)

Chloroform was cleaned by adding SBD-H₂O (10 ml) to chloroform (400 ml) in a Teflon separating funnel. The mixture was shaken for 5 minutes. The water layer was separated and discarded. This procedure was repeated 10 times. The cleaned chloroform was stored with a surface film of SBD-H₂O in an ultra clean FEP bottle (1000 ml) and used within 36 hours of preparation.

e) Complexant

A mixed complexant was prepared by accurately weighing out ammonium pyrrolidine dithiocarbamate (APDC) (2.0 g) and diethylammonium diethyldithiocarbamate (DDDC) (2.0 g) and dissolving in SBD-H₂O (100 ml) to produce a 2% w/v solution.

The solution was mixed, and filtered using vacuum, through a glass fibre filter (Whatman GF/C, 47 mm). The filtrate was transferred to a Teflon separating funnel and pre-cleaned chloroform (10 ml), see step (d), was added. The mixture was shaken and the chloroform was discarded. To ensure complete removal of metal traces this procedure was repeated 10 times. Due to the short lifetime of the complexant solution (3-4 days) (Parker, 1999), the complexant was stored refrigerated and used within 24 hours of preparation.

2.3.5. Preconcentration and back-extraction

The preconcentration and back-extraction steps were carried out in a clean room under a Class-100 laminar wet station. Teflon funnels used for the separation were cleaned prior to each extraction run. This involved addition of pre-cleaned chloroform (3ml) and complexant (4 ml). Funnels were shaken for 5 min, and the content was discarded. To reduce sample carry over, this step was repeated between each extraction. Figure 10 illustrates a flow diagram of the employed procedure.

An aliquot (approximately 100.0 g) of each sample was accurately weighed into a Teflon separating funnel (500 ml) and neutralised with ID-NH₄OH (200-300 µl). The neutralisation step was performed to ensure the correct pH for complete extraction of the metals under investigation (Statham, 1985). The exact amount of ID-NH₄OH required for neutralising the sample to a pH between 6.5 to 8 varied depending on the sample batch. The amount was determined by stepwise addition of ID-NH₄OH to a separate aliquot (20 ml) from each sample batch. Teflon funnels were shaken to ensure complete neutralisation. After the extraction step the pH of the samples was re-confirmed to be between pH 6.5 and 8.

To each sample, APDC-DDDC complexant (2% w/v) (4 ml) and chloroform (3 ml) were added. The Teflon funnels were mounted in a plastic frame and rotated automatically for 5 minutes (for the mechanisation of the extraction step see Statham, 1985). The aqueous and chloroform layers were allowed to settle and the chloroform extracts were run off and collected into ultra clean Teflon pots (Saville, 30 ml). Care was taken not to transfer any of the aqueous phases with the chloroform extracts. Two additional extraction steps, each using 3 ml aliquots of chloroform were done. The additional chloroform extracts were added to the first.

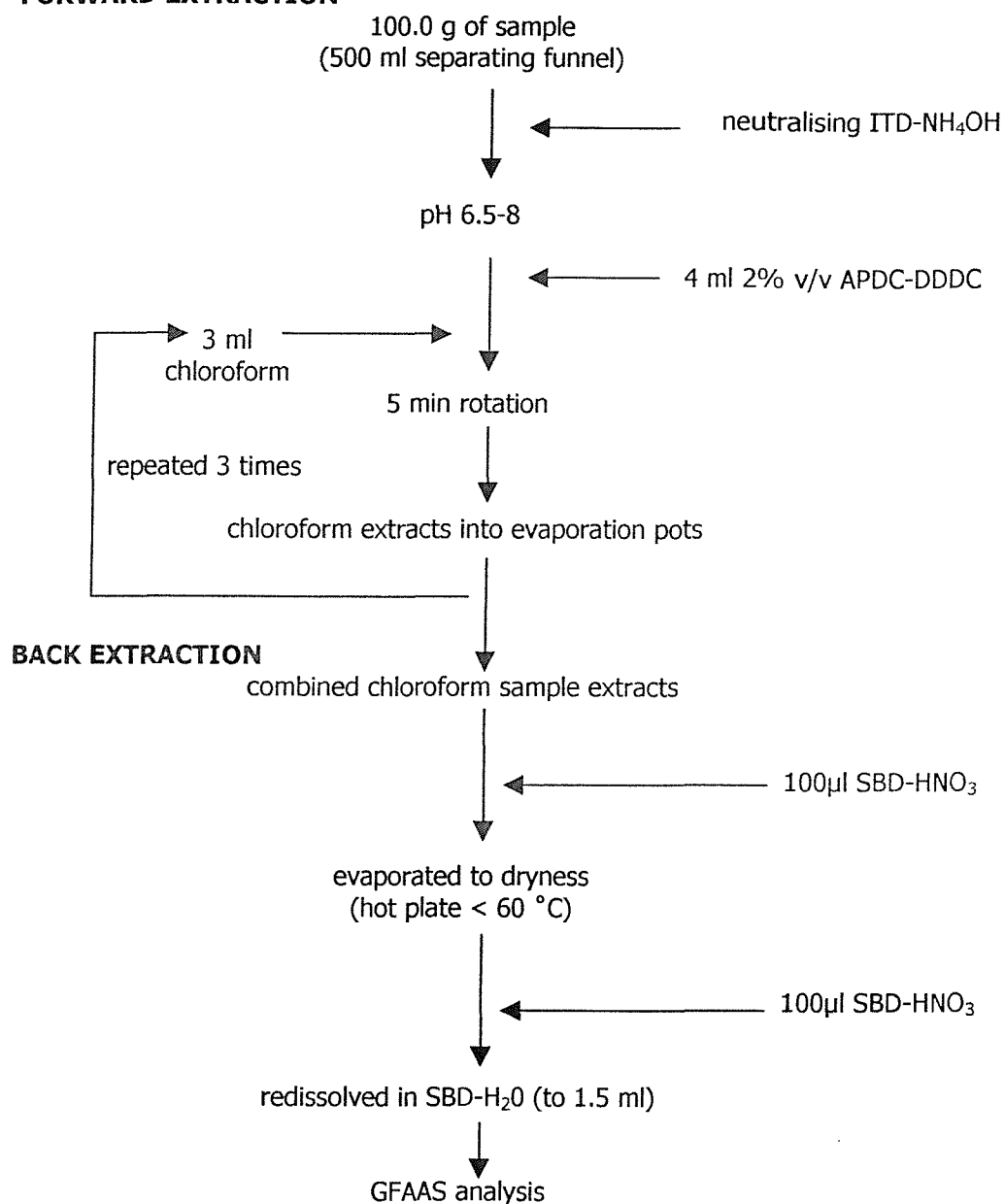
FORWARD EXTRACTION

Figure 10. Flow diagram of the extraction procedure (see text for details).

To oxidise the matrix component, SBD-HNO₃ (100 µl) was added to each combined chloroform extracts. Parker (1999) noted that this early addition of acid helped reduce fuming, noted upon addition of SBD-HNO₃ after the evaporation step. The sample pots were transferred to a hot plate and evaporated to dryness (50 °C, 24 hrs). The temperature of the hot plate was kept constant at 50 °C during the evaporation, in order to avoid any loss of metal, as a result of boiling and splashing of the chloroform (CHCl₃ b.p. 61.2 °C). To the evaporated extracts, further SBD-HNO₃ (100 µl) was added and the acid was allowed to evaporate on the hot plate (50 °C, 24 hrs). The hot plate was turned off and the samples allowed to cool.

The samples were redissolved in concentrated SBD-HNO₃ (100 µl). The extract was then made up to a final volume of 1.5 ml by the addition of SBD-H₂O (1400 µl) using a micropipette. This gave a final acid concentration of ~ 7% v/v, assuming no acid remained in the final sample residue. The back extract for each sample was transferred using a micropipette to an acid cleaned screw capped polypropylene tube.

In order to assess the analytical quality of the technique and comparability of consecutive sample batches, blanks (SBD-H₂O, 100.0 g to which complexant (4 ml) and chloroform (3 x 3 ml) were added), LMSW (Low Metal Seawater) and certified reference seawater (CASS-3) were analysed with each sample batch.

2.3.6. Determination of total dissolved trace metals by GFAAS

The total dissolved trace metal concentrations in the back extracts were measured by Graphite Furnace Atomic Absorption Spectrophotometry (GF-AAS) using a Perkin-Elmer 1100B AAS equipped with an AS-70 autosampler and an HGA-700 graphite furnace. For the analysis of Mn, a deuterium hollow cathode lamp (HCL) background correction system was used. All elements were analysed by injection of the sample into a pyrocoated tube with fixed L'vov platform. Furnace conditions were adapted from the manufacture recommendations (see Table 4). Samples and standards were placed in 2 ml polyethylene sample cups and introduced to the GFAAS by the use of an autosampler. For the analysis of Co multiple plating was employed, whereby three 40 µl injections were separated by a drying stage (350 °C) prior to the atomisation stage (2500 °C).

Table 4. GFAAS conditions for analysis of back extracts.

ELEMENT	Mn	Co
Wavelength (nm)	279.5	241.2
Lamp current (mA)	10	8
Slitwidth (nm)	0.2	0.2
Injection volume (µl)	20	40 x 3
Injection temp (°C)	100	100
Drying temp (°C)	120	120
Ramp time (sec)	10	10
Hold time (sec)	10	10
Char (°C)	1300	1600

Ramp time (sec)	15	15
Hold time (sec)	15	15
Atomisation (°C)	2200	2500
Ramp time (sec)	0	0
Hold time (sec)	3	3
Burnout (°C)	2400	2600
Ramp time (sec)	2	2
Hold time (sec)	3	3
Calibration range ($\mu\text{g l}^{-1}$)	0-100	0-10

2.3.7. Calculation of dissolved sample concentration

The final metal concentration in the samples was obtained by subtracting the average analytical blank from each sample and by correcting for the concentration factor (final volume of the back extract over the initial volume). The result was converted from $\mu\text{g l}^{-1}$ into nM, by dividing by the atomic weight (g mol^{-1} times a factor of 1000) for the element of interest.

The limit of detection (LOD) (Table 5) was calculated as three times (3σ) the standard deviation (STDEV) of replicate blanks in nM (for Co a LOD of two times the STDEV was used). The precision of the analysis was calculated from replicate analysis of low metal seawater (LMSW) used as an internal reference (see Table 5).

Table 5. Average blanks, detection limits and recovery data for Mn and Co.

ELEMENT	Mn	Co
Average blank (nM)	0.20 (n=28)	0.006 (n=28)
Detection limit (nM)	0.80	0.022
%Recovery (recovery of added Mn/Co to an internal reference material)	93	110
Precision (RSDEV, %)	10	6
CASS-3 certified value (nM)	45.69 \pm 6.55	0.696 \pm 0.153
CASS-3 analysis (n=3) (nM)	46.54 \pm 4.44	0.720 \pm 0.011

2.4. Use and development of an in-situ detection technique

2.4.1. Introduction

Our understanding of geochemical processes in the marine environment is strongly dependent on the analytical tools we use to monitor the system under investigation. The wide availability of continuous profiling instruments for measuring physical parameters including conductivity, salinity and pressure has greatly enhanced this understanding. There is, however, a need for instrumentation capable of measuring continuously, in-situ and in real time, the concentrations of dissolved trace metals in seawater. A number of automated chemical analysers have been proposed in the past. From the initial discrete sampling techniques, early developments involved systems where the seawater was pumped on board a ship for subsequent analysis. These systems were based on a sample stream segmented by air-bubbles and, due to the pressure differences with depth in the water column, they turned out to be difficult techniques to further adapt to in-situ analysis. New possibilities came with the development of Flow Injection Analysis (FIA) in the 1970s (Ruzicka and Hansen, 1988). Flow Injection Analysis is based on the injection of a sample directly into an unsegmented reagent stream (alternatively, a reagent can be injected into a sample stream, denoted reversed-FIA). Recently, a range of chemical and trace metal analysers have been developed employing FIA for the mixing of sample and reagent (Johnson *et al.*, 1986; Chapin *et al.*, 1991; Chin *et al.*, 1992; Mallini and Shiller, 1993; Nowicki *et al.*, 1994; Blain and Tréguer, 1995; Daniel *et al.*, 1995). The chemical FIA-manifold can be used in combination with various detectors such as fluorometric (Klinkhammer, 1994), chemiluminescent (Okamura *et al.*, 1998; Cannizzaro *et al.*, 1999) and colourimetric devices (Chin *et al.*, 1992; Gamo *et al.*, 1994). Although a wide variety of chemical manifolds and detector systems now exists, only a limited number of these have been adapted to truly *in-situ* use (see Johnson *et al.*, 1986; Chin *et al.*, 1992; Gamo *et al.*, 1994).

In-situ chemical analysers offer numerous advantages for the measurements of dissolved trace metals in seawater compared to the more commonly used wireline hydrocast techniques. First, by allowing the sampling frequency to be increased it is possible to obtain more detailed information concerning the distribution of the element under investigation. Second, by reducing sample handling the risk of contamination is minimised.

The present study was part of one of the Autosub special topics projects aimed at creating a 3D map of the distribution of dissolved and particulate Mn in two Scottish Lochs (Loch Etive and Loch Fyne) using the Autosubs unique contour hugging dive profiling abilities. The project was coordinated by Dr. Statham and Dr. German at the SOC together with Dr. Overnell at the DML. In addition, the principal researchers working on the project were Dr. Connelly (SOC) and Tim Brand (DML). Initial development work of the in-situ colorimetric technique, was carried out at the SOC by Dr. Statham and Dr. Connelly. In addition to the measurements of particulate and dissolved Co and Mn, the present study was concerned with the development of the chemical aspects of this in-situ chemical analyser for the analysis of dissolved Mn, as detailed below. All work presented in the MPhil (unless otherwise stated) was the work of the author and represents an integral and important part of the development process. The obtained results from the use of the in-situ analyser are reported in Section 3.8.

In this study, in-situ detection of dissolved Mn in seawater was based on the colorimetric method developed by Chin *et al.* (1992). The reagent 1-(2-pyridylazo)-2-naphthol (PAN) forms a coloured complex with Mn(II) that can be detected using a spectrophotometer at λ 560 nm. Watanabe (1974) showed that the solubility of PAN, which generally is low in aquatic solutions could be increased by using a surfactant. Chin *et al.* (1992) solubilised the PAN in Triton X-100, also used in this study. Using the Mn-PAN complexation method, iron was shown to be a strong potential interference. This is because it can compete with Mn, also to form a coloured complex with PAN. The Fe-PAN compound absorption band overlaps with that of the Mn-PAN complex (see further Section 2.4.4). In a system such as Loch Etive, where hypoxic waters overly anoxic sediments a high concentration of dissolved Fe may diffuse into the water column from the sediments (Slomp *et al.*, 1997; Schoemann *et al.*, 1998). The iron interference was, therefore, suppressed using desferrioxamine B, an iron-specific chelating agent (Chin *et al.*, 1992).

2.4.2. Chemical manifold

The reagent was added to the sample using a chemical manifold (Figure 11). Reagent and sample were passed through the manifold using a peristaltic pump (Ismatec, 8 rolls, model MS/CA4-E/08/100) providing an overall flow rate of 1.6 ml min^{-1} (with a ratio of sample to reagent of 5.3). The sample and reagent were transported through the

manifold using PTFE (Teflon) tubing (i.d. 0.5-0.8 mm) connected with flanged tube fittings. From the external reagent bag the sample was added to the reagent through a T-fitting and mixed using a knitted mixing coil (see Section 2.4.5). The coloured complex was detected by allowing the solution to pass through a detector system.

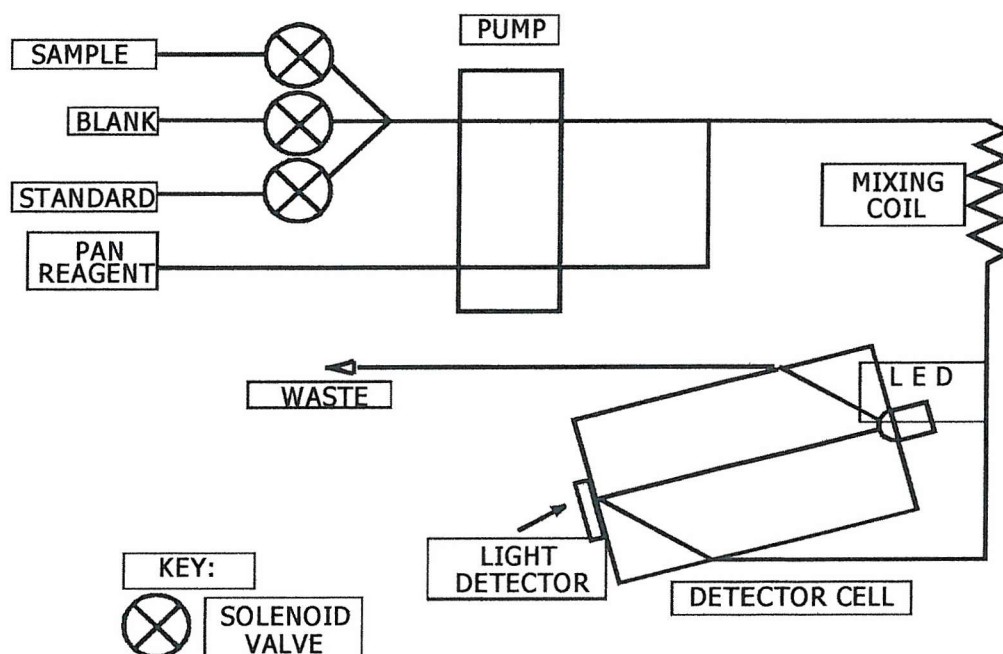
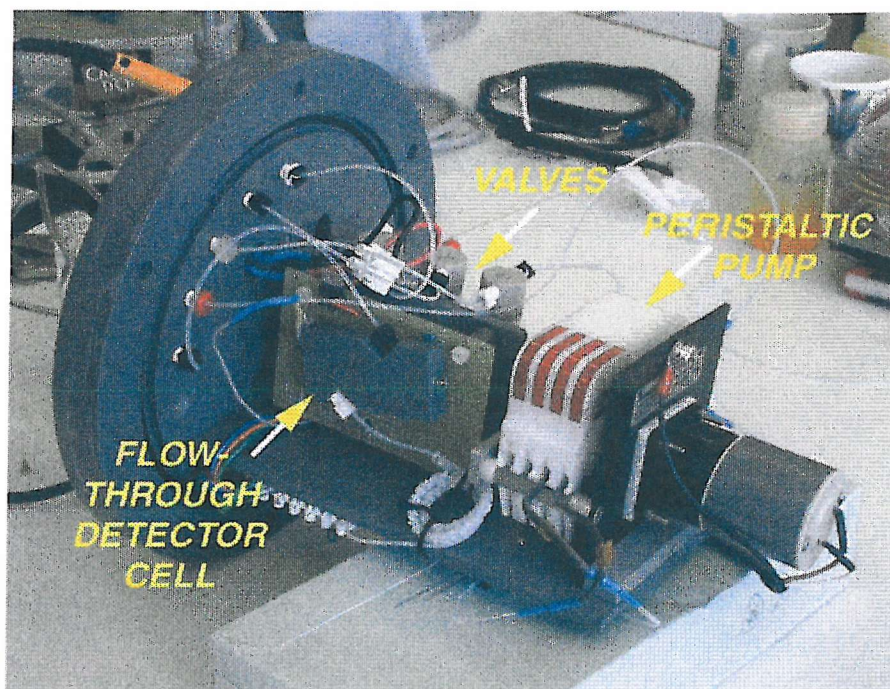


Figure 11. Photograph (above) and schematic layout (below) of the chemical manifold.

The detector system consisted of a PVC flow-through cell with a high intensity light emitting diode (LED) attached on one end of a narrow sample channel (2 mm i.d., 50 mm in length). On the opposite end was a combined silicon photodiode – CMOS amplifier (TAOS, TSL235) where the light intensity was converted to a TTL output frequency.

2.4.3. Optimisation of the surfactant concentration

Tests of the analytical method in the laboratory indicated problems of adsorption of the PAN complex in the manifold. Therefore, to obtain a reagent that would be less prone to adsorption, the effect of increasing the surfactant used for solubilising the PAN compound was investigated. Tests were performed manually using a spectrophotometer (Hitachi, U-2000). For these experiments, reagents and samples were mixed in batch in the same proportions as obtained in the FIA system of Chin *et al.* (1992). Initial testing indicated that the coloured (yellow) Mn-PAN complex was formed immediately upon mixing of sample and reagent. The absorbance at λ 560 nm increased linearly with increased dissolved Mn concentration. To enhance the solubilisation of PAN and hence reduce the adsorption in the manifold, investigations were made of the effect of increasing the amount of Triton X-100. A more concentrated Triton X-100 reagent solution (20ml Triton X-100 to 60 ml of Milli-Q water per 0.05 g of PAN compared to 5 ml of surfactant to 50 ml of Milli-Q water for an equivalent amount of PAN as used by Chin *et al.* 1992), did not influence the linear calibration. Moreover, it was observed that a higher concentration of surfactant could positively reduce any adsorbance on the walls of the detection cell and on tubing in the manifold. Hence, the optimised amount of Triton X-100 was shown to be approximately three times that of the amount used by Chin *et al.* (1992) (5 ml of Triton-X per 0.05 g of PAN added to 50 ml of Milli-Q water) (Table 6).

Table 6. Optimised %Triton X-100 in the PAN solution.

% Triton X-100	Author
33.3 %	Present study
20.0 %	Chin <i>et al.</i> , 1992

2.4.4. Test of the iron interference

The iron interference was investigated using a spectrophotometer (U-2000) set to a wavelengths scan mode. The absorbance of the Mn-PAN complex reached a broad maximum at λ 560 nm. The Fe-PAN complex had a negative absorbance at λ 510 nm, followed by a significant high absorbance at λ 560 nm. The addition of Desferal suppressed the iron interference. It was, however, noted that the addition of Desferal to the PAN reagent had a strong influence upon the final pH of the reagent. The effect of the pH of the absorbance of the PAN complex was investigated by Chin *et al.* (1992) and the optimal pH range of the reagent was found to be at a pH of 9.7 - 10.0. Due to the high iron concentrations expected in Loch Etive, the amount of Desferal used during the April cruise was kept at 400 μ l per 250 ml of PAN solution (Chin *et al.*, 1992). For work carried out in a less reducing environment, this amount should be adjusted in order to gain an optimal balance between final pH and effective reduction of the Fe-interference. The concentration of Desferal used in the present study effectively eliminated the iron interference in addition to agreeing well with previously published data.

2.4.5. Choice of mixing coil design

The mixing efficiency of two types of mixing columns, a knitted PTFE column and a packed glass bead columns, were investigated using a bench top version of the manifold connected in-line with the U-2000 spectrophotometer. The knitted column was designed by the method described by Selavka *et al.* (1987), whereby overhand knots of alternate directions are created on the PTFE tube using a backbone to hinder complete deformation of the tube. The packed column was made using a PVC tube with a central axial hole 40 mm in length passing through it. A frit was placed on one end of the axial hole and the column was packed with glass beads (0.45-0.5 mm diameter). A second frit was placed on the opposite end to keep the packed column intact (Van Der Berg *et al.*, 1980; Reijn *et al.*, 1981). Testing involved comparison with reagent-sample solutions mixed manually and comparison between the efficiency of the two types of columns. Results from the testing of the two types of columns did not indicate any difference in mixing efficiency. In the in-situ manifold a knitted column (80 mm in length) was used.

2.4.6. Analytical method

The analytical method employed in this study was based on that used by Chin *et al.* (1992) but with a different optical cell and with more surfactant (see below).

A borate (H_3BO_3) buffer solution (pH 10) was prepared by dissolving H_3BO_3 (0.618 g) in NaOH (0.1 M, 100 ml).

The mixed reagent was prepared by adding PAN (0.05 g) and Triton X-100 (20 ml) to Milli-Q water (60 ml). The mixture was stirred with a magnetic stirrer on a hot plate (80 °C, 5 hrs). The solution was removed from the hotplate and allowed to cool. To the cooled mixture, borate buffer (pH 10, 100 ml) was added and the solution made up to a final volume (250 ml) using Milli-Q water. The pH of the final solution was adjusted to be between pH 9.7 to 10.0 using a pH meter (Orion Research, EA920) and further additions of buffers, if needed.

Desferrioxamine B, pharmaceutical grade (trade name Desferal) was prepared by adding Milli-Q water (3.05 ml) to the Desferal (500 mg). To the cooled PAN solution, desferrioxamine solution (400 μl) was added followed by thorough stirring.

The prepared PAN reagent was placed in a pre-cleaned transfusion bag (500 ml). This was the standard bag type used for the reagent, blank and standards throughout the sampling procedure. The bags were directly connected to the manifold.

In order to allow for in-situ calibration of the system, two additional reagent bags were attached to the chemical manifold. Firstly, a blank solution, containing seawater stripped of Mn using Chelex-100. Secondly, a Mn standard (a blank solution spiked with dissolved Mn to obtain a final concentration of 1 μM). Each inlet was equipped with an electrically operated PEEK/PTFE valve (12V, Biochem-Valve Inc., model 075T2NC12-32-5). Electro-mechanical (Finder) timers were used to control the valves and allow the inlet to be switched between sample, blank and standard (40:4:4 min).

2.4.7. In-situ housing

For the system to work under water it was necessary to isolate all electrical components as well as to pressure compensate any pump tubing and other manifold constituents. Electrical components were therefore housed in a 4 inch sealed pressure case. To allow the pumping to work under ambient pressure the manifold and associated components were immersed in silicon oil (Gamo *et al.*, 1994). The manifold and oil were placed in an acrylic tube (200 mm i.d.) sealed with a PVC bottom plate and with a removable top

plate. The reagent, blank and standard bags could be directly attached to the top plate. Once sealed, a diaphragm on the top plate allowed for changes in pressure and this volume with depth and temperature.

The components were attached inside the front of the Autosub with the sample inlet mounted on top. A coarse filter (glass wool) was attached to the inlet to prevent any large material entering the manifold. Power to the electrical pressure housing was obtained directly from the Autosub. The 48V DC Autosub supply was reduced to the appropriate voltage for the pump and detector system with a solid state regulator. The output frequency obtained from the detector was logged from the Autosub to the onboard mission control system.

2.5. Particulate trace metal analysis

2.5.1. Sample preparation and analysis

The dissolved samples were filtered upon collection (Section 2.3.3). The leaching of the samples and the detection of Mn by Flame AAS were carried out at the Dunstaffnage Marine Laboratory (DML) by T. Brand. The filters were dried in an oven at 60-70 °C and allowed to cool to room temperature in a desiccator. The weights of the cooled samples were accurately recorded. The dried filters were placed in polypropylene centrifuge tubes and leached with HCl (1M, 3 ml) on a rotating table for 16 hours at room temperature. The samples were then centrifuged (1500 rpm, 10 min). The supernatant was transferred to a LDPE tube and analysed for Mn, using a Flame AAS (Pye Unicam SP9) with deuterium hollow cathode lamp (HCL) background correction. The Co analysis was performed at the Southampton Oceanography Center and carried out using a GFAAS (see Section 2.3.6).

2.5.2. Calculation of particulate sample concentration

The particulate Mn concentration ($\mu\text{g g}^{-1}$) in the samples was calculated by multiplying volume corrected Mn ($\mu\text{mol l}^{-1}$) by the atomic weight ($54.938 \text{ g mol}^{-1}$) and dividing by the suspended solid load (mg l^{-1}) times a factor of 1000. The particulate Co concentration was calculated from the $\mu\text{g l}^{-1}$ (obtained from the GFAAS converted to mg l^{-1}) multiplied by the digest volume (3 ml) and divided by the amount of suspended particulate matter (g).

Chapter 3. Results and discussion

3.1. Data processing

The data processing for the CTD casts was described in Section 2.3.7. The Autosub raw data was obtained as ASCII files with values recorded at 1-sec intervals. Post processing was made using SEABIRD software. Data were averaged over 10-sec intervals and stored as ASCII files that could be imported into Microsoft Excel. The data were then categorised according to mission number and averaged over the time each water bag on the Aqua Monitor (AqM) was sampled. When Autosub was rapidly diving or surfacing the AqM was sampling whilst passing through sharp concentration gradients. An AqM sample obtained during such an ascent or descent would be an integrated value and hence not truly representative of the average depth. To identify these ascents and descents, the standard deviation (SD) and coefficient of variation (CV) were calculated for each parameter and sample. Data were discarded for samples where the depth parameter had a CV larger than 15%, since, generally, CV was below 10% or above 20%. Hence, 15% was determined to be a suitable cut off value.

All data for the dissolved and particulate trace metal analysis and relevant hydrographic parameters (salinity, temperature and dissolved oxygen) are listed in Appendix 1.

In the following discussion, trace metal data (dissolved and particulate Co and Mn concentrations) will be considered in combination with the hydrographic data (salinity, oxygen and temperature). As mentioned previously (see Section 1.1) the water column at the time of sampling is expected to represent a stratified system. Based on the hydrographic data (see below), therefore, the water column is divided into surface and deep water, respectively. The term *surface water* will be used to denote water above the oxycline. Similarly, *deep water* will be used to denote water below the oxycline. The main oxycline corresponds to the main thermocline and halocline in each season.

3.2. Hydrographic data

3.2.1. General overview

The oxygen, salinity and temperature data from the November and April sampling cruises are presented in Figure 12 and 13. The November profile was obtained by plotting the hydrographic data for all CTD station against depth. For April, however, due to the large number of data points, the profile represents data averaged over 100 seconds. Although these profiles do not give information on the hydrographic conditions at a specific location in the Loch, this data processing employed provides an overall characterisation of the conditions in the surface and deep water, respectively. In November the salinity in surface waters ranged from 6.0 to 14.2 (Figure 12), progressively increasing with depth to values up to 27.4 in deep waters. The salinity in surface waters showed large variations, as expected considering the riverine freshwater inputs and the connection to the coastal waters at the lower part of the loch. Similarly to the salinity data, the temperature depth profile for November indicated large variations in surface samples (9 - 11 °C) followed by a decrease in temperature with depth. Below 20 – 60 m, the water had a relatively stable intermediate temperature (12.8 °C). A marked change occurred at 60 metres, below this value the temperature decreasing with increased depth to a stable value of 11.9 °C below 90 metres. At 80 m, another “step” in the temperature profile was observed. These marked changes were also reflected in the oxygen profile. In general, the dissolved oxygen concentration in November decreased with depth from an average concentration of 8.6 ml l⁻¹, above 10 metres, to 1.9 ml l⁻¹ (30 % saturation²) below 90 m, with two marked changes in oxygen concentration at 60 and 80 m, respectively (Figure 12).

In April, the salinity in surface waters ranged from 18.2 to 20.1 (Figure 13) with an average salinity in the top 10 m of the water column of 18.7. This was followed by an increase with depth to a stable value of 27.2 below 100 m (Figure 13). The vertical temperature profile from April indicated an initial increase with depth (0 to 47 m). At 47 m depth, the trend was reversed, the temperature decreasing slowly with increasing depth. This change, located at approximately 50 m, was also observed in the oxygen profile. The dissolved oxygen data decreased throughout the water column from an

² The % saturation was calculated using the Weiss equation (for details see Weiss, 1970). Calculations were based on averaged data from the surface and deep water, from both seasons, respectively.

initial average value of 9.2 in surface waters, to 1.2 ml l⁻¹ (19 % saturation) below 90 m, with a lower decreasing rate observed below 50 m (Figure 13).

Deep-water renewal is driven by gravitational forces and caused by overlying waters being denser than that in the deeper basins of the loch. The temperature, salinity and oxygen data from November strongly indicate stratification in the water column, with a warm, less dense surface layer about 10-15 m in thickness. Within this layer, estuarine circulation would develop.

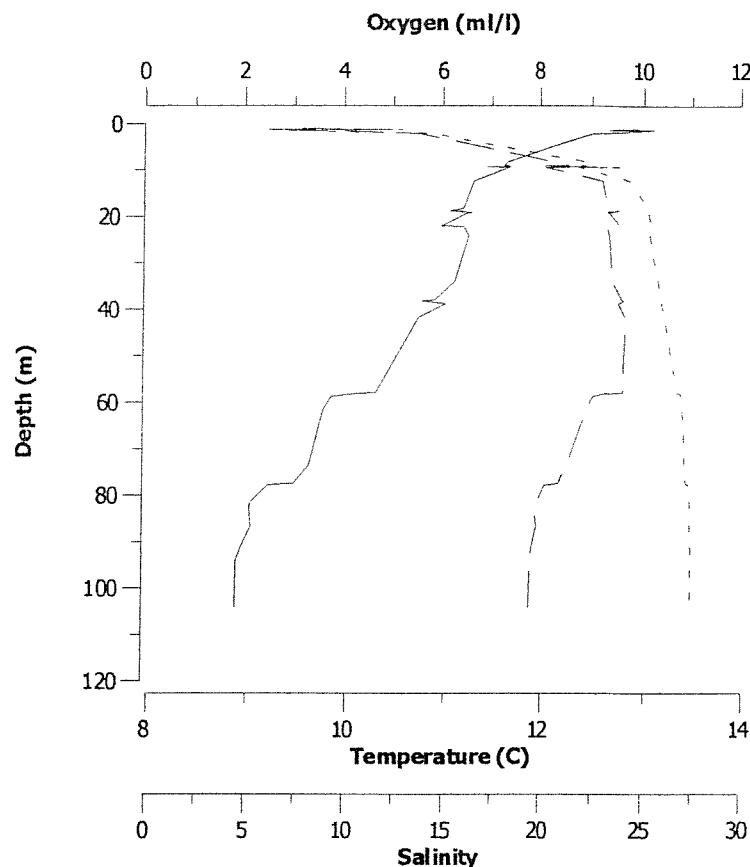


Figure 12. Oxygen (solid line), temperature (dashed line) and salinity (dotted line) data, Loch Etive November 1999.

The initial “step” observed in the oxygen profile for November at about 10 m (Figure 12) is therefore an indication of the existence of a primary pycnocline, separating outgoing brackish water from the more saline incoming seawater. The sharp changes with depth can also be due to variability in oxygen concentrations across the loch at these depths.

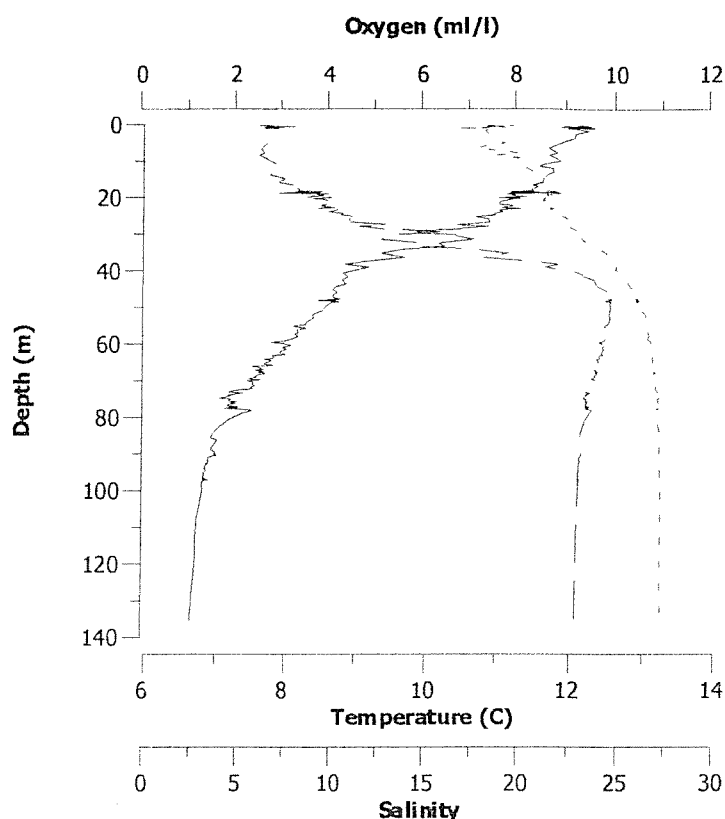


Figure 13. Oxygen (solid line), temperature (dashed line) and salinity (dotted line) data, Loch Etive April 2000.

Below this top layer, the temperature remains relative constant from 20 to 60 m, with the presence of a secondary pycnocline at 60 m (this will be denoted the *oxycline*). Due to data processing, assigning the position of the oxycline must be done with caution, as the value obtained would be an average value over a large Loch area. Despite this, it gives a good indication of the different characteristics of the deep water and surface waters. Deep water had a low oxygen concentration, constant high salinity and a low but stable temperature. Below 80 m, the higher temperature and salinity compared to those in surface waters indicate that little or no vertical mixing between these two water masses has recently occurred. The constant temperature and slowly increasing salinity between 20 to 60 metres, however, would suggest that the waters in Loch Etive at this time of the year cannot be considered only as a simple two-layered system. Vertical mixing may take place at the interface between the surface and deep layer through the mechanism of turbulence and molecular diffusion. Vertical mixing could also be enhanced by the formation of internal waves (Stigebrandt, 1976;

Liungman, 2000). This suggests the occurrence at the time of sampling of an intermediate, relatively mixed layer about 40 m in thickness (at 20 to 60 m). In addition to the sharp change at 60 m (oxycline), the change in the oxygen and temperature profiles at 80 m suggests that the water sampled below this depth represents a separate layer of deep water.

Both salinity and temperature profiles in April followed a similar trend to those in November, with similar values recorded in deep water. This indicates the presence of a warm, less dense surface layer, similarly to the situation observed in November. In contrast, the temperature depth profile in April (Figure 13) did not indicate the presence of an intermediate layer, but rather the presence of two stratified bodies of water. The upper, warmer layer was characterised by increasing temperature with depth. A sharp change was observed at 47 m, in parallel with a sharp decrease in the dissolved oxygen concentration. It seems, therefore, that during the April sampling cruise the oxycline occurred at 47 m. The deep water concentration of dissolved oxygen was lower than that recorded by Edwards and Edelsten (1977), who recorded concentrations of 4 ml l^{-1} in the deep water of Loch Etive in April 1974. The annual phytoplankton bloom, occurring at the end of March-beginning of April (Overnell *et al.*, 1996), would lead to increased productivity in the upper water column and an associated flux of organic matter downward. The utilisation of dissolved oxygen in the breakdown of this flux of organic matter, resulting from this bloom would be consistent with the more reducing conditions observed in April, compared to November. This is reflected in the % dissolved oxygen saturation, which decreased from 30 to 19 % in April. Interestingly, during both November and April the oxygen concentration in the bottom waters was low but the water column did not become anoxic.

3.2.2. Comparison of two depth-transects

A detailed understanding of the seasonal changes in the hydrographic conditions of the basin requires a comparison between data from similar water masses. In this section, data from two Autosub depth-transects, made in November and April, respectively (Mission 212, 3rd November 1999 and Mission 227, 6th April 2000), are compared. These two missions were made at similar geographical positions, with M212 covering only the deeper part of the water column and M227 covering both surface and deep parts. Transects were made along the deepest part of the Loch (approximately from WP

5 –27, refer to Figure 7), routes of the two selected Autosub missions being shown in Figure 14. Data were processed as described in Section 3.1.

Oxygen data for these two Autosub missions are plotted against depth in Figure 15. The limited number of data points for the November mission is due to missing of data during recording, residual data presented here corresponding, for each individual sample, to the beginning and the end of the Aqua Monitor sampling period.

The oxygen concentration in November in the top 50 m of the water column shows a large variation, values ranging from 6.8 to 7.5 ml l⁻¹ (n = 23). These concentrations are higher than those obtained from the CTD transects in November. This could be the result of the difference in geographical position and hence water column structure between the depth transect and the sampling location of the CTD samples (refer to Table 2). Compared to the depth transects, the CTD samples were located further northeast and consequently closer to the fresh water source. Similarly, large variations were observed at 80 m depth. This was followed by a rapid decrease in the oxygen concentration below 80 m from an average concentration of 7.2 at 78-80 m (n = 9) to 2.1 ml l⁻¹ at 81-93 m depth (n = 7). The oxygen concentration below 90 m is similar to that observed in Section 3.2.1. (1.9 ml l⁻¹ below 90 m).

Similarly large variation characterises the April data. This confirms the previous suggestion, *i.e.* that a complex stratified system occurs in the upper part of the water column. The average oxygen concentration in surface waters (top 10 m) was 9.3 ml l⁻¹ (n = 82), similar to values shown in the previous section. The average oxygen concentration in waters below 90 m was 1.4 ml l⁻¹ (n = 202), slightly higher than the oxygen concentration shown in the previous section. This difference could reflect spatial variations in oxygen concentrations as a result of changes in the input of organic matter and variations in bottom topography. It is interesting to note that the oxygen concentration in the deep water during each season remains relatively constant, but with a distinct decrease occurring between seasons. This confirms the suggestion that at the time of sampling, although the upper part of the water column displays varied oxygen concentration, there was a deep stagnant layer of water. The small decrease observed in deep water between the sampling occasion would be expected if the sediments act as a sink for the oxygen. Since from November to April no renewal took place, the oxygen concentration of this water mass decreased further between these periods.

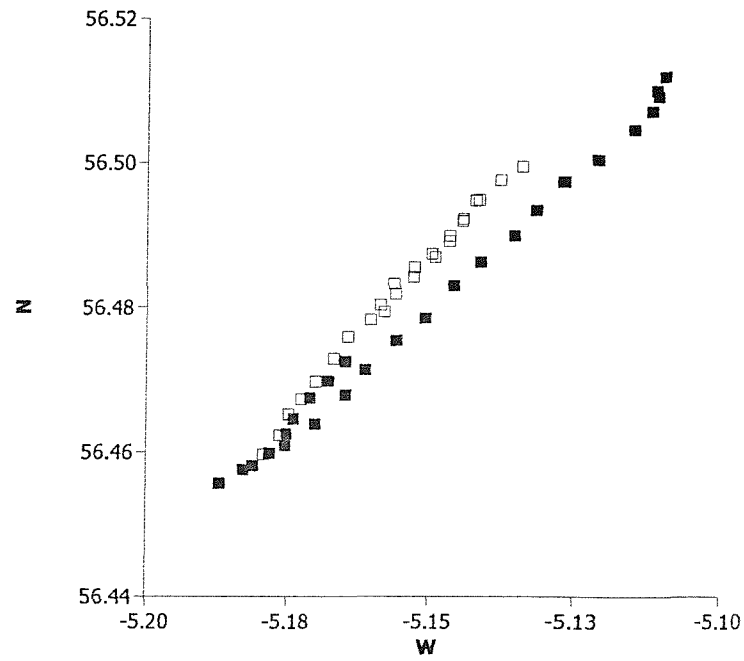


Figure 14. The geographical sampling positions of M212 (November 1999), open squares, and M227 (April 2000), closed squares, Loch Etive.

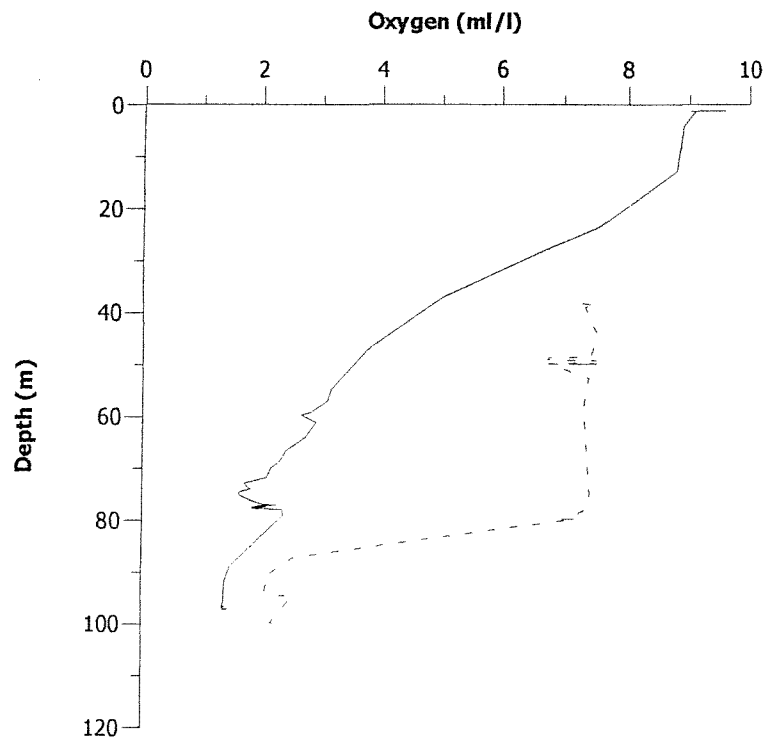


Figure 15. Oxygen data (ml l^{-1}) vs depth (m) for missions M212 (November 1999), dashed line, and M227 (April 2000), solid line, Loch Etive.

3.3. Dissolved manganese

3.3.1. General overview

The dissolved manganese (Mn_d) data from November (total CTD casts and Autosub mission run M212) and April (Autosub mission runs 226-231) are presented in Figures 16 and 17. The concentration for dissolved Mn observed in November ranged from 19.4 to 224 nM (Figure 16). In April the recorded concentrations were higher, from 62.0 to 828 nM (Figure 17). As expected, when compared to open ocean concentrations these values were significantly higher (Landing and Bruland, 1980, 1987; Statham *et al.*, 1998), but match well with concentrations recorded in low oxygen/anoxic systems such as in the Saanich Inlet (intermittently hypoxic) and in the Northwestern Black Sea. In the Saanich Inlet, Jacobs and Emerson (1982) recorded dissolved Mn concentrations of 100 – 500 nM (above the O_2/H_2S interface). In the Northwestern Black Sea, Tankéré *et al.* (submitted) measured dissolved Mn concentrations of 1.2-1350 nM. Compared to permanently anoxic basins, for example Framvaren, where the dissolved Mn concentration has been shown to be in the order of 15 to 20 μM (Jacobs *et al.*, 1985), the concentrations recorded in Loch Etive are lower by two orders of magnitude.

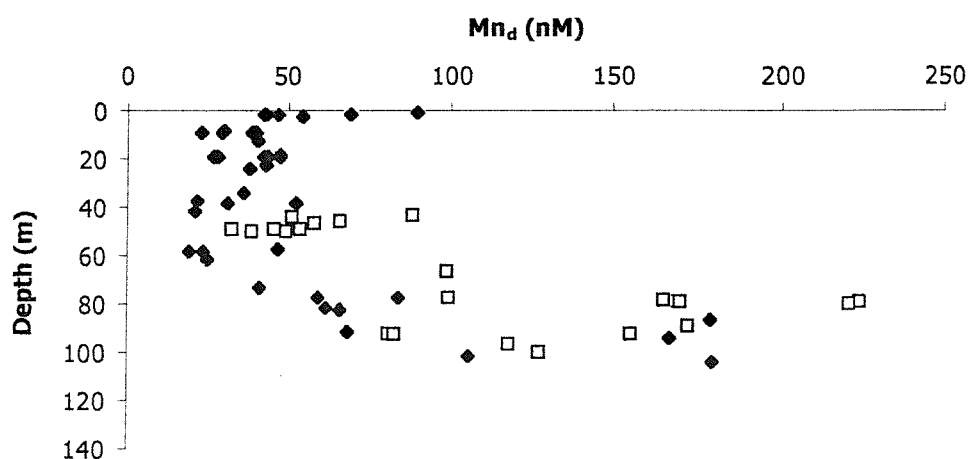


Figure 16. Dissolved Mn (nM) vs depth (m) for total CTD casts (November 1999, closed squares) and M212 (3rd November 1999, open squares), Loch Etive.

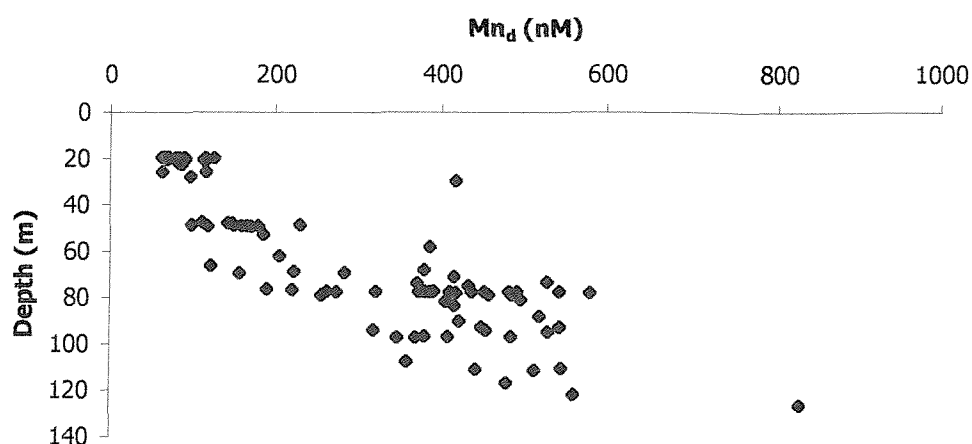


Figure 17. Dissolved Mn (nM) vs depth (m) Loch Etive April 2000 (Autosub M226-231).

3.3.2. Surface water

The processes controlling the dissolved and particulate Mn concentrations in the upper part of the water column will be considered separately from those of the deeper waters. This is because of the stratification occurring within the water column shown by the analysis of the hydrographic parameters (see Section 3.2).

The general depth trend of the dissolved Mn concentrations (Figure 16 and 17) indicates low dissolved Mn concentration in surface waters, values progressively increasing with depth. In November, in the upper layer, the average Mn concentration was 44.5 nM ($n = 20$), with a small dissolved Mn enrichment (89.7 nM) followed by a decrease towards the oxycline at 60 m. In April, the shallowest samples were obtained from Mission 231 where the Autosub followed a route at a constant depth of about 20 m. The average dissolved Mn concentration was 79.8 nM ($n = 22$), similar to surface concentrations observed in November.

Surface enrichment is a characteristic feature of the oceanic distribution of dissolved Mn. This enrichment has been related to several factors such as desorption from aerosols, river runoff and diffusion out from nearshore reducing sediments (Bender *et al.*, 1977; Jones and Murray, 1985; Statham and Chester, 1988).

Atmospheric inputs are known to influence the concentration of dissolved trace metals in coastal waters (*e.g.* Slinn, 1983). For any atmospheric input to have a substantial influence on the dissolved Mn concentration, dissolution of the Mn introduced on the particles must take place. Studies on eolian dust show that dissolution

processes take place on a time scale of minutes once the particles are mixed with seawater (Szekiela, 1978; see also Hodge *et al.*, 1978). Loch Etive receives high annual rainfall (ca 200 cm a⁻¹, Williams *et al.*, 1988) that may result in wet deposition of particles and associated trace metals to surface waters. Hall *et al.* (1996) estimated the wet depositional flux of dissolved Mn to upper Loch Linnhe, a nearby Scottish sea loch located north of Loch Etive. The wet deposition (66 g a⁻¹) was insignificant compared to that of the riverine input of 30000 g a⁻¹. Due to the proximity of the two lochs it is reasonable to extend these estimates also to Loch Etive. Atmospheric inputs, therefore, do not have a major influence on the Mn concentration in Loch Etive.

In order to evaluate the importance of riverine inputs, the correlation of Mn with salinity and sample location was investigated. In November, in the top 10 m of the water column, the salinity ranged from 8.0 to 23.8. Dissolved Mn was significantly correlated with salinity (Pearson correlation: $r = -0.745$, $P < 0.005$; linear regression: $R^2 = 0.55$, $F_{1,11} = 13.71$, $P < 0.005$), with increasing values associated to lower salinity. In deeper water (below 20 m) the salinity ranged from 25.3 to 27.5, with Mn showing a weaker ($R^2 = 0.31$) and opposite correlation with salinity. The Estimated Zero Salinity End Member Concentration (EZSEM) of dissolved Mn, extrapolated from linear regression of data related to the top 10 m, was 79.5 nM. Data of the dissolved Mn concentration in the rivers Awe, Etive, and Kinglass are not available for comparison. However, comparing the results with dissolved Mn data from the adjacent Loch Linnhe, values are within a similar range (Hall *et al.*, 1996; Statham, pers. comm.). The highest surface concentrations of dissolved Mn were observed at station AT07 (89.7 nmol l⁻¹, depth 1.0 m) and station AT10 (69.0 nmol l⁻¹, depth 1.6 m). Station AT10 was located on a transect line starting from the river Glen Liver, while AT07 was located further northeast on the centre line of the loch. The location of these two sampling stations suggests that the surface concentration of dissolved Mn would be influenced by freshwater inflow although sampling in closer proximity to the individual river outflows would be necessary in order to establish the strengths of these sources.

Surface enrichments of dissolved Mn can also be produced as a result of diffusion of Mn from reducing nearshore sediments (Bender *et al.*, 1977). Since Loch Etive is a predominantly reducing system, release from very shallow reducing sediments may influence the surface concentrations, but such impact would be expected to be localised.

3.3.3. Deep water

In November, the concentration of dissolved Mn in the deep water, below the oxycline at 60 m, varied from 25.1 at 62 m to a maximum of 224 nM at 80 m, with an average concentration of 120 nM ($n = 23$). In April, the dissolved Mn concentration from water sampled below the oxycline (47 m) varied from 111 nM at 47 m to a maximum of 828 nM at 126 m, with an average concentration of 358 nM ($n = 67$). Compared to surface concentrations, therefore, deep-water concentrations were higher with an eight-fold increase at certain depths.

In an oxygenated system Mn reduction is not likely to take place, unless there is the presence of micro-reducing zones (see the next section). Therefore, mechanisms whereby high dissolved Mn concentration in deep waters is expected are (1) sediment inputs, and (2) resuspension of particulate matter with particulate Mn being reduced in-situ in the water column. Several previous studies (*e.g.* Hunt and Kelly, 1988; Aller, 1994; Thamdrup, 1994a,b) have verified that reducing sediments may act as a source of dissolved trace metals. Due to the hypoxic conditions of the water column the bottom sediments in Loch Etive are likely to be reducing. During the decomposition of organic matter, therefore, particulate Mn in the sediments would undergo spontaneous reduction to form dissolved Mn(II). Once reduced, Mn can cycle internally in the sediments (Section 1.3, Figure 5), or be remobilised and returned to the water column by advective sediment-water exchange, bioturbation or diffusive processes (Hunt and Kelly, 1988). The concentration of pore water Mn(II) in the bottom sediments of Loch Etive has been investigated by Overnell *et al.* (1996). The authors recorded Mn(II) pore water concentrations of 400 μM . These concentrations are higher than those generally reported for marine sediments (*e.g.* Sugai, 1987). In addition, as the concentrations of dissolved Mn recorded in this study were 2 orders of magnitude lower, it is suggested that the sediment in Loch Etive can act as a source of dissolved Mn(II) to the overlying water column.

The high dissolved Mn(II), moreover, could reflect resuspended particulate Mn that is reduced in-situ in the water column (Balls, 1990). In order to test this hypothesis it is necessary to consider the variation of total Mn concentration (leachable and dissolved) with depth. The variation of total Mn with depth is presented in Figures 18 and 19: the trend follows the same pattern as observed for dissolved Mn. This leads to the suggestion that the sediments are acting as a source of dissolved Mn to the water column. Furthermore, the results imply that although the sediments also are acting as a

source of particulate Mn, a fraction of the particulate Mn is in fact re-precipitated Mn from the water column. This suggests that deep-water entrapment from a sedimentary source is likely to be the controlling mechanism in producing the observed trend in the dissolved Mn concentration (see further Section 3.4.3).

A further point that should be noticed (see Figure 16, 17 and also Figure 18 and 19) is the greater noise in the Autosub data compared to the CTD data. This is due to the broader area sampled by the Autosub, inferring spatial variability in the Mn concentrations (see further the following section).

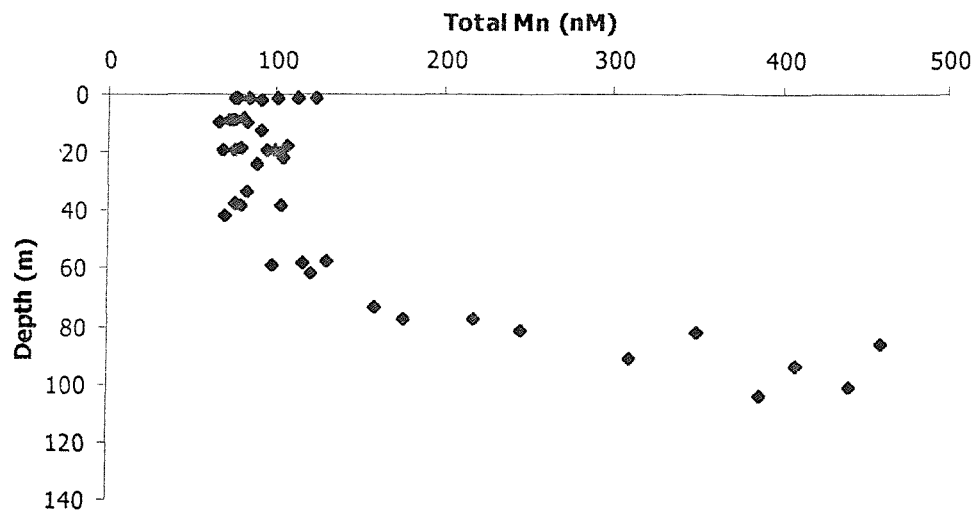


Figure 18. Total Mn (nM) vs depth (m), Loch Etive Nov 1999 (CTD casts).

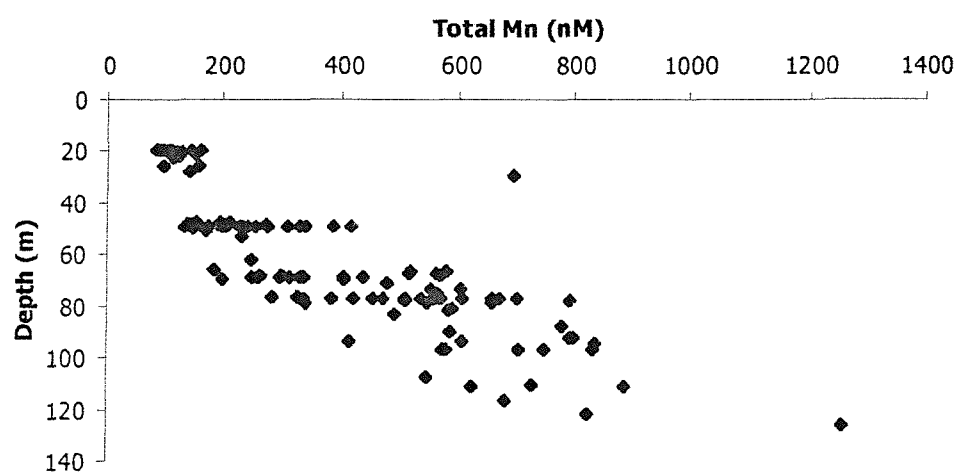


Figure 19. Total Mn (nM) vs depth (m), Loch Etive April 2000 (Autosub M226-231, AqM samples).

Comparison of Mn data from AqM samples from November and April

In order to compare trace metal data from the same water mass, in the following section the results from two depth transects (M212, 3rd November 1999 and M227, 6th April 2000, see Section 3.2.2) are compared. The dissolved Mn versus depth for M212 and M227 are presented in Figure 20. In November (M212), the average dissolved Mn concentration varied from 43.7 nM at 50 m ($n = 5$) to 127 nM at 100 m ($n = 12$). In general, the concentration of dissolved Mn above the oxycline (60 m) was lower (average concentration 53.4 nM ($n = 9$)) than for the samples taken below 60 m (average concentration 143 nM ($n = 12$)). Hence, the trend shown by data from November is similar to that previously observed, *i.e.* increasing dissolved Mn with depth. There is, however, a large scatter in the data, especially in deep water, that characterised also the April data (M227) where no clear trend was recognised. This could reflect both a combination of lack of analytical precision and real differences between samples, arising, for example, from variations in the input of organic carbon, bottom topography, bioturbation and the presence of micro-reducing zones.

A reliable estimation of the analytical precision of data is provided by the % standard deviation (for details see Table 5, Chapter 2). This value is 10%, showing satisfactory analytical precision and placing more importance on real differences for justifying the variation among data.

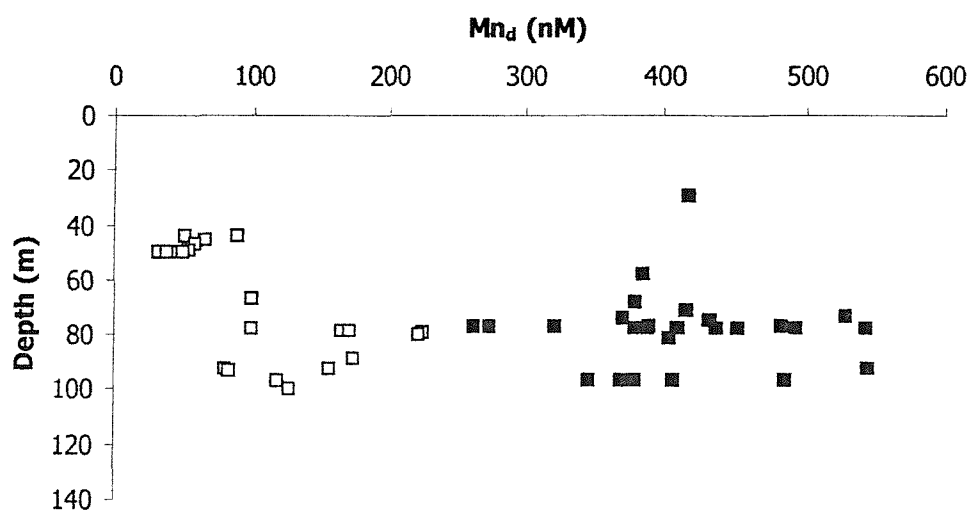


Figure 20. Dissolved Mn (nM) vs depth (m) for M212 (3rd November 1999, open squares) and M227 (6th April 2000, closed squares), Loch Etive.

The input of organic carbon has an indirect effect upon the oxygen utilisation and consequently on the oxygen content of the water column (Aller, 1994; Stumm and Morgan, 1996). Hence, the input of organic carbon plays an important role in the recycling efficiency of Mn, implying that low input of organic carbon leads to higher dissolved oxygen concentrations. In such areas, therefore, a deeper section of the bottom sediment would be oxidising and hence retaining Mn(II) in the form of particulate Mn(IV). In contrast, where the input of organic carbon is high Mn(IV) would be reduced, releasing Mn(II) from the sediments.

Alternatively, variations in bottom topography could explain the observed variability. This factor is closely linked to the above discussed mechanism since it plays an important role in controlling the accumulation of organic matter and fine-grained sediment to the deepest part of the Loch (Overnell *et al.*, 1996). Particulate matter controls the behaviour of many trace metals in a variety of marine environments (Balls, 1990; Santschi *et al.*, 1990). As such, under reducing conditions, areas with high amount of fine-grained sediments and accumulated particulate matter act as a source of dissolved Mn to the overlying water column.

The exchange of solutes between sediment and water column is influenced by bioturbation, particularly by the burrowing habit of benthic macrofauna (Aller, 1988). Several studies show that this results in enhanced oxygen consumption (*e.g.* Koike and Mukai, 1983; Ziebis *et al.*, 1996) and therefore increases the fluxes of metals across the sediment-water interface (Santschi *et al.*, 1990). Such benthic organisms produce characteristic bottom surface features. In Loch Fyne, a survey of the bottom conditions was performed using a towed sledge carrying a video recorder (Howson and Davies, 1991). This showed well-developed burrows and mounds. A similar survey in Loch Etive would help in order to determine the importance of bioturbation, as well as establishing small variations in bottom topography as controlling factors producing the observed scatter in the dissolved Mn concentration.

The presence of micro-reducing zones, *i.e.* localised zones with reducing conditions, is a factor that has been little investigated. Such zones might exist for example within marine aggregates and may produce localised reducing conditions in oxidising parts of the water column. In order to establish the impact of micro-reducing zones further laboratory investigations would be required.

3.4. Particulate Mn

3.4.1. General overview

The concentration of Mn in suspended particulate matter (SPM) (Mn_p) from November (total CTD casts) and April (Autosub mission runs 226-231) are presented in Figures 21 and 22. The concentrations of particulate Mn show a similar trend to the depth profiles of dissolved Mn. In November, the particulate Mn concentration ranged from 23.2 to 334 nM ($9.76 \times 10^2 - 2.63 \times 10^4 \mu g g^{-1}$) (Figure 21). In April, the observed surface concentrations were lower, varying from 15.7 nM in surface waters to 428 nM in deep waters ($1.17 \times 10^3 - 7.70 \times 10^4 \mu g g^{-1}$) (Figure 22). During both seasons, the lowest concentrations were recorded in surface waters. In addition, similarly to the trend for dissolved Mn, large variability was observed in the top 20 m of the water column. The concentrations of particulate Mn were equivalent to concentrations recorded in the Drammensfjord (Öztürk, 1995). Öztürk (1995) recorded highest particulate Mn concentrations ranging from 240 to 1400 nM depending on the season. Comparing the recorded values in the present study to the particulate Mn concentrations recorded in shale (for total Mn, $850 \mu g g^{-1}$, IM HCl leach (Statham, pers. comm.)), deep water concentrations are concentrated in Mn relative to estimates of the Mn in background sediments. Between the two seasons, with isolation of deep water, the concentrations of Mn increased. Surface water concentrations are in the range of total Mn shale concentrations.

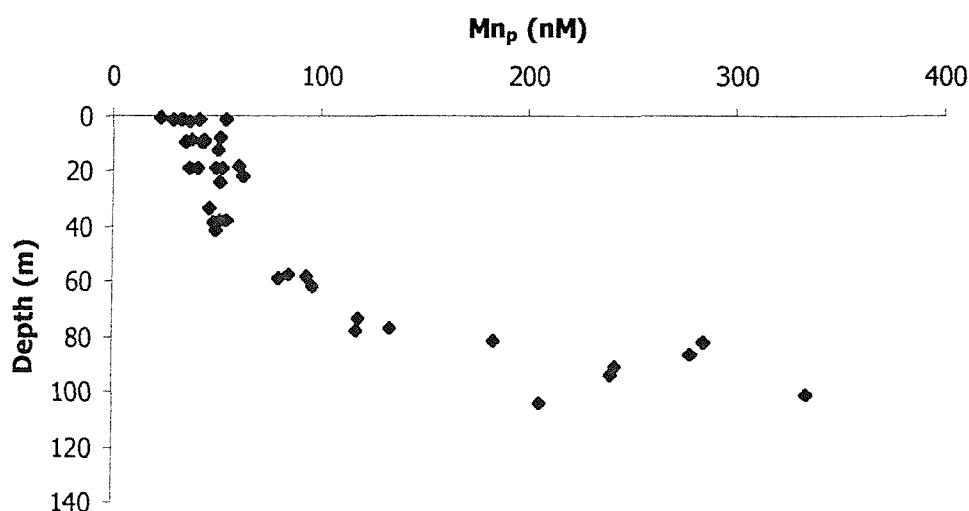


Figure 21. Particulate Mn (nM) vs depth (m) Loch Etive November 1999 (CTD casts).

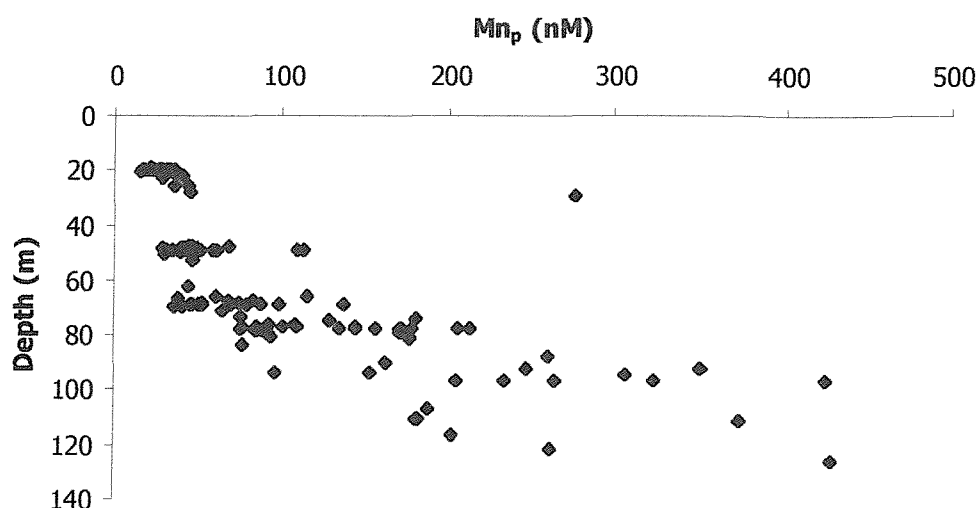


Figure 22. Particulate Mn (nM) vs depth (m) Loch Etive April 2000 (Autosub M226-231, AqM samples).

3.4.2. Surface water

In surface water the depth trend of the particulate Mn concentration (Mn_p) (Figure 21 and 22) is similar to that observed for the dissolved Mn, low surface concentrations increasing with depth. In November, large variation in Mn_p was observed in the top 10 m of the water column with an average concentration of 39.0 nM ($n = 13$). This was followed by an increase in the concentration of Mn_p towards the oxycline, located at 60 m. In April, the Mn_p concentration of the surface samples taken at 20m were comparable to those recorded in November, with an average concentration of 19.7 nM ($n = 22$) increasing towards the oxycline.

Particulate Mn concentration is influenced by a large number of processes, including the introduction of terrigenous material, scavenging and/or resuspension of Mn enriched particles, type of particles constituting the SPM and changes in dissolved Mn concentrations. Among these factors, the input of river-borne terrestrial material, with high SPM load, is likely to be an important source particularly to surface waters. SPM concentrations versus depths for November and April are shown in Figure 23. For both seasons, a large variation in SPM is observed throughout the water column. When the SPM concentrations are compared to the Mn_p concentrations for samples in close vicinity to river-mouths no clear trend is observed. Consequently, other factors would be suggested to dominate in producing the observed concentration trends.

The seasonal changes in the concentration Mn_p may have been influenced by changes in the particles constituting the SPM. The Mn_p concentrations in surface waters were higher in November compared to April, this trend being also reflected in the concentration of SPM. The high Mn concentration observed in autumn could reflect the presence of a larger lithogenous component in the SPM followed by scavenging of sediment-derived Mn (Tappin *et al.*, 1995). On the other hand, the spring phytoplankton bloom would dilute this component, weakening the lithogenous signal. Hence, the lower Mn_p concentrations recorded in surface waters in spring could indicate increasing organic material constituting the SPM. Data on contributions from lithogenous and organic material in the SPM are not available and therefore further investigation would be required to assess the effect of scavenging of sediment-derived Mn.

In oxygenated surface water, dissolved Mn is readily oxidised to form particulate Mn. The amount of particulate Mn present in the water column, therefore, is indirectly influenced by the amount of dissolved Mn present. Dissolved Mn assumes biological importance as it is taken up by species such as *Phaeocystis* spp. (Lubbers *et al.*, 1990, Schoemann *et al.*, 1998) and, consequently, the occurrence of a spring bloom would reduce the overall dissolved Mn concentration in surface waters. Dissolved Mn concentrations in surface waters in April were not different to those recorded in November (see Section 3.3.2). This comparison, however, was constrained by the lack of samples collected above 20 m in April.

3.4.3. Deep water

In November, Mn_p concentration in deep-water, *i.e.* below the oxycline at 60 m, showed a clear, increasing trend with depth. The concentration varied from 96.3 nM at 62 m to 334 nM at 101 m, with an average concentration of 204 nM ($n = 11$). In April, the Mn_p concentration from water below the oxycline (47 m) varied from 180 nM at 48 m ($n = 5$) to a maximum of 428 nM at 126 m, the average being 115 nM ($n = 98$).

Compared to the surface (Section 3.4.2), the deep-water concentrations were generally one order of magnitude higher. Three plausible mechanisms could explain this result: (1) input from terrestrial material, (2) resuspension of Mn-enriched particles, and (3) sedimentary source and scavenging of Mn in the water column.

The importance of terrestrial material was discussed in Section 3.4.2: this source would be expected to have a minor influence on the Mn concentrations trend in deep water, although it cannot be excluded that such input could affect the scatter in the data.

In order to investigate the importance of resuspension of Mn-enriched particles it is necessary to consider the SPM distribution in relation to that of the particulate Mn concentration. If the SPM is the major controlling factor in producing the observed profile the trend with depth of SPM should be similar to that of the particulate Mn, whereas, as shown in Figure 23, the two sets of data are clearly not related.

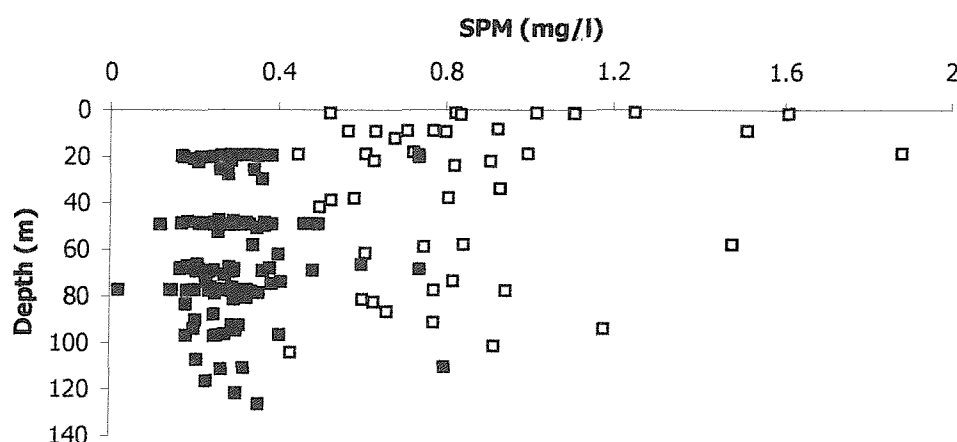


Figure 23. SPM (mg l^{-1}) vs depth (m) for all CTD data 2nd November 1999 (open squares) and collected Autosub data M226-M231, 6-7th April 2000 (closed squares), Loch Etive.

Data on the concentration of solid phase from sediments in the deep basin of Loch Etive has been previously recorded by Overnell *et al.* (1996): the extractable fraction of Mn from these sediments was about 1% (wt. %). Results from this study give comparable values for November, 1.6% from samples below 60 m (mean concentration $1.57 \times 10^4 \mu\text{g g}^{-1}$, $n = 11$), but different results for April, 5.2% from samples below 95 m (mean concentration $5.22 \times 10^4 \mu\text{g g}^{-1}$, $n = 12$). Since in April the wt. % obtained in this study is as much as five times larger compared to the wt. % obtained from the extractable fraction of Mn in the sediments, the concentration of particulate Mn recorded in the deep waters cannot be explained only by resuspension of Mn-enriched particles.

The third mechanism whereby high particulate Mn can be observed in deep water is through a sedimentary source of dissolved Mn followed by scavenging of Mn in the water column. This mechanism was discussed in Section 3.3.3 (see also Section

1.3): the reducing conditions in the bottom sediments in Loch Etive at the time of sampling may cause particulate Mn-oxides to undergo reduction to form the more soluble Mn(II). The reduced Mn(II) can be remobilised and returned to the water column by advective sediment-water exchange. As the Mn(II) reaches more oxygenated waters, some will be spontaneous oxidised to form Mn-oxides. Consequently, the release of Mn from the sediments will enrich the bottom water in dissolved and particulate Mn that can be entrapped and transported to surface waters by diffusion processes.

3.5. Manganese oxidation rates

Data from the present study, i.e. two sampling occasions in November and April, do not provide a suitable time base for rate calculations. Hence, in order to give an indication of the time scale of the Mn-oxidation processes, this section considers results from a study by Overnell *et al.* (in press). The authors measured the concentrations of dissolved and particulate Mn and dissolved oxygen as a function of depth at two stations in the upper basin of Loch Etive, over a 17 months period (including the time frame for the present study). By assuming steady state and the return of solid phase manganese to the sediment, the authors applied rate constant as calculated by Yeats and Strain (1990) and subsequently estimated the rate of oxidation of dissolved Mn(II) in Loch Etive. The rate expressions used by Yeats and Strain (based on work by Stumm and Morgan, 1970) were:

$$-d[\text{Mn}^{2+}]/dt = k[\text{Mn}^{2+}][\text{Mn}_p][\text{O}_2] \quad (1)$$

$$-d[\text{Mn}^{2+}]/dt = k_1[\text{Mn}^{2+}][\text{O}_2] + k_2[\text{Mn}^{2+}][\text{Mn}_p][\text{O}_2] \quad (2)$$

Both expressions contain an autocatalytic term for the Mn particulate concentration. Several studies investigating manganese oxidation (*e.g.* Emerson *et al.*, 1979; Tebo *et al.*, 1984; Moffett, 1997) have found that the rate of manganese oxidation is too fast to be purely accounted for inorganic mechanisms hence inferring that biological catalysis must be occurring. The autocatalytic term, therefore, may represent a bacterial mediated oxidation process on particle surfaces. The results from the study by Overnell *et al.* (in press) indicate that these rate expressions also can be applied to Loch Etive with a calculated manganese oxidation rate of the order of 2.2 – 5.4 mmol.m⁻².d⁻¹.

Using the calculated oxidation rates the authors calculated the *removal time* (dissolved manganese concentration divided by the oxidation rate). This typically decreased from approximately 25 days near sill depth to 7 days near the bottom sediments. As seen from the hydrographic data both in the present study and by Overnell *et al.* (in press), the deep water of Loch Etive did not overturn between the sampling occasions, thus verifying that the time scale of the overturning process (month-year) is much slower than the manganese removal time (days). This suggests that the overall removal and production of dissolved Mn in the water column is in an almost steady state. This steady state would be maintained by an increase flux of dissolved Mn from the sediment as the oxygen concentration decreases producing more reducing conditions. The increase of Mn would in turn result in increasing Mn concentration in the water column, thus producing an increase in the overall Mn inventory.

Although the time series measurements at a single station gives suitable data for rate calculations, no information on the spatial variation of the manganese and oxygen concentration within the loch can be obtained. The present study presented high resolution spatial measurements of the Mn concentration and it would consequently be expected that similar calculations using this data would show lateral variability, not observed using regular sampling techniques.

3.6. Dissolved and particulate Co

3.6.1. General overview

The dissolved cobalt (Co_d) data from November (total CTD casts) and April (Autosubmission runs 226-231) are presented in Figures 24 and 25. In November, the concentrations of dissolved Co observed in Loch Etive ranged from 35 to 288 pM (Figure 24). In April, concentrations fell within a similar range, varying from concentrations below detection limit (22 pM) to a maximum of 246 pM (Figure 25). These concentrations are generally higher than those previously recorded in the open ocean. In the Northeast Pacific, Martin (1985) recorded Co_d concentrations in the range of 60 – 100 pM, decreasing with depth to less than 50 pM. In the Sargasso sea, Jickells and Burton, (1988) reported Co_d concentrations 20 - 40 pM in surface waters decreasing rapidly with depth to less than 15 – 20 pM. More recently, Wong *et al.* (1995) recorded similarly low concentration in the western Philippine Sea, with surface values of 95 pM decreasing to less than 25 pM below 1000 m. Values recorded in this study are higher

than those mentioned so far but similar to concentrations recorded in the Mediterranean and the Strait of Dover. Huynh-Ngoc and Whitehead (1986) recorded Co_d surface concentration in the Mediterranean ranging from 80 to 250 pM, decreasing to 30 – 50 pM in deep water; James *et al.* (1993) reported mean Co_d concentrations in the order of 230 pM.

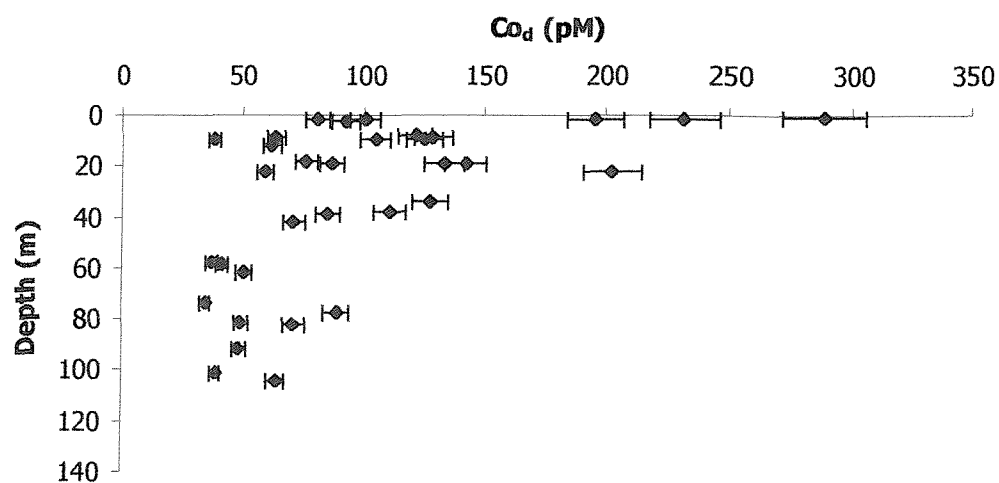


Figure 24. Dissolved Co (pM) vs depth (m) Loch Etive, November 1999 (CTD casts). Error bars representing $\pm 6\%$ as based on the precision analysis.

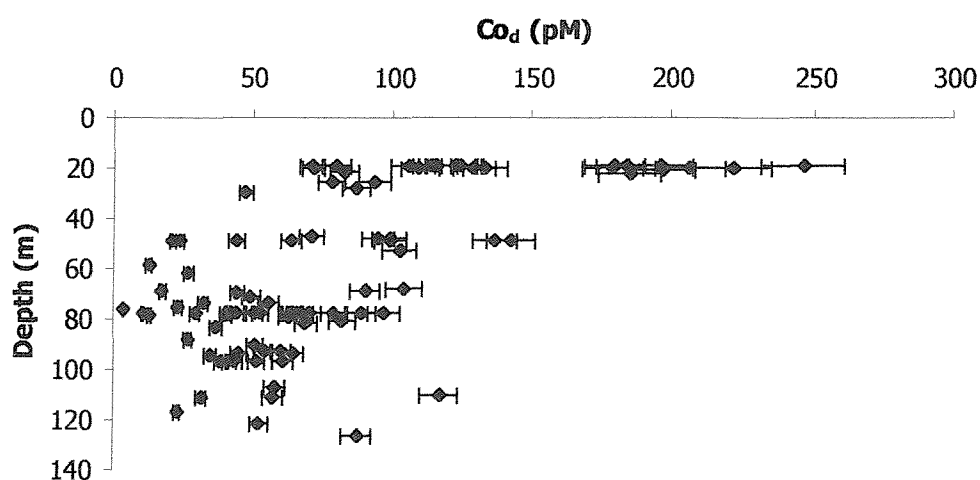


Figure 25. Dissolved Co (pM) vs depth (m) Loch Etive, April 2000 (Autosub M226-231, AqM samples). Error bars representing $\pm 6\%$ as based on the precision analysis.

3.6.2. Surface water

The Co_d concentration in surface water displayed large variations during both sampling periods. In November, Co_d concentrations in the top 5 m varied from 81 to 288 pM, the concentration in the top ten metres being 131 pM ($n = 12$) and decreasing at the oxycline to 43 pM ($n = 3$). Similarly, large variations were observed from the surface samples collected in April, the Co_d concentration varying from 71 (samples from 19–20 m, $n = 22$) to 246 pM. The Co_d concentration decreased towards the oxycline to an average of 75 pM (at 47–49 m, $n = 11$). In April, moreover, large variations were observed in the Co_d concentrations at intermediate depths. Considering the range of spatial environments sampled, and the satisfactory analytical precision (% standard deviation, 6% for the Co analysis), these variations may reflect spatial variability in the concentrations of Co in this Loch system. This was also reflected in the Mn data (see Section 3.3.3). Processes that can determine the trend observed in surface water include external sources, such as freshwater and atmospheric inputs, biological processes and mixing processes.

Loch Etive receives freshwater inputs from two main rivers, the River Etive and the River Awe, in addition to large annual rainfall. Although no data of dissolved Co for these rivers are available, the variation of dissolved Co concentration with salinity shows pronounced, negative correlation ($R^2 = 0.42$ in November and 0.44 in April, respectively), with higher dissolved Co concentrations observed for samples with lower salinity. This Co-salinity “mirror-image” relationship has previously been described by Knauer *et al.* (1982), which explained higher Co_d concentrations in surface waters as a result of inputs from continental weathering (see also Kremling and Hydes, 1988). In this study, a more detailed investigation into the origin of samples with highest Co_d did not show any clear trend with vicinity to freshwater inputs. Hence, in order to establish the strengths of this source, further studies of the Co_d concentrations of the fresh-water sources to Loch Etive would be required.

Surface enrichment in the concentration of Co_d has also been linked to atmospheric inputs, for example in the Western Philippine Sea (Wong *et al.*, 1995) and in the Sargasso Sea (Jickells and Burton, 1988). Loch Etive receives high annual rainfall that in turn may lead to the deposition of associated trace metals of natural and/or anthropogenic origin. Although the data obtained in this study do not allow estimation of the relative importance of these sources, their influencing role in Loch Etive cannot be excluded.

As the central metal cofactor in vitamin B₁₂ Co is an essential micronutrient for organisms (Carlucci and Cuhel, 1977; Swift, 1981) and thus Co_d should be taken up by phytoplankton. This nutrient-like behaviour of Co has previously been observed in the northeast Pacific (Martin, 1985). Such a removal process in Loch Etive should be largest during the spring, *i.e.* during the annual phytoplankton bloom, resulting in a lower Co_d concentration in surface waters observed during this time. Following uptake, regeneration in deep water should occur as a result of the breakdown of organic matter. Shallow regeneration of Co has been suggested to take place in the Philippine Sea (Wong *et al.*, 1995). In this study, Co_d concentrations were not lower in April than in November, suggesting that if the phytoplankton uptake process does occur, the rate of surface inputs may exceed removal. Below the oxycline, the average concentration increased slightly between the two seasons, mean values being 56 pM (n = 8) in November (below 60 m), and 78 pM (n = 63) in April (below 47 m). Since these concentrations are similar, it is difficult without nutrient data to assess whether or not a regeneration process is taking place in deep water.

A third mechanism whereby decreasing Co concentrations with depth would be expected is through the process of mixing. Thus, the observed decreasing concentration in dissolved Co may be the result of mixing processes between high Co concentrations surface waters and deep water with low Co concentrations. As such, the decreasing depth trend is not necessarily explained only by invoking strong biochemical control.

3.6.3. Deep water

In November, the concentration of dissolved Co in the deep water below the oxycline showed an average concentration of 56 ± 14 pM (n = 8). Despite some variations the concentration remained low but stable with depth. In April, the concentration of dissolved Co from water samples below the oxycline showed an average concentration of 78 ± 20 pM (n = 63). Compared to surface water, the deep water concentration were lower, but no important changes in the Co concentration at depth are observed from November to April. Concentrations in deep water were similar to those recorded previously in open ocean areas (see Section 3.6.1).

Main interpretations of the trend observed in deep water could be (1) that addition rates and removal rates are of equal magnitudes and/or (2) that not truly dissolved Co is being measured.

Concerning the former interpretation, inputs of dissolved Co in deep water can originate from desorption of Co from Mn-oxides, regeneration of Co associated with organic matter, plus a possible influence of microreducing zones.

Scavenging of Co onto Mn-oxides has been suggested to control the behaviour of Co_d in the water column of the Baltic Sea (Kremling, 1983). Under oxic conditions Co shows a strong adsorption affinity for Mn-oxides (Murray and Brewer, 1975; Murray and Dillard, 1979). Cobalt adsorption and oxidation occurring on the surfaces of Mn-oxides in the water column could therefore be a significant process for Co_d removal. Cobalt associated with Mn-oxides would be released under the prevailing reducing conditions in the sediments, acting as a source of dissolved Co. The underlying mechanism of this oxidation process, however, is not clearly understood. Earlier studies suggest that the oxidation of Co_d could occur spontaneously through surface catalysis (Murray and Dillard, 1979). Thermodynamically, oxidation of Co(II) by Mn-oxides is a spontaneous process (Burns, 1976). More recent studies, however, have linked the process to microbial oxidation of Mn(II), suggesting that Mn(II)-oxidising microorganisms could directly catalyse the oxidation of Co(II): $2\text{Co}^{2+} + 1/2\text{O}_2 + 3\text{H}_2\text{O} \rightarrow 2\text{CoOOH} + 4\text{H}^+$. Alternatively, Co(II) oxidation could occur indirectly through a coupled redox reaction, whereby attached Co(II) to the surface of Mn-oxides would lower the activation energy required for the oxidation process (Lee and Tebo, 1994). Both mechanisms require a close relationship between Co and Mn. In this study, the relationship between these two variables was investigated for both seasons, assuming that if Co_d is associated with Mn-oxides an inverse relationship between Co_d and Mn_p should occur. In November, a weak correlation ($R^2 = 0.30$) was found for samples above the oxycline with higher Mn_p concentrations associated with lower Co_d , whereas in April no significant correlation was found. Similarly, in April, no correlation was observed when plotting Co_d concentration versus Mn_p . In November, a weak, positive correlation ($R^2 = 0.36$) was observed for samples above the oxycline. A more direct test for solid phase removal mechanisms is to consider the correlation, if any, between particulate Co and Mn. In November, the particulate Co concentration ranged from below detection limit (22 pM) to 274 pM. Data were very scattered and no clear trend was observed. In April, the concentrations ranged from below detection limit to 80 pM. Similarly to the November data, no trend with depth could be seen. Therefore, for both seasons the correlation with particulate Mn was investigated but no correlation was observed. The weak correlation between these two variables suggests

that the addition processes in the deep water cannot be due only to desorption processes. An additional process that is expected to occur in surface water is the uptake of Co as a micronutrient. In deep water, Co associated with organic matter is released as the organic matter is broken down, resulting in a source of dissolved Co in deep water.

Another important source of Co in deep water could be through a benthic source. However, a comparison of the dissolved Co concentration in deep water between the two seasons indicates no significant increase. Thus, if Co is being released as a result of Mn-oxide reduction, either it does not leave the sediments or it is rapidly removed onto the Mn-oxides in the water column near to the seafloor. Regarding the first suggestion, few studies have in detail investigated the Co fluxes from sediments. As such it is difficult to hypothesise the exact mechanism by which Co may be trapped. Heggie and Lewis (1984) studied Co in pore waters of marine sediments and found that Co may precipitate as insoluble Co-sulphides. From results from thermodynamic equilibrium modelling, however, this appears to be unlikely (Landing and Lewis, 1991). An alternative suggestion is through co-precipitation with Fe-sulphides (Lewis and Landing, 1992) or, possibly, through any Fe-oxide phase forming in the surface sediments. The Co removal onto Mn-oxides near the seafloor implies a correlation between the particulate Mn and Co, but, as discussed previously, in the present study no correlation was observed. Consequently, in order to further understand these mechanisms, a more detailed investigation of the behaviour of Co near the sediment-water interface in the Loch is required.

The main removal process of dissolved Co would be expected to be microbial oxidation. This process has been suggested to be of importance above the oxic-anoxic interface in areas such as the Saanich inlet (intermittently anoxic) and Framvaren (Tebo *et al.*, 1984). Recent studies have shown that Co can be oxidised by microbes, independently of the presence of Mn-oxide surfaces (Lee and Fisher, 1993; Lee and Tebo, 1994). The distinction between microbial oxidation rather than adsorption process is of geochemical significance since if the oxidation of Co occurs by a microbial pathway it will depend mainly on the abundance and activity of such organisms rather than the abundance of Mn-oxides. In the present study no correlation between Co and Mn was observed, suggesting that in hypoxic areas the dissolved Co concentration is controlled by a mechanism independent from the presence of Mn-oxides. This supports the results from the study by Lee and Fisher (1993), who found no increase in the formation of particulate Co as a result of increased concentration of particulate Mn.

Considering the uncertainties in estimating the above outlined addition and removal processes, it is not possible to establish if these are of equal magnitude.

Concerning the second explanation of the Co trend observed in deep water, in the present study it was assumed that the recorded Co was in a truly dissolved form. If the dissolved Co was present in a colloidal form or organically complexed, Co would neither be biological available, nor available for adsorption onto Mn-oxides. Few studies have examined the speciation of Co in seawater. Zhang *et al.* (1990) determined the Co-complexing capacity for samples from the Scheldt Estuary and the Menai Strait and found that a highly variable fraction (between 46 and 100 %) of the total dissolved Co concentration occurred as organic complexes. Complexes of small size could pass through a 0.45 μm filter and consequently would be recorded as dissolved but with the implication that this fraction would be present in a biological unavailable form.

3.7. Manganese and cobalt correlations

The correlation between Co and Mn was discussed in Section 3.6. In the present study, a comparison between these two elements in deep water did not show any correlation and only a slight correlation was observed in the oxic part of the water column for dissolved samples from November. Assuming a solid phase removal mechanisms, a correlation would be expected between particulate Co and Mn. This was investigated (see Section 3.6.3), but no correlation was observed. Since several previous studies have concluded that the geochemistry of Co and Mn are closely related (*e.g.* Lee and Tebo, 1994; Moffett and Ho, 1996), it is necessary to consider the reasons for the observed decoupling observed in Loch Etive.

To the author's knowledge this is the first time that detailed data investigating this correlation in a hypoxic environment have been reported. Hence, due to the relatively few previous studies concerning this topic (none specifically looking at Co and Mn in a hypoxic area), the direct comparison is difficult.

One reason for the similarities observed in the geochemical behaviour of Co and Mn could be the result of microbially mediated Co oxidation (Lee and Fisher, 1993). Similarly to the present study, these authors observed no increase in the formation of particulate Co with increasing particulate Mn concentration, suggesting that the formation of particulate Co was directly mediated by microorganisms. Further evidence for a direct cobalt oxidation mechanisms was presented by Lee and Tebo (1994). Their

study gives evidence of the formation of particulate Co by the marine manganese(II)-oxidising *Bacillus* sp. Strain SG-1 in the absence of added dissolved Mn, suggesting a decoupling between the two elements. Moreover, Moffett and Ho (1996) observed a decoupling between Co and Mn in their study carried out in the Sargasso Sea, due to a combination of lower activity of Mn oxidising bacteria and higher biological demand for Co. Considering that Loch Etive is a nutrient rich system, and bearing in mind that the concentrations recorded in this study are higher than those in oceanic areas, the above explanation is unlikely to apply to the present study. Results, however, confirm that a correlation between these two elements would be sensitive to environmental factors. A biological removal mechanism is strongly dependent on factors such as oxygen, temperature and pH. It is therefore assumed that as a result of the hypoxic conditions in Loch Etive the relative importance of such direct removal mechanism would be altered. Furthermore, since in natural environments the concentration of dissolved Mn is orders of magnitude higher than that of dissolved Co, it is likely that if microorganisms as for example the SG-1 were active in the marine environment, Co(II) oxidation could occur simultaneously via both a direct mechanism and an indirect mechanism involving oxidation by Mn-oxides. Further research is required to establish whether in hypoxic systems the environmental conditions would enhance the importance of a direct oxidation mechanism or diminish its importance in favour of indirect oxidation and/or alternative removal mechanisms (See Section 4.1).

3.8. In-situ measurements

In the present study an in-situ technique for the measurement of dissolved Mn in seawater was developed and tested in collaboration with Dr. D. Connelly and Dr. P. Statham. Initial testing was performed using a bench top version of the manifold connected to a spectrophotometer (U-2000) (see Section 2.4). Iron interference and mixing efficiency were investigated, leading to some modifications from the method initially used by Chin *et al.* (1992) (Section 2.4). A modified in-situ chemical analyser was carried on-board the Autosub during the April sampling period. The result from mission 225 is presented in Figure 26. Unfortunately, no bagged samples were obtained using the Aqua Monitor during this mission. The concentration of dissolved Mn, however, ranged from approximately 50 to 700 nM, corresponding well to concentrations recorded during subsequent missions from the Aqua Monitor samples.

The use of the technique with Autosub thus proved highly successful. In the field, the limitation for obtaining trace metal data, remains the difficulties in assuring clean sampling and treatment procedures. As such, the further development of the method used by Chin *et al.* (1992) will greatly enhance the number of reliable trace metal data that can be obtained and hence will enable a more detailed investigation of the behaviour of these elements in the marine environment.

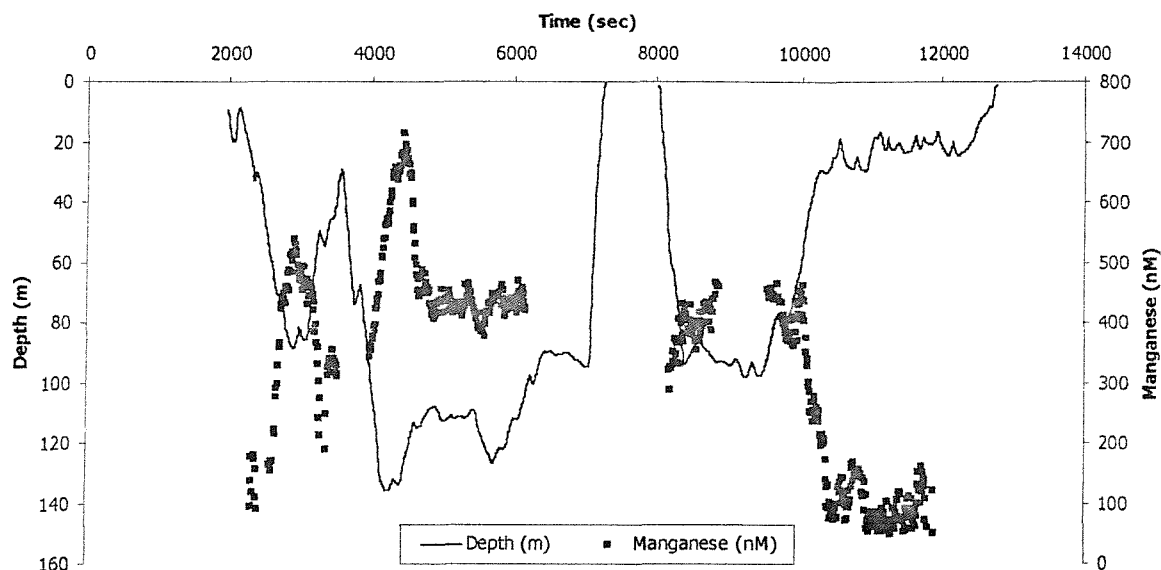


Figure 26. Results from the in-situ chemical Mn-analyser for M225 Loch Etive, April 2000. Data shown are frequency response from the instrument which is inversely proportional to the concentration (right hand Y axis). Missing data points are periods when internal calibration was carried out.

Chapter 4. Conclusions

4.1. Dissolved and particulate Mn and Co

Trace metal sampling was performed in Loch Etive by using an Aqua Monitor carried on the Autosub, an autonomous underwater vehicle able to carry out unique contour hugging and seesaw dive-profiling. Thus, an extensive picture of the dissolved and particulate concentrations of Mn and Co in the loch has been obtained. Because of the *hypoxic* conditions in Loch Etive at the time of sampling, data assumes particular importance as a step for further understanding the biogeochemical behaviour of these elements.

The analysis of the hydrographic data at the time of sampling (November 1999 and April 2000) indicates that Loch Etive could not be considered only as a simple two-layered system. Further analysis suggests that the upper part of the water column during both sampling occasions is a complex stratified system, within which estuarine circulation would develop. Contrary, in deep water, the data gave evidence for the presence of a deep stagnant layer of water with decreasing oxygen concentration from November 1999 to April 2000.

Dissolved manganese (Mn_d) concentrations were significantly higher than those recorded for the open ocean but matched well with concentrations recorded in hypoxic-anoxic regions such as the Saanich Inlet and the northwestern Black Sea. Although a small surface enrichment of dissolved Mn was observed, the general distribution with depth indicated low surface concentration values progressively increasing with depth. Surface enrichment is a characteristic feature of the oceanic distribution of dissolved Mn. In the case of Loch Etive, although atmospheric input could occur, such enrichment is probably mainly from riverine inputs.

Since Mn reduction is not likely to take place in oxygenated seawater, high dissolved Mn in deep waters would be expected as a result of in-situ reduction of particulate Mn or through a sedimentary source. Comparative analysis between the recorded trace metal concentration and the concentration of SPM suggests that a sedimentary source is the controlling mechanism. Data on pore water for the bottom sediments of Loch Etive (Overnell *et al.*, 1996) indicate that the concentrations of dissolved Mn are about two orders of magnitude higher than the highest water column

concentration recorded in the present study. This confirms that the sediments are acting as a source of dissolved Mn to the overlying water column.

The dissolved Mn concentration showed pronounced seasonal variability with increasing concentrations from November to April. This would be expected on the basis of the hydrographic data, indicating decreasing oxygen conditions between the two seasons. The comparatively low Mn concentrations recorded in November were characteristic of pre-bloom conditions. In early spring, however, increased biological activity and associated oxygen utilisation in the breakdown of this organic matter produced increasing reducing conditions that in turn favours Mn reduction.

Several previous studies reporting the variations of Mn concentrations are based on widely spaced measurements. In the present study the unique sampling technique has allowed for the collection of high-resolution data not previously obtained. As well as verifying the generally observed depth trend for dissolved Mn, the results give evidence for the presence of localised variations. More research is required to better understanding the processes producing these variations (see Section 4.2), possible factors including inputs of organic carbon, variations in bottom topography, bioturbation and the presence of micro-reducing zones.

The concentrations of particulate Mn (Mn_p) show a similar trend to the depth profiles of dissolved Mn. In surface water the input of river-borne terrestrial material, having a high SPM load is likely to be an important source. In oxygenated surface water, the oxidation of Mn(II) is a spontaneous process and hence the amount of particulate Mn is indirectly influenced by the amount of dissolved Mn. Increased biological activity in surface water decreases the concentration of dissolved Mn, this having an indirect effect on the concentration of particulate Mn. Compared to the surface, the deep-water concentrations of particulate Mn were generally one order of magnitude higher. The trend in SPM observed in the present study, in addition to previously recorded Mn sediment concentrations (Overnell *et al.*, 1996) suggest that the observed Mn water column concentrations cannot be explained solely by resuspension of Mn-enriched particles. Rather, scavenging of dissolved Mn from a sedimentary source is suggested to be the major factor for producing the observed trend.

The seasonal variations of the particulate Mn concentrations were small, concentrations slightly decreasing in surface waters from November to April, while an opposite trend was observed in deep water. The seasonal variations could be the result of a combination of the changes in dissolved Mn concentrations and the type of

particles constituting the SPM. The lower Mn_p concentrations recorded in spring, therefore, may be the result of increased organic component of the SPM during this time, while in deep water the scavenging of dissolved Mn derived from the sediments is the main controlling process.

Relatively few studies have investigated the biogeochemical behaviour of Co in the marine environment, making it difficult to directly compare the results from the present study. The dissolved Co (Co_d) concentrations in this study were higher than those recorded in the open ocean but comparable to those recorded for example in the Strait of Dover and in the Mediterranean. The highest Co concentrations were recorded in surface waters, decreasing with depth. Co showed a weak, negative correlation with salinity, suggesting that the higher surface concentrations might be due to riverine input.

Despite some variations, the concentration of dissolved Co in deep water remained low but stable with depth. This scenario is suggested to occur as a result of addition and removal processes being of equal magnitudes. The addition of Co could take place through a combination of two main processes: (1) desorption from Mn-oxides and (2) regeneration of Co associated with organic matter. The main removal mechanism is microbial oxidation. Recent studies (*e.g.* Lee and Fisher, 1993; Lee and Tebo, 1994) have shown evidence for Co oxidation by microbes in the absence of Mn-oxide surfaces. In the present study, no correlation was observed between Co and Mn, hence supporting the view that microbial oxidation may be an important removal mechanism for dissolved Co in Loch Etive.

Further interpretation of these results leads to the conclusion that in low oxygen environments, such as the bottom waters of Loch Etive, the biochemical processes affect Mn and Co differently, resulting in a geochemical separation of these two elements.

An in-situ chemical analyser (based on the method used by Chin *et al.*, 1992) was developed and tested for the determination of dissolved Mn. The initial testing shows that this technique successfully can record the dissolved Mn concentration. In the field the limitation for obtaining trace metal data remains the difficulties in assuring contamination-free sampling procedures. By using an in-situ technique, the contamination risk is brought to a minimum. The further development of high resolution sampling techniques will, therefore, enable a more detailed understanding of the behaviour of redox sensitive trace metals and in the case of Mn and Co an insight into the processes controlling their distribution.

4.2. Recommendations for further work

Loch system can be conceptually considered as intermediate between a mesocosm and the open coastal environment (Hall *et al.*, 1999). Consequently, their semi-enclosed basins facilitate quantification of input of freshwater and associated trace metals to the system. The present study would have benefited from a more detailed investigation of the magnitude of these inputs, in particular the trace metal load of the riverine sources to the loch.

Results indicate that the presence of localised features such as benthic activities, changes in bottom topography and the presence of microreducing zones are responsible for producing the observed scatter in the data. Benthic organisms produce characteristic features, visible at the surface of the bottom sediments. Video recording techniques have previously proven successful for the identification and estimation of this type of bottom activities (Howson and Davies, 1991). A similar survey in Loch Etive would help in order to determine the importance of bioturbation as well as establishing small variations in bottom topography as controlling factors for variations in the concentrations of the trace metal data.

The presence of microreducing zones is a factor that has been little investigated. Such zones could be responsible for producing reducing conditions in otherwise oxidising parts of the water column, for example within marine aggregates. Initial laboratory studies of environmental samples would be required in order to understand their occurrence and impact.

The results from the present study suggest that the controlling mechanisms of the biogeochemical behaviour of Mn and Co are different. Although the behaviour of Mn in the marine environment is now well understood, more research into the behaviour of Co is required. Factors of particular interest are: (1) speciation and complexation of Co in marine waters and (2) microbial Co oxidation. The biological availability of Co is determined by its speciation. If Co is organically complexed or in a colloidal form, it might be measured as dissolved Co, but these fractions may not be present in a biological available form, or may not interact with particles and manganese oxides in the same way as ionic cobalt.

Microbially-mediated Co oxidation is still a process that is poorly understood. Scope for further work involves establishing its mechanisms as well as the sensitivity to environmental factors such as temperature, salinity and oxygen.

In the present study, the use of an in-situ technique has proven to offer numerous advantages including minimisation of contamination risks and the possibility of increased sampling frequency. Further development of in-situ techniques will, therefore, facilitate a more detailed investigation of the processes controlling the behaviour of trace metals in the marine environment.

References

- Aller, R.C., 1978. The effects of animal-sediment interaction on geochemical processes near the sediment-water interface. In: M.L. Wiley (Editor), *Estuarine interactions*. Academic Press, London, pp. 157-172.
- Aller, R.C., 1980. Diagenetic processes near the sediment-water interface of Long Island Sound. II. Fe and Mn. *Advances in Geophysics*, 22: 351-415.
- Aller, R.C., 1988. Benthic fauna and biogeochemical processes in marine sediments: the role of burrow structures. In: T.H. Blackburn and J. Sorenson (Editors), *Nutrient cycling in coastal marine environments*. John Wiley & Sons Ltd, New York, pp. 301-338.
- Aller, R.C., 1994. The sedimentary Mn cycle in Long Island Sound: Its role as intermediate oxidant and the influence of bioturbation, O₂, and C_{org} flux on diagenetic reaction balances. *Journal of Marine Research*, 52: 259-295.
- Anderson, J.J. and Devol, A.H., 1973. Deep water renewal in the Saanich Inlet, an intermittently anoxic basin. *Estuarine and Coastal Marine Science*, 1: 1-10.
- Arimoto, R., Duce, R.A. and Ray, B.J., 1989. Concentrations, sources and air-sea exchange of trace elements in the atmosphere over the Pacific Ocean. In: J.P. Riley, R. Chester and R.A. Duce (Editors), *Chemical oceanography*. vol. 10., SEAREX: The sea/air exchange program, Academic Press, London, pp. 107-149.
- Armannsson, H., 1979. Dithizone extraction and flame atomic absorption spectrometry for the determination of cadmium, zinc, lead, copper nickel, cobalt, and silver in sea water and biological tissues. *Analytica Chimica Acta*, 110: 21-28.
- Bacon, M.P., Brewer, P., G, Spencer, D.W., Murray, J.W. and Goddard, J., 1980. Lead-210, polonium-210, manganese and iron in the Cariaco Trench. *Deep-Sea Research*, 27: 119-135.
- Balistrieri, L.S. and Murray, J.W., 1986. The surface chemistry of sediments from the Panama Basin: the influence of Mn oxides on metal adsorption. *Geochimica et Cosmochimica Acta*, 50: 2235-2243.
- Balls, P.W., 1990. Distribution and composition of suspended particulate material in the Clyde Estuary and associated sea lochs. *Estuarine, Coastal and Shelf Science*, 30: 475-487.
- Balzer, W., 1982. On the distribution of iron and manganese at the sediment/water interface: thermodynamic vs kinetic control. *Geochimica et Cosmochimica Acta*, 46: 1153-1161.
- Baturin, G.N., 1988. The geochemistry of manganese and manganese nodules in the ocean. D. Reidel, Dordrecht, 342 pp.

- Bender, M.L., Klinkhammer, G.P. and Spencer, D.W., 1977. Manganese in seawater and the marine manganese balance. *Deep-Sea Research*, 24: 799-812.
- Bewers, J.M., Sundby, B. and Yeats, P.A., 1976. The distribution of trace metals in the western North Atlantic off Nova Scotia. *Geochimica et Cosmochimica Acta*, 40: 687-696.
- Blain, S. and Treguer, P., 1995. Iron(II) and iron(III) determination in sea-water at the nanomolar level with selective online preconcentration and spectrophotometric determination. *Analytica Chimica Acta*, 308(1-3): 425-432.
- Boyle, E.A. and Edmond, J.M., 1977. Determination of copper, nickel, and cadmium in seawater by APDC chelate coprecipitation and flameless atomic absorption spectrometry. *Analytica Chimica Acta*, 91: 189-197.
- Brandhorst, W., 1958. Nitrite accumulation in the northeast Tropical Pacific. *Nature*, 182: 679.
- Breck, W.G., 1974. Redox levels in the sea. In: E.D. Goldberg (Editor), *The sea*. Wiley-Interscience, New York, pp. 181-196.
- Bruland, K.W., 1983. Trace elements in seawater. In: J.P. Riley and R. Chester (Editors), *Chemical oceanography*. Academic press, New York, pp. 157-221.
- Bruland, K.W., Coale, K.H. and Mart, L., 1985. Analysis of seawater for dissolved Cd, Cu and Pb: an intercomparison of voltametric and atomic absorption methods. *Marine Chemistry*, 17: 285-300.
- Bruland, K.W., Franks, R.P., Knauer, G.A. and Martin, J.H., 1979. Sampling and analytical methods for the determination of copper, cadmium, zinc, and nickel at the nanogram per litre level in seawater. *Analytica Chimica Acta*, 105: 233-245.
- Burns, R.G., 1976. The uptake of cobalt into ferromanganese nodules, soils, and synthetic Mn(IV) oxides. *Geochimica et Cosmochimica Acta*, 40: 95-102.
- Burton, J.D. and Statham, P.J., 1990. Trace metals in seawater. In: R.W. Furness and P.S. Rainbow (Editors), *Heavy metals in the marine environment*. CRC Press, Boca Raton, pp. 5-25.
- Cannizzaro, V., Bowie, A.R., Sax, A., Achterberg, E.P. and Worsfold, P.J., 1999. Determination of cobalt and iron in estuarine and coastal waters using flow injection with chemiluminescence detection. *Analyst*, 125: 51-57.
- Carlucci, A.F. and Cuhel, R.L., 1977. Vitamins in the south polar seas; distribution and significance of dissolved and particulate vitamin B₁₂, thiamine and biotin in the southern Indian Ocean. In: G.A. Liano (Editor), *Adaptations within marine ecosystems*. Smithsonian Institute, pp. 115-128.

- Chapin, T.P., Johnson, K.S. and Coale, K.H., 1991. Determination of manganese in seawater by flow injection analysis with chemiluminescence detection. *Analytica Chimica Acta*, 249: 469-478.
- Chin, C.S., Johnson, K.S. and Coale, K.H., 1992. Spectrophotometric determination of dissolved manganese in natural waters with 1-(2-pyridylazo)-2-naphthol: application to analysis in situ in hydrothermal plumes. *Marine Chemistry*, 37: 65-82.
- Cline, J.D. and Richards, F.A., 1972. Oxygen deficient conditions and nitrate reduction in the eastern tropical North Pacific Ocean. *Limnology and Oceanography*, 17(6): 885-900.
- Codispoti, L.A., Friederich, G.E., Murray, J.W. and M, S.C., 1991. Chemical variability in the Black Sea: implications of continuous vertical profiles that penetrated the oxic/anoxic interface. *Deep-Sea Research*, 38(suppl.): S691-S710.
- Codispoti, L.A. and Richards, F.A., 1976. An analysis of the horizontal regime of denitrification in the eastern tropical North Pacific. *Limnology and Oceanography*, 21(3): 379-388.
- Ćosović, B., Degobbi, D., Bilinski, H. and Branica, M., 1982. Inorganic cobalt species in seawater. *Geochimica et Cosmochimica Acta*, 46: 151-158.
- Daniel, A., Birot, D., Blain, S., Treguer, P., Leilde, B. and Menut, E., 1995. A submersible flow-injection analyzer for the in-situ determination of nitrite and nitrate in coastal waters. *Marine Chemistry*, 51(1): 67-77.
- Danielsson, L.-G., 1980. Cadmium, copper, iron, lead, nickel and zinc in Indian Ocean water. *Marine Chemistry*, 8: 199-215.
- Danielsson, L.G., Magnusson, B. and Westerlund, S., 1978. An improved metal extraction procedure for the determination of trace metals in seawater by atomic absorption spectrometry with electrothermal atomisation. *Analytica Chimica Acta*, 98: 47-57.
- Deuser, W.G., 1973. Cariaco Trench: Oxidation of organic matter and residence time of anoxic water. *Nature*, 242: 601-603.
- Deuser, W.G., 1975. Reducing environments. In: J.P. Riley and G. Skirrow (Editors), *Chemical oceanography*. vol. 3., 2nd ed., Academic press, London, pp. 1-37.
- Diem, D. and Stumm, W., 1984. Is dissolved Mn^{2+} being oxidized by O_2 in absence of Mn-bacteria or surface catalysts? *Geochimica et Cosmochimica Acta*, 48: 1571-1573.
- Donat, J.R. and Bruland, K.W., 1995. Trace elements in the oceans. In: B. Salbu and E. Steinnes (Editors), *Trace elements in natural waters*. CRC Press Inc., Boca Raton, pp. 247-281.

- Dyrssen, D. and Kremling, K., 1990. Increasing hydrogen sulfide concentration and trace metal behaviour in the anoxic Baltic waters. *Marine Chemistry*, 48: 329-342.
- Edwards, A., 1989. The Loch Obisary surveys. Report to the Nature Conservancy Council., Scottish Marine Biological Association, 23 pp.
- Edwards, A., Baxter, M.S., Ellett, D.J., Martin, J.A.H., Meldrum, D.T. and Griffiths, C.R., 1986. Clyde Sea hydrography. *Proceedings of the Royal Society of Edinburgh*, 90B: pp 67-83.
- Edwards, A. and Edelsten, D.J., 1977. Deep water renewal of Loch Etive: a three basin Scottish fjord. *Estuarine and Coastal Marine Science*, 5: 575-595.
- Edwards, A. and Grantham, B.E., 1986. Inorganic nutrient regeneration in Loch Etive bottom water. In: S. Skreslet (Editor), *The role of freshwater outflow in coastal marine ecosystem*. NATO ASI G7. Springer-Verlag, Berlin, pp. 195-204.
- Emerson, S., Cranston, R.E. and Liss, P.S., 1979. Redox species in a reducing fjord: equilibrium and kinetic considerations. *Deep-Sea Research*, 26A: 859-878.
- Emerson, S., Kalhorn, S., Jacobs, L., Tebo, B.M., Nealson, K.H. and Rosson, R.A., 1982. Environmental oxidation rate of manganese(II): bacterial catalysis. *Geochimica et Cosmochimica Acta*, 46: 1073-1079.
- Fanning, K.A. and Pilson, M.E.Q., 1972. A model for the anoxic zone of the Cariaco Trench. *Deep-Sea Research*, 19: 847-863.
- Fergusson, J.E., 1990. *The heavy elements: chemistry, environmental impact, and health effects*. Pergamon Elsevier, Netherlands, 614 pp.
- Froelich, P.N., Klinkhammer, G.P., Bender, M.L., Luedtke, N.A., Heath, G.R., Cullen, D., Dauphin, D., Hammond, B., Hartman, B. and Maynard, V., 1979. Early oxidation of organic matter in pelagic sediments of the eastern equatorial Atlantic: suboxic diagenesis. *Geochimica et Cosmochimica Acta*, 43: 1075-1090.
- Gade, H.G. and Edwards, A., 1980. Deep water renewal in fjords. In: H.J. Freeland and D.M. Farmer (Editors), *Fjord oceanography*. Plenum, New York, pp. 453-489.
- Gamo, T., Sakai, H., Nakayama, E., Ishida, K. and Kimoto, H., 1994. A submersible flow-through analyser for in-situ colourimetric measurement down to 2000 m depth in the ocean. *Analytical Sciences*, 10(6): 843-848.
- Grasshoff, K., 1975. The hydrochemistry of landlocked basins and fjords. In: J.P. Riley and G. Skirrow (Editors), *Chemical oceanography*. vol. 2., Academic press, London, pp. 455-597.

- Griffiths, C.R., Millard, N.M., McPhail, S.D., Stevenson, P., Perrett, J.R., Pebody, M., Webb, A.T. and Meldrum, D.T., 1998. Towards environmental monitoring with the autosub autonomous underwater vehicle, IEEE Conference, Underwater Technology '98, Tokyo, Japan.
- Griffiths, G., Millard, N.M., Pebody, M. and McPhail, S.D., 1997. The end of research ships? Autosub - an autonomous underwater vehicle for ocean science, Underwater Technology International. Society for Underwater Technology, Aberdeen, pp. 349-362.
- Guieu, C., Martin, J.-M., Tankéré, S.P.C., Mousty, F., Trincherini, P., Bazot, M. and Dai, M.H., 1998. On trace metal geochemistry in the Danube river and western Black Sea. *Estuarine, Coastal and Shelf Science*, 47: 471-485.
- Hall, I.R., Hydes, D.J., Statham, P.J. and Overnell, J., 1996. Dissolved and particulate trace metals in a Scottish sea loch: an example of a pristine environment? *Marine Pollution Bulletin*, 32(12): 846-854.
- Hall, I.R., Hydes, D.J., Statham, P.J. and Overnell, J., 1999. Seasonal variations in the cycling of aluminium, cadmium and manganese in a Scottish sea loch: biogeochemical processes involving suspended particles. *Continental Shelf Research*, 19: 1783-1808.
- Haraldsson, C. and Westerlund, S., 1988. Trace metals in the water columns of the Black Sea and Framvaren fjord. *Marine Chemistry*, 23: 117-424.
- Heggie, D. and Lewis, T., 1984. Cobalt in pore waters of marine sediments. *Nature*, 311(4): 453-455.
- Hodge, V., Johnson, S.R. and Goldberg, E.D., 1978. Influence of atmospherically transported aerosols on surface ocean water composition. *Geochemical Journal*, 12: 7-20.
- Hong, H. and Kester, D.R., 1986. Redox state of iron in the offshore waters of Peru. *Limnology and Oceanography*, 31: 512-524.
- Howard, A.G. and Statham, P.J., 1993. Inorganic trace analysis; philosophy and practice. John Wiley & Sons Ltd, Chichester, 182 pp.
- Howson, C.M. and Davies, L.M., 1991. Marine nature conservation review, surveys of Scottish sealochs. A towed video survey of Loch Fyne. Volume-1, Report to the Nature Conservancy Council from the Marine biological station, Millport, 40 pp.
- Hunt, C.D., 1983a. Incorporation and deposition of Mn and other trace metals by flocculent organic matter in a controlled marine ecosystem. *Limnology and Oceanography*, 28: 302-308.
- Hunt, C.D., 1983b. Variability in the benthic Mn flux in coastal ecosystem resulting from temperature and primary production. *Limnology and Oceanography*, 28: 913-923.

- Hunt, C.D. and Kelly, J.R., 1988. Manganese cycling in coastal regions: response to eutrophication. *Estuarine, Coastal and Shelf Science*, 26: 527-558.
- Huynh-Ngoc, L. and Whitehead, N.E., 1986. Nickel and cobalt determination in the northwestern Mediterranean by differential pulse cathodic stripping voltammetry. *Oceanologica Acta*, 9(4): 433-438.
- Jacobs, L. and Emerson, S., 1982. Trace metal solubility in an anoxic fjord. *Earth and Planetary Science Letters*, 60: 237-252.
- Jacobs, L., Emerson, S. and Husted, S.S., 1987. Trace metal geochemistry in the Cariaco Trench. *Deep-Sea Research*, 34(5/6): 965-981.
- Jacobs, L., Emerson, S. and Skei, J., 1985. Partitioning and transport of metals across the O₂/H₂S interface in a permanently anoxic basin: Framvaren Fjord, Norway. *Geochimica et Cosmochimica Acta*, 49: 1433-1444.
- James, R.H., Statham, P.J., Morley, N.H. and Burton, J.D., 1993. Aspects of the geochemistry of dissolved and particulate Cd, Cu, Ni, Co and Pb in the Dover Strait. *Oceanologica Acta*, 16(5-6): 553-564.
- Jickells, T.D. and Burton, J.D., 1988. Cobalt, copper, manganese and nickel in the Sargasso Sea. *Marine Chemistry*, 23: 131-144.
- Jickells, T.D. and Knap, A.H., 1984. The distribution and geochemistry of some trace metals in the Bermuda coastal environment. *Estuarine, Coastal and Shelf Science*, 18: 245-262.
- Johnson, K.S., Beehler, C.L. and Sakamoto-Arnold, C.M., 1986. A submersible flow analysis system. *Analytica Chimica Acta*, 179: 245-257.
- Jones, C.J. and Murray, J.W., 1985. The geochemistry of manganese in the northeast Pacific Ocean off Washington. *Limnology and Oceanography*, 30: 81-92.
- Jongsma, D., Fortuin, A.R., Huson, W., Troelstra, S.R., Klaver, G.T., Peters, J.M., Von Harten, D., De Lange, G.J. and Ten Haven, H.L., 1983. Discovery of an anoxic basin within the Strabo Trench, eastern Mediterranean. *Nature*, 305: 795-797.
- Kingston, H.M., Barnes, I.L., Brady, T.J., Rains, T.C. and Champ, M.A., 1978. Separation of eight transition elements from alkali and alkaline earth elements in estuarine and sea water with chelating resins and their determination by graphite furnace atomic absorption spectrometry. *Analytical Chemistry*, 50: 2064-2070.
- Klinkhammer, G.P., 1980. Determination of manganese in seawater by flameless atomic absorption spectrometry after preconcentration with 8-hydroxyquinoline in chloroform. *Analytica Chimica Acta*, 52: 117-120.
- Klinkhammer, G.P., 1994. Fiber optic spectrometers for in-situ measurements in the ocean: the ZAPS probe. *Marine Chemistry*, 47: 13-20.

- Klinkhammer, G.P. and Bender, M.L., 1980. The distribution of manganese in the Pacific Ocean. *Earth and Planetary Science Letters*, 46: 361-384.
- Knauer, G.A., Martin, J.H. and Gordon, R.M., 1982. Cobalt in north-east Pacific waters. *Nature*, 297: 49-51.
- Koike, I. and Mukai, H., 1983. Oxygen and inorganic nitrogen contents and fluxes in burrows of the shrimps *Callinassa japonica* and *Upogebia major*. *Marine Ecology-Progress Series*, 12(2): 185-190.
- Kremling, K., 1983. The behaviour of Zn, Cd, Cu, Ni, Co, Fe and Mn in anoxic Baltic waters. *Marine Chemistry*, 13: 87-108.
- Kremling, K. and Hydes, D., 1988. Summer distribution of dissolved Al, Cd, Co, Cu, Mn and Ni in surface waters around the British Isles. *Continental Shelf Research*, 8(1): 89-105.
- Kremling, K., Wenck, A. and Pohl, C., 1987. Summer distribution of dissolved Cd, Co, Cu, Mn and Ni in central North Sea waters. *Deutsche Hydrographische Zeitschrift*, 40: 103-113.
- Landing, W.M. and Bruland, K.W., 1980. Manganese in the North Pacific. *Earth and Planetary Science Letters*, 49: 45-56.
- Landing, W.M. and Bruland, K.W., 1987. The contrasting biogeochemistry of iron and manganese in the Pacific Ocean. *Geochimica et Cosmochimica Acta*, 51: 29-43.
- Landing, W.M. and Lewis, B.L., 1991. Thermodynamic modelling of trace metal speciation in the Black Sea. In: E. Izdar and J.W. Murray (Editors), *Black Sea Oceanography*. Kluwer Academic Publishers, Netherlands, pp. 125-160.
- Lee, B.-G. and Fisher, N., S., 1993. Microbially mediated cobalt oxidation in seawater revealed by radiotracer experiments. *Limnology and Oceanography*, 38(8): 1593-1602.
- Lee, Y. and Tebo, B.M., 1994. Cobalt(II) oxidation by the marine manganese(II)-oxidizing *Bacillus* sp. strain SG-1. *Applied and Environmental Microbiology*, 60(8): 2949-2957.
- Lewis, B.L. and Landing, W.M., 1991. The biochemistry of manganese and iron in the Black Sea. *Deep-Sea Research*, 38(suppl.): S773-S803.
- Lewis, B.L. and Landing, W.M., 1992. The investigation of dissolved and suspended-particulate trace metal fractionation in the Black Sea. *Marine Chemistry*, 40: 105-141.
- Lienemann, C.-P., Taillefert, M., Perret, D. and Gaillard, J.-F., 1997. Association of cobalt and manganese in aquatic systems: Chemical and microscopic evidence. *Geochimica et Cosmochimica Acta*, 61(7): 1437-1446.

- Lilley, M.D., Freely, R.A. and Trefry, J.H., 1995. Chemical and biochemical transformations in hydrothermal plumes. In: S.E. Humphris (Editor), Seafloor hydrothermal systems: physical, chemical, biological, and geological interactions. AGE Geophysical Monograph 91. American Geophysical Union, Washington D.C., pp. 369-391.
- Liungman, O., 2000. Tidally forced internal wave mixing in a k-e model framework applied to fjord basins. *Journal of Physical Oceanography*, 30: 352-368.
- Lubbers, G.W., Gieskes, W.W.C., del Castillo, P., Salomons, P. and Bril, J., 1990. Manganese accumulation in the high pH microenvironment of *Phaeocystis* sp. (Haptophyceae) colonies from the North Sea. *Marine Ecology-Progress Series*, 59: 285-293.
- Mackay, D.W. and Halcrow, W., 1976. The distribution of nutrients in relation to water movements in the Firth of Clyde. In: S. Skreslet (Editor), *Freshwater on the sea*. Association of Norwegian Oceanographers, Oslo, pp. 246.
- Magnusson, B. and Westerlund, S., 1981. Solvent extraction procedures combined with back-extraction for trace metals determinations by atomic absorption spectrometry. *Analytica Chimica Acta*, 131: 63-72.
- Mallini, L.J. and Shiller, A.M., 1993. Determination of dissolved manganese in seawater by flow-injection analysis with colorimetric detection. *Limnology and Oceanography*, 38(6): 1290-1295.
- Manheim, F.T., 1991. Geological Survey Ferromanganese Crust Data Set. <http://www.ngdc.noaa.gov/mgg/geology/usgscrust.html>.
- Martin, J.H., 1985. Iron and cobalt in NE Pacific waters. *Eos*, 66(51): 1291.
- Martin, J.H. and Knauer, G.A., 1984. VERTEX: manganese transport through oxygen minima. *Earth and Planetary Science Letters*, 67: 35-47.
- Moffett, J.W., 1997. The importance of microbial Mn oxidation in the upper ocean: a comparison of the Sargasso Sea and equatorial Pacific. *Deep-Sea Research*, 44(8): 1277-1291.
- Moffett, J.W. and Ho, J., 1996. Oxidation of cobalt and manganese in seawater via a common microbially catalyzed pathway. *Geochimica et Cosmochimica Acta*, 60(18): 3415-3424.
- Morgan, J.J., 1967. Chemical equilibria and kinetic properties of manganese in natural waters. In: S.D. Faust and J.V. Hunter (Editors), *Principles and applications of water chemistry*. John Wiley & Sons Ltd, New York, pp. 561-624.
- Morris, A.W., Bale, A.J. and Howland, J.M., 1982. The dynamics of estuarine manganese cycling. *Estuarine, Coastal and Shelf Science*, 14: 175-192.

- Murray, J.W., 1975. The interaction of cobalt with hydrous manganese oxide. *Geochimica et Cosmochimica Acta*, 39: 653-647.
- Murray, J.W. and Brewer, P., G, 1975. Mechanisms of removal of manganese, iron and other trace metals from sea water. In: G.P. Glasby (Editor), *Marine manganese deposits*. Elsevier, New York, pp. 292-325.
- Murray, J.W. and Dillard, J.G., 1979. The oxidation of cobalt(II) absorbed on manganese dioxide. *Geochimica et Cosmochimica Acta*, 43: 781-787.
- Murray, J.W. and Izdar, E., 1989. The 1988 Black Sea oceanographic expedition: overview and new discoveries. *Oceanography*, 2: 15-21.
- Murray, J.W., Jannasch, H.W., Honjo, S., Anderson, R.F., Reeburgh, W.S., Top, Z., Friederich, G.E., Codispoti, L.A. and Izdar, E., 1989. Unexpected changes in the oxic/anoxic interface in the Black Sea. *Nature*, 338(30): 411-413.
- Nowicki, J.L., Johnson, K.S., Coale, K.H., Elrod, V.A. and Lieberman, 1994. Determination of zinc in seawater using flow-injection analysis with fluorometric detection. *Analytical Chemistry*, 66(17): 2732-2738.
- Okamura, K., Gamo, T., Obata, H., Nakayama, E., Karatani, H. and Nozaki, Y., 1998. Selective and sensitive determination of trace manganese in sea water by flow through technique using luminol hydrogen peroxide chemiluminescence detection. *Analytica Chimica Acta*, 377(2-3): 125-131.
- Overnell, J., Harvey, S.M. and Parkes, R.J., 1996. A biochemical comparison of sea loch sediments. Manganese and iron contents, sulphate reduction and oxygen uptake rates. *Oceanologica Acta*, 19(1): 41-55.
- Overnell, J., Brand, T., Bourgeois, W. and Statham, P.J., 2001. Manganese and iron dynamics in the water column of the upper basin of Loch Etive, a Scottish fjord. *Estuarine, Coastal and Shelf Science*., in press.
- Öztürk, M., 1995. Trends of trace metal (Mn, Fe, Co, Ni, Cu, Zn, Cd and Pb) distributions at the oxic-anoxic interface and in sulfidic water of the Drammensfjord. *Marine Chemistry*, 48: 329-342.
- Pacyna, J.M., 1984. Estimation of the atmospheric emission of trace elements from anthropogenic sources in Europe. *Atmospheric Environment*, 18: 41-50.
- Pai, S., Whung, P. and Lai, R., 1988. Pre-concentration efficiency of chelex-100 resin for heavy-metals in seawater. 1. Effects of pH and salts on the distribution rations of heavy metals. *Analytica Chimica Acta*, 211(1-2): 257-270.
- Pan, P.J. and Susak, N.J., 1991. The speciation of cobalt in seawater and freshwater at 25 °C. *Geochemical Journal*, 25: 411-420.

- Parker, E.R., 1999. The role of colloidal material in the fate and cycling of trace metals in estuarine and coastal waters. PhD Thesis, University of Southampton, Southampton, 346 pp.
- Price, N.B. and Calvert, S.E., 1973. A study of the geochemistry of suspended particulate matter in coastal waters. *Marine Chemistry*, 1: 169-189.
- Reijn, J.M., Van Der Linden, W.E. and Poppe, H., 1981. Dispersion in open tubes and tubes packed with large glass beads. *Analytica Chimica Acta*, 123: 229-237.
- Richards, F.A., 1965. Anoxic basins and fjords. In: J.P. Riley and G. Skirrow (Editors), *Chemical oceanography*. vol. 1., Academic press, London, pp. 611-645.
- Richards, F.A. and Vaccaro, R.F., 1956. The Cariaco Trench, an anaerobic basin in the Caribbean Sea. *Deep-Sea Research*, 3: 214-228.
- Ridgway, I.M. and Price, N.B., 1987. Geochemical associations and post-depositional mobility of heavy metals in coastal sediments: Loch Etive, Scotland. *Marine Chemistry*, 21: 229-248.
- Robertson, D.E., 1970. The distribution of cobalt in oceanic waters. *Geochimica et Cosmochimica Acta*, 34: 553-567.
- Rue, E.L., Smith, G.J., Cutter, G.A. and Bruland, K.W., 1997. The response of trace element redox couples to suboxic conditions in the water column. *Deep-Sea Research*, 44(1): 113-134.
- Ruzicka, J. and Hansen, E.H., 1988. *Flow injection analysis*. 2nd ed. John Wiley & Sons, New York, 498 pp.
- Saager, P.M., De Baar, H.J.W. and Burkill, P.H., 1989. Manganese and iron in Indian Ocean waters. *Geochimica et Cosmochimica Acta*, 53: 2259-2267.
- Santschi, P., Höhener, P., Benoit, G. and Buchholtz-Ten Brink, M., 1990. Chemical processes at the sediment-water interface. *Marine Chemistry*, 30: 269-315.
- Santschi, P.H., Adler, D.M. and Admurer, M., 1983. The fate of particles and particle reactive trace metals in coastal waters: radioisotope studies in microcosms. In: C.S. Wong, E. Boyle, K.W. Bruland, D.J. Burton and E.D. Goldberg (Editors), *Trace metals in sea water*. Plenum Press, New York, pp. 331-349.
- Schoemann, V., De Baar, H.J.W., de Jong, J.T.M. and Lancelot, C., 1998. Effects of phytoplankton blooms on the cycling of manganese and iron in coastal waters. *Limnology and Oceanography*, 43(7): 1427-1441.
- Selavka, C.M., Jiao, K.-S. and Krull, I.S., 1987. Construction and comparison of open tubular reactors for postcolumn reaction detection in liquid chromatography. *Analytical Chemistry*, 59: 2221-2224.

- Sen Gupta, R. and Naqvi, S.W.A., 1984. Chemical oceanography of the Indian Ocean, north of the equator, a review. *Deep-Sea Research*, 31: 671-706.
- Sillén, L.G., 1965. Oxidation states of earth's ocean and atmosphere: a model calculation on earlier states. The myth of the prebiotic soup. *Arkiv for kemi*, 24: 431-456.
- Slater, R.D. and Kroopnick, P., 1984. Controls on dissolved oxygen distribution and organic carbon deposition in the Arabian Sea. In: B.U. Haq and J.D. Milliman (Editors), *Marine geology and oceanography of Arabian Sea and coastal Pakistan*. Van Nostrand Reinhold Company, London, pp. 305-313.
- Slinn, W.G.N., 1983. Air-to-sea transfer of particles. In: P.S. Liss and W.G.N. Slinn (Editors), *Air-sea exchange of gases and particles*. D. Reidel Publishing company, Dordrecht, pp. 299-405.
- Slomp, C.P., Malschaert, J.F.P., Lohse, L. and Van Raaphorst, W., 1997. Iron and manganese cycling in different sedimentary environments on the North Sea continental margin. *Continental Shelf Research*, 17(9): 1083-1117.
- Smith, R.G. and Windon, H.L., 1980. A solvent extraction technique for determining nanogram per liter concentrations of cadmium, copper, nickel and zinc in seawater. *Analytica Chimica Acta*, 113: 39-46.
- Spencer, D., W and Brewer, P., G, 1971. Vertical advection diffusion and redox potentials as controls on the distribution of manganese and other trace metals dissolved in waters of the Black Sea. *Journal of Geophysical Research*, 76(24): 5877-5892.
- Statham, P.J., 1985. The determination of dissolved manganese and cadmium in sea water at low nmol l^{-1} concentrations by chelation and extraction followed by electrothermal atomic absorption spectrometry. *Analytica Chimica Acta*, 169: 149-159.
- Statham, P.J. and Burton, J.D., 1986. Dissolved manganese in the North Atlantic Ocean, 0-35°N. *Earth and Planetary Science Letters*, 79: 55-65.
- Statham, P.J. and Chester, R., 1988. Dissolution of manganese from marine atmospheric particulates into seawater and rainwater. *Geochimica et Cosmochimica Acta*, 52: 2433-2437.
- Statham, P.J., Yeats, P.A. and Landing, W.M., 1998. Manganese in the eastern Atlantic Ocean: processes influencing deep and surface water distributions. *Marine Chemistry*, 61: 55-68.
- Stigebrandt, A., 1976. Vertical diffusion driven by internal waves in a sill fjord. *Journal of Physical Oceanography*, 6(4): 486-495.

- Stone, A.T. and Morgan, J.J., 1984a. Reduction and dissolution of manganese(III) and manganese(IV) oxides by organics. 1. Reaction with hydroquinone. *Environmental Science and Technology*, 18: 450-456.
- Stone, A.T. and Morgan, J.J., 1984b. Reduction and dissolution of manganese(III) and manganese(IV) oxides by organics. 2. Survey of the reactivity of organics. *Environmental Science and Technology*, 18: 617-624.
- Stone, A.T. and Morgan, J.J., 1987. Reductive dissolution of metal oxides. In: W. Stumm (Editor), *Aquatic surface chemistry*. Wiley, New York, pp. 221-254.
- Stumm, W. and Morgan, J.J., 1970. *Aquatic chemistry, an introduction emphasising chemical equilibria in natural waters*. Wiley-Interscience, New York, 538 pp.
- Stumm, W. and Morgan, J.J., 1981. *Aquatic chemistry*. 2nd ed. Wiley, New York, 780 pp.
- Stumm, W. and Morgan, J.J., 1996. *Aquatic chemistry: chemical equilibria and rates in natural waters*. 3rd ed. John Wiley & Sons, New York, 1022 pp.
- Sturgeon, R.E., Bergman, S.S., Desaulniers, J.A.H., Mykytiuk, A.P. and Russell, D.S., 1980. Pre-concentration of trace metals from sea-water for determination by graphite-furnace atomic-absorption spectrometry. *Talanta*, 27: 85-94.
- Sugai, S.F., 1987. Temporal changes in the sediment geochemistry of two southeast Alaskan fjords. *Deep-Sea Research*, 34: 913-925.
- Swift, D.G., 1981. Vitamin levels in the Gulf of Maine and ecological significance of vitamin B₁₂ there. *Journal of Marine Research*, 39: 375-403.
- Szekiela, K.-H., 1978. Eolian dust into the northeastern Atlantic. *Oceanography and Marine Biology-Annual Review*, 16: 11-41.
- Tankéré, S.P.C., Muller, F.L.L., Burton, D.J., Statham, P.J., Guieu, C. and Martin, J.-M., submitted. Biogeochemical cycling of trace metals of the continental shelf of the northwestern Black Sea.
- Tappin, A.D., 1988. *Studies of trace metals in shelf waters of the British Isles*. Ph. D. Thesis, University of Southampton, 279 pp.
- Tappin, A.D., Millward, G.E., Statham, P.J., Burton, J.D. and Morris, A.W., 1995. Trace metals in the central and southern North Sea. *Estuarine, Coastal and Shelf Science*, 41: 275-323.
- Tebo, B.M., Nealson, K.H., Emerson, S. and Jacobs, L., 1984. Microbial mediation of Mn(II) and Co(II) precipitation at the O₂/H₂S interface in two anoxic fjords. *Limnology and Oceanography*, 29(6): 1247-1258.

- Tett, P., Gowen, R., Grantham, B. and Jones, K., 1986. The phytoplankton ecology of the Firth of Clyde sea-lochs Striven and Fyne. *Proc. Royal Soc. Edinburgh*, 90B: 223-238.
- Thamdrup, B., Fossing, H. and Jørgensen, B.B., 1994a. Manganese, iron, and sulphur cycling in a coastal marine sediment, Aarhus Bay, Denmark. *Geochimica et Cosmochimica Acta*, 58(23): 5115-5129.
- Thamdrup, B., Glud, R.N. and Hansen, J.W., 1994b. Manganese oxidation and *in situ* fluxes from coastal sediment. *Geochimica et Cosmochimica Acta*, 58: 2563-2570.
- Van Der Berg, J.H.M., Deelder, R.S. and Egberink, G.M., 1980. Dispersion phenomena in reactors for flow analysis. *Analytica Chimica Acta*, 114: 91-104.
- Van Der Sloot, H.A., Hoede, D., Hamburg, G., Woittiez, J.R.W. and Van Der Weijden, C.H., 1990. Trace elements in suspended matter from the anoxic hypersaline Tyro and Bannock Basins (eastern Mediterranean). *Marine Chemistry*, 31: 187-203.
- Warren, B.A., 1994. Context of the suboxic layer in the Arabian Sea. In: D. Lal (Editor), *Biochemistry of the Arabian Sea*. Thomson Press, India, pp. 203-216.
- Watanabe, H., 1974. Spectrophotometric determination of cobalt with 1-(2-pyridylazo)-2-naphthol and surfactants. *Talanta*, 21: 295-302.
- Weiss, R.F., 1970. The solubility of nitrogen, oxygen and argon in water and seawater. *Deep-Sea Research*, 17: 721-735.
- Westerlund, S. and Öhman, P., 1991. Cadmium, copper, cobalt, nickel, lead and zinc in the water column of the Weddell Sea, Antarctica. *Geochimica et Cosmochimica Acta*, 55: 2127-2146.
- Whitfield, M. and Turner, D., 1987. The role of particles in regulating the composition of seawater. In: W. Stumm (Editor), *Aquatic surface chemistry*. Wiley, New York, pp. 457-493.
- Williams, T.M., McKenzie, A.B., Scott, R.D., Price, N.B. and Ridgway, I.M., 1988. Radionuclide distributions in the surface sediments of Loch Etive. In: J.G. Guary, P. Guegueniat and R.J. Pentreath (Editors), *Radionuclides, a tool for oceanography*. Cherbourg, pp. 341-350.
- Wollast, R., Billen, G. and Duinker, J.C., 1979. Behaviour of manganese in the Rhine and Scheldt estuaries. *Estuarine and Coastal Marine Science*, 9: 161-169.
- Wong, G., T F, Pai, S.-C. and Chung, S.-W., 1995. Cobalt in the western Philippine Sea. *Oceanologica Acta*, 18(6): 631-638.
- Wyrski, K., 1962. The oxygen minima in relation to ocean circulation. *Deep-Sea Research*, 9: 11-23.

- Yeats, P.A. and Bowers, J.M., 1985. Manganese in the western north Atlantic Ocean. *Marine Chemistry*, 17: 255-263.
- Yeats, P.A. and Strain, P.M., 1990. The oxidation of manganese in seawater: rate constants based on field data. *Estuarine, Coastal and Shelf Science*, 31: 11-24.
- Zhang, H., Van den Berg, C.M.G. and Wollast, R., 1990. The determination of interactions of cobalt(II) with organic compounds in seawater using cathodic stripping voltammetry. *Marine Chemistry*, 28: 285-300.
- Ziebis, W., Huettel, M. and Foster, S., 1996. Impact of biogenic sediment topography on oxygen fluxes in permeable seabeds. *Marine Ecology-Progress Series*, 140(1-3): 227-237.

Appendix

Table 7 (ref. Figures 12,13 and 15). Hydrographic parameters. Data presented in Figure 13 are here shown every 5th value.

November 1999 CTD data (Figure 12)			
Depth (m)	Temp (°C)	Salinity	Oxygen (ml l ⁻¹)
1.07	9.5	8.00	9.9
1.28	10.4	12.76	9.4
1.28	9.6	8.44	9.5
1.28	9.2	6.01	10.2
1.44	9.7	8.08	9.9
1.51	9.8	8.71	9.7
1.64	10.1	8.46	9.7
2.10	10.7	14.24	9.0
8.24	12.1	22.14	7.3
9.01	12.2	22.36	7.3
9.01	12.0	21.79	7.4
9.11	12.2	22.38	7.3
9.22	12.2	22.14	7.4
9.28	12.5	23.75	6.9
9.36	12.0	21.75	7.4
12.18	12.6	24.15	6.7
18.17	12.6	25.08	6.4
18.76	12.7	25.12	6.2
18.91	12.6	25.14	6.5
18.94	12.7	25.13	6.4
19.07	12.6	25.16	6.6
19.29	12.6	25.10	6.5
21.94	12.7	25.27	6.0
22.09	12.6	25.30	6.5
24.09	12.6	25.19	6.6
33.89	12.7	25.64	6.3
37.89	12.8	25.81	5.9
38.11	12.8	25.86	5.6
38.66	12.7	25.84	6.1
41.73	12.8	26.01	5.5
57.91	12.8	26.69	4.7
57.99	12.6	26.84	4.3
58.75	12.5	26.91	3.8
61.62	12.4	26.96	3.6
73.49	12.2	27.11	3.3
77.39	12.2	27.17	3.0
77.81	12.0	27.29	2.5
81.49	11.9	27.37	2.2
82.53	11.9	27.39	2.2
86.71	12.0	27.38	2.2
91.37	11.9	27.43	2.0
94.11	11.9	27.44	1.9
101.41	11.9	27.45	1.9
104.17	11.9	27.46	1.9

April 2000 Hydrographic data (Figure 13)				April 2000 Hydrographic data (cont.)			
Depth (m)	Temp (°C)	Salinity	Oxygen (ml l ⁻¹)	Depth (m)	Temp (°C)	Salinity	Oxygen (ml l ⁻¹)
0.30	7.8	18.21	9.4	48.36	12.5	25.96	4.1
0.36	7.6	19.65	9.2	48.42	12.5	25.95	4.2
0.44	7.7	19.13	9.3	48.97	12.5	26.08	4.0
0.58	7.9	18.18	9.4	53.85	12.5	26.42	3.6
0.65	8.0	18.59	9.1	56.74	12.5	26.51	3.4
0.73	7.7	18.52	9.3	59.29	12.4	26.69	3.0
0.83	7.9	19.16	8.9	61.00	12.4	26.65	3.0
1.08	7.7	17.82	9.4	62.78	12.4	26.67	3.1
2.66	7.7	18.28	9.2	64.44	12.4	26.78	2.8
8.44	7.6	18.77	8.7	66.05	12.3	26.89	2.4
12.01	7.8	20.39	8.7	67.04	12.3	26.88	2.5
16.57	8.1	20.77	8.3	67.30	12.3	26.86	2.6
18.45	8.4	21.83	8.0	67.39	12.3	26.87	2.5
18.54	8.2	21.75	8.4	67.48	12.3	26.86	2.6
18.59	8.3	21.80	8.2	67.56	12.3	26.85	2.6
18.62	8.4	21.88	8.0	67.63	12.3	26.88	2.6
18.64	8.3	21.89	8.2	67.68	12.3	26.90	2.5
18.67	8.2	21.82	8.4	67.71	12.3	26.90	2.5
18.69	8.1	21.79	8.5	67.76	12.3	26.89	2.6
18.70	8.0	21.81	8.6	67.92	12.3	26.88	2.6
18.72	8.0	21.97	8.7	69.04	12.3	26.90	2.5
18.75	8.1	21.75	8.5	70.63	12.3	26.95	2.4
18.80	8.3	21.75	8.2	72.32	12.3	26.98	2.3
18.88	8.5	21.83	8.1	73.10	12.2	27.08	1.9
19.54	8.5	21.44	7.9	74.11	12.2	27.06	1.9
20.76	8.6	21.24	7.8	75.06	12.2	27.05	1.9
22.41	8.5	21.39	7.9	76.51	12.2	27.10	1.9
23.95	8.6	21.49	7.7	76.85	12.2	27.10	1.9
26.65	8.9	22.10	7.4	76.97	12.2	27.08	1.9
29.00	10.0	22.81	5.9	77.08	12.2	27.08	1.9
31.38	9.3	23.06	7.1	77.17	12.2	27.06	2.0
36.41	10.8	24.27	5.6	77.22	12.2	27.07	2.0
40.57	12.1	25.10	4.3	77.30	12.2	27.07	2.0
45.19	12.5	25.79	4.1	77.36	12.2	27.05	2.1
47.55	12.5	25.93	4.2	77.40	12.2	27.07	1.9
47.67	12.5	25.89	4.3	77.44	12.2	27.05	2.0
47.76	12.5	25.93	4.1	77.48	12.2	27.08	1.9
47.81	12.5	25.96	4.1	77.55	12.2	27.09	1.9
47.85	12.5	25.97	4.0	77.67	12.2	27.03	2.0
47.88	12.5	25.91	4.1	78.28	12.3	26.93	2.4
47.91	12.5	25.93	4.1	85.53	12.1	27.18	1.5
47.94	12.5	25.91	4.1	89.49	12.1	27.16	1.6
47.97	12.5	25.92	4.1	90.60	12.1	27.17	1.6
48.00	12.5	25.93	4.0	92.57	12.1	27.19	1.4
48.04	12.5	25.88	4.1	94.04	12.1	27.19	1.4
48.04	12.5	25.88	4.1	96.47	12.1	27.21	1.3
48.11	12.5	25.92	4.0	96.80	12.1	27.21	1.3
48.13	12.5	25.90	4.0	97.01	12.1	27.21	1.4
48.14	12.5	25.98	3.9	97.17	12.1	27.20	1.4
48.16	12.5	25.93	3.9	105.17	12.1	27.22	1.2
48.18	12.5	25.96	3.9	110.95	12.1	27.23	1.2
48.20	12.5	25.93	4.1	112.84	12.1	27.23	1.2
48.24	12.5	25.91	4.1	121.62	12.1	27.23	1.2
48.27	12.5	25.94	4.1	133.56	12.1	27.24	1.1
48.31	12.5	25.92	4.1				

Nov. M212 (Figure 15)		April M227 (Figure 15)		April M227 (cont.)	
Depth (m)	Oxygen (ml l ⁻¹)	Depth (m)	Oxygen (ml l ⁻¹)	Depth (m)	Oxygen (ml l ⁻¹)
38.10	7.3	0.93	9.6	77.40	1.9
38.52	7.5	1.02	9.6	77.42	1.9
38.88	7.4	1.04	9.4	77.43	1.9
44.31	7.5	1.06	9.4	77.44	2.0
48.47	7.4	1.09	9.3	77.45	2.1
48.62	6.8	1.11	9.0	77.46	1.9
49.00	6.8	1.15	9.1	77.47	1.9
49.17	7.5	4.10	8.9	77.48	1.9
49.20	7.5	12.64	8.8	77.50	1.8
49.29	7.4	23.37	7.6	77.52	2.0
49.69	7.5	37.00	5.0	77.54	1.9
49.70	7.4	47.05	3.8	77.55	1.9
49.73	7.5	54.67	3.2	77.57	1.9
49.75	6.8	56.90	3.1	77.59	1.9
49.75	6.8	59.11	2.8	77.63	1.8
49.77	6.8	59.59	2.7	77.69	1.9
49.78	7.5	61.11	2.9	77.83	2.3
49.78	7.3	63.84	2.7	78.93	2.4
49.78	7.3	66.41	2.4	88.72	1.5
49.80	7.5	68.61	2.3	91.54	1.4
49.83	6.8	69.76	2.2	93.96	1.4
49.84	7.4	71.72	2.1	95.62	1.4
49.84	6.8	72.74	1.7	96.23	1.4
52.58	7.4	73.03	1.7	96.59	1.3
58.09	7.3	73.43	1.7	96.66	1.4
74.71	7.4	73.93	1.8	96.71	1.3
76.57	7.4	74.21	1.7	96.76	1.4
77.87	7.4	74.51	1.6	96.80	1.3
77.91	7.4	74.75	1.6	96.84	1.3
78.56	7.3	75.13	1.6	96.88	1.3
78.75	7.3	76.03	1.8	96.92	1.4
79.21	7.1	76.83	2.0	96.98	1.4
79.64	7.2	77.01	2.2	97.02	1.4
79.66	7.1	77.06	2.1	97.04	1.4
79.69	6.9	77.09	2.0	97.07	1.4
79.72	7.2	77.12	1.9	97.09	1.4
87.09	2.5	77.15	2.1	97.12	1.4
90.91	2.1	77.19	2.0	97.20	1.4
90.91	2.1	77.20	2.0	97.33	1.4
91.06	2.1	77.21	2.0		
91.39	2.1	77.23	2.0		
93.31	2.1	77.25	2.1		
94.02	2.1	77.27	1.9		
94.33	2.1	77.29	1.9		
94.52	2.5	77.32	2.0		
99.70	2.2	77.35	2.0		
99.77	2.2	77.36	2.0		
99.77	2.2	77.39	2.0		

Table 8 (ref. Figures 16 and 17). Dissolved Mn data.

Nov. 1999 (Figure 16)		April 2000 (Figure 17)		April 2000 (cont.)		April 2000 (cont.)	
Depth (m)	Mn (nM)	Depth (m)	Mn (nM)	Depth (m)	Mn (nM)	Depth (m)	Mn (nM)
1.1	89.7	19.4	62.0	52.7	185.2	93.9	454.4
1.3	46.4	19.4	66.7	58.0	385.7	94.7	529.8
1.3	42.5	19.5	68.9	62.0	205.1	96.5	380.3
1.4	68.9	19.5	64.9	66.1	122.2	96.7	408.4
1.5	43.2	19.5	68.1	68.0	379.7	96.8	485
1.6	69.0	19.5	89.4	68.6	222.2	96.9	346.9
2.1	54.4	19.5	70.3	69.0	283.6	97.1	369.3
8.2	29.7	19.5	70.7	69.4	156.9	107.3	358.9
9.0	38.3	19.5	65.5	70.9	415.8	110.5	546
9.0	29.1	19.5	78.6	73.3	528.5	110.9	442.3
9.2	39.3	19.5	80.6	73.7	370.9	111.3	513.8
9.3	39.5	19.5	83.3	74.8	433.1	116.6	479.8
9.4	23.2	19.5	71.6	76.3	190.0	121.8	561.1
12.2	40.7	19.6	79.7	76.4	220.5	126.3	827.8
18.2	47.2	19.6	125.9	77.2	261.7		
18.8	42.4	19.6	115.7	77.2	390.9		
18.9	27.0	19.7	66.1	77.3	321.2		
18.9	47.5	19.9	69.8	77.3	482.5		
19.1	27.7	20.2	90.9	77.3	273.7		
19.3	43.6	20.3	86.7	77.3	373.1		
22.1	42.6	20.3	68.4	77.3	389.1		
24.1	38.2	20.4	112.7	77.4	386.6		
33.9	35.9	21.0	114.8	77.4	410.6		
37.9	21.8	22.0	83.2	77.4	543.7		
38.1	52.4	22.4	85.9	77.4	492		
38.7	30.9	25.6	62.8	77.5	451.7		
41.7	20.9	25.7	116.1	77.5	380.2		
57.9	46.9	27.7	97.2	77.5	437		
58.0	23.4	29.6	417.6	77.9	418		
58.7	19.4	47.4	111.3	77.9	580.4		
61.6	25.1	47.8	142.7	78.7	255.7		
73.5	41.0	47.9	148.7	78.8	457.8		
77.4	83.8	48.4	98.8	78.9	485.7		
77.8	58.8	48.5	229.8	80.8	496.5		
81.5	61.5	48.7	149.7	81.5	405.2		
82.5	65.8	48.7	149.7	83.4	416.2		
86.7	180.0	48.9	159.5	87.9	519.5		
91.4	68.3	48.9	166.0	90.1	422.3		
94.1	167.3	49.0	118.2	92.6	544		
101.4	106.0	49.1	179.5	92.6	449		
104.2	180.6	49.2	171.3	93.8	318.6		

Table 9 (ref. Figures 18 and 19). Total Mn.

Nov. 1999 (Figure 18)		April 2000 (Figure 19)		April 2000 (cont.)		April 2000 (cont.)	
Depth (m)	Mn (nM)	Depth (m)	Mn (nM)	Depth (m)	Mn (nM)	Depth (m)	Mn (nM)
1.1	112.9	19.4	83.3	48.9	276.3	76.3	283.0
1.3	75.7	19.4	84.9	49.0	176.5	76.4	328.7
1.3	83.8	19.5	90.9	49.0	231.4	77.2	338.4
1.4	101.4	19.5	86.8	49.1	199.5	77.2	535.3
1.5	77.5	19.5	91.3	49.1	231.0	77.3	423.1
1.6	123.3	19.5	110.5	49.1	205.1	77.3	568.5
2.1	91.7	19.5	87.5	49.2	205.8	77.3	384.0
8.2	81.0	19.5	95.4	49.2	243.5	77.3	508.0
9.0	76.1	19.5	87.3	49.2	329.0	77.3	561.4
9.0	72.8	19.5	111.5	49.3	255.9	77.4	471.4
9.2	74.4	19.5	109.3	49.3	341.3	77.4	555.7
9.3	83.4	19.5	105.1	49.4	417.3	77.4	701.0
9.4	65.9	19.5	98.1	49.4	309.4	77.4	670.7
12.2	91.2	19.6	107.2	49.4	388.3	77.5	658.5
18.2	107.0	19.6	161.9	49.8	147.2	77.5	455.7
18.8	79.7	19.6	146.5	50.8	172.5	77.5	608.1
18.9	76.5	19.7	97.2	52.7	232.3	77.9	509.8
18.9	99.7	19.9	103.6	62.0	249.9	77.9	794.4
19.1	68.7	20.2	122.0	66.1	184.0	78.7	341.1
19.3	95.6	20.3	119.4	66.3	518.7	78.8	546.6
22.1	104.9	20.3	104.4	67.0	579.2	78.9	657.1
24.1	89.6	20.4	128.3	67.5	517.0	80.8	590.6
33.9	82.8	21.0	151.1	67.7	562.9	81.5	582.5
37.9	76.0	22.0	124.4	68.0	569.3	83.4	493.8
38.1	103.6	22.4	115.4	68.3	261.9	87.9	780.0
38.7	79.1	25.6	98.6	68.5	299.7	90.1	585.8
41.7	70.5	25.7	160.2	68.6	260.3	92.6	791.1
57.9	131.0	27.7	143.3	68.6	405.3	92.6	800.8
58.0	116.8	29.6	693.7	68.9	250.0	93.8	415.3
58.7	98.5	47.4	156.5	68.9	260.5	93.9	608.3
61.6	121.4	47.8	211.9	69.0	338.7	94.7	837.2
73.5	158.9	47.9	195.4	69.0	330.1	96.5	703.9
77.4	217.1	48.4	206.6	69.1	312.5	96.7	831.7
77.8	176.0	48.4	148.7	69.2	298.4	96.8	749.2
81.5	245.9	48.4	140.0	69.2	329.6	96.9	581.6
82.5	351.8	48.5	273.1	69.2	332.6	97.1	574.3
86.7	459.5	48.5	191.5	69.2	440.1	107.3	547.2
91.4	311.3	48.7	140.5	69.3	405.4	110.5	728.1
94.1	408.0	48.7	191.1	69.4	197.4	110.9	623.2
101.4	440.3	48.9	231.0	70.9	480.7	111.3	887.5
104.2	387.4	48.9	134.3	73.3	604.7	116.6	683.0
48.9	205.2	74.8	562.9	73.7	551.9	121.8	823.4
						126.3	1255.7

Table 10 (ref. Figure 20). Dissolved Mn (nM)
for M212 (November) and M227 (April).

November M212		April M227	
Depth (m)	Mn (nM)	Depth (m)	Mn (nM)
43.7	88.2	29.6	417.6
43.9	50.9	58.0	385.7
45.6	65.7	68.0	379.7
47.1	57.6	70.9	415.8
49.5	53.4	73.3	528.5
49.5	32.5	73.7	370.9
49.5	45.4	74.8	433.1
49.7	38.3	77.2	261.7
49.8	49.0	77.2	390.9
66.4	98.9	77.3	321.2
77.7	99.6	77.3	482.5
78.2	165.2	77.3	273.7
78.8	170.4	77.3	389.1
79.5	223.8	77.4	410.6
79.7	220.7	77.4	543.7
89.0	172.7	77.4	492.0
92.4	80.8	77.5	451.7
92.5	155.5	77.5	380.2
92.8	83.0	77.5	437.0
97.1	118.3	81.5	405.2
99.7	127.2	92.6	544.0
		96.5	380.3
		96.7	408.4
		96.8	485.0
		96.9	346.9
		97.1	369.3

Table 11 (ref. Figures 21 and 22). Particulate Mn (nM).

Nov. 1999 (Figure 21)		April 2000 (Figure 22)		April 2000 (cont.)		April 2000 (cont.)	
Depth (m)	Mn (nM)	Depth (m)	Mn (nM)	Depth (m)	Mn (nM)	Depth (m)	Mn (nM)
1.1	23.2	19.4	21.3	48.9	45.7	69.2	52.8
1.3	29.3	19.4	18.2	48.9	110.3	69.2	40.3
1.3	41.3	19.5	21.9	49.0	46.8	69.3	36.7
1.4	32.5	19.5	21.9	49.0	113.3	69.4	40.5
1.5	34.3	19.5	23.2	49.1	52.0	70.9	64.8
1.6	54.3	19.5	21.1	49.1	51.5	73.3	76.2
2.1	37.3	19.5	17.2	49.1	30.9	73.7	181.0
8.2	51.3	19.5	24.7	49.2	34.4	74.8	129.8
9.0	37.8	19.5	21.7	49.2	44.0	76.3	93.0
9.0	43.7	19.5	32.9	49.2	61.5	76.4	108.2
9.2	35.1	19.5	28.7	49.3	48.5	77.2	76.7
9.3	43.9	19.5	21.8	49.3	50.8	77.2	144.4
9.4	42.7	19.5	26.5	49.4	46.9	77.3	101.9
12.2	50.5	19.6	27.5	49.4	59.7	77.3	86.0
18.2	59.8	19.6	36.0	49.4	51.5	77.3	110.3
18.8	37.3	19.6	30.9	48.9	45.7	77.3	134.8
18.9	49.5	19.7	31.1	48.9	110.3	77.3	172.3
18.9	52.2	19.9	33.8	49.0	46.8	77.4	84.8
19.1	41.0	20.2	31.1	49.0	113.3	77.4	145.1
19.3	52.0	20.3	32.7	49.1	52.0	77.4	157.2
22.1	62.3	20.3	36.0	49.1	51.5	77.4	178.7
24.1	51.4	20.4	15.7	49.1	30.9	77.5	206.8
33.9	46.9	21.0	36.3	49.2	34.4	77.5	75.5
37.9	54.2	22.0	41.2	49.2	44.0	77.5	171.1
38.1	51.2	22.4	29.5	49.2	61.5	77.9	91.8
38.7	48.2	25.6	35.8	49.3	48.5	77.9	214.0
41.7	49.6	25.7	44.1	49.3	50.8	78.7	85.4
57.9	84.1	27.7	46.1	49.4	46.9	78.8	88.9
58.0	93.4	29.6	276.1	49.4	59.7	78.9	171.4
58.7	79.1	47.4	45.2	49.4	51.5	80.8	94.1
61.6	96.3	47.8	69.2	49.8	40.0	81.5	177.3
73.5	117.9	47.9	46.6	50.8	30.3	83.4	77.5
77.4	133.3	48.4	39.6	52.7	47.1	87.9	260.5
77.8	117.2	48.4	49.9	62.0	44.7	90.1	163.5
81.5	184.4	48.4	41.7	66.1	61.8	92.6	247.1
82.5	286.0	48.5	43.3	66.3	116.3	92.6	351.9
86.7	279.5	48.5	42.3	67.0	39.1	93.8	96.7
91.4	243.0	48.7	29.1	67.5	83.5	93.9	153.9
94.1	240.7	48.7	41.4	67.7	69.2	94.7	307.3
101.4	334.3	48.9	59.5	68.0	70.6	96.5	323.6
104.2	206.8	48.9	39.0	68.3	52.9	96.7	423.3
				68.5	75.0	96.8	264.2
				68.6	38.0	96.9	234.7
				68.6	137.3	97.1	205.0
				68.9	80.1	107.3	188.3
				68.9	87.9	110.5	182.1
				69.0	99.6	110.9	180.9
				69.0	46.4	111.3	373.8
				69.1	69.9	116.6	203.1
				69.2	50.4	121.8	262.3
				69.2	47.2	126.3	427.9

Table 12 (ref. Figure 23). SPM data (mg l^{-1}).

November 1999		April 2000		April 2000 (cont.)		April 2000 (cont.)	
Depth (m)	SPM (mg l^{-1})	Depth (m)	SPM (mg l^{-1})	Depth (m)	SPM (mg l^{-1})	Depth (m)	SPM (mg l^{-1})
1.1	1.25	19.4	0.35	49.0	0.33	76.3	0.24
1.3	1.02	19.4	0.32	49.1	0.38	76.4	0.29
1.3	0.82	19.5	0.34	49.1	0.12	77.2	0.14
1.3	1.11	19.5	0.31	49.1	0.12	77.2	0.33
1.4	0.52	19.5	0.29	49.2	0.38	77.3	0.15
1.5	1.11	19.5	0.38	49.2	0.50	77.3	0.02
1.6	1.61	19.5	0.29	49.2	0.31	77.3	0.20
2.1	0.84	19.5	0.35	49.3	0.25	77.3	0.31
8.2	0.92	19.5	0.29	49.3	0.30	77.3	0.26
9.0	1.51	19.5	0.27	49.4	0.28	77.4	0.27
9.0	0.77	19.5	0.27	49.4	0.29	77.4	0.32
9.1	0.71	19.5	0.29	49.4	0.25	77.4	0.19
9.2	0.63	19.5	0.28	49.8	0.37	77.4	0.30
9.3	0.57	19.6	0.17	50.8	0.35	77.5	0.19
9.4	0.80	19.6	0.27	52.7	0.26	77.5	0.27
12.2	0.68	19.6	0.29	58.0	0.34	77.5	0.24
18.2	0.72	19.7	0.30	62.0	0.40	77.9	0.34
18.8	1.88	19.9	0.35	66.1	0.21	77.9	0.29
18.9	0.61	20.2	0.18	66.3	0.60	78.7	0.35
18.9	1.00	20.3	0.25	67.0	0.19	78.8	0.31
19.1	0.45	20.3	0.22	67.5	0.28	78.9	0.25
19.3	0.74	20.4	0.74	67.7	0.17	80.8	0.33
21.9	0.63	21.0	0.20	68.0	0.18	81.5	0.30
22.1	0.91	22.0	0.29	68.0	0.38	83.4	0.18
24.1	0.82	22.4	0.21	68.3	0.17	87.9	0.25
33.9	0.93	25.6	0.26	68.5	0.30	90.1	0.21
37.9	0.81	25.7	0.34	68.6	0.21	92.6	0.29
38.1	0.58	27.7	0.28	68.6	0.74	92.6	0.31
38.7	0.53	29.6	0.36	68.9	0.25	93.8	0.20
41.7	0.50	47.4	0.26	68.9	0.48	93.9	0.30
57.9	0.84	47.8	0.29	69.0	0.23	94.7	0.30
58.0	1.48	47.9	0.18	69.0	0.23	96.5	0.27
58.7	0.75	48.4	0.24	69.1	0.21	96.7	0.41
61.6	0.61	48.4	0.21	69.2	0.23	96.8	0.26
73.5	0.82	48.4	0.31	69.2	0.30	96.9	0.18
77.4	0.77	48.5	0.32	69.2	0.23	97.1	0.25
77.8	0.94	48.5	0.37	69.2	0.36	107.3	0.21
81.5	0.60	48.7	0.17	69.3	0.29	110.5	0.80
82.5	0.63	48.7	0.32	69.4	0.24	110.9	0.32
86.7	0.66	48.9	0.49	70.9	0.27	111.3	0.27
91.4	0.77	48.9	0.22	73.3	0.23	116.6	0.23
94.1	1.18	48.9	0.46	73.7	0.41	121.8	0.30
101.4	0.92	48.9	0.47	74.8	0.39	126.3	0.35
104.2	0.43	49.0	0.21				

Table 13 (ref. Figures 24 and 25). Dissolved Co (pM).

Nov. 1999 (Figure 24)		April 2000 (Figure 25)		April 2000 (cont.)		April 2000 (cont.)	
Depth (m)	Co (pM)	Depth (m)	Co (pM)	Depth (m)	Co (pM)	Depth (m)	Co (pM)
1.1	288.3	19.4	116.1	48.5	99.1	77.9	52.9
1.3	100.5	19.4	122.6	48.7	23.6	78.7	13.2
1.3	232.6	19.5	114.2	48.7	23.6	78.8	40.6
1.4	196.0	19.5	122.7	48.9	142.8	78.9	63.4
1.5	80.7	19.5	124.9	48.9	63.6	80.8	82.2
2.1	92.6	19.5	105.8	49.0	21.4	81.5	69
8.2	121.5	19.5	70.9	49.2	136.9	83.4	36.8
9.0	63.6	19.5	105.6	52.7	102.7	87.9	26.7
9.0	128.7	19.5	79.8	58.0	12.7	90.1	50.9
9.2	104.6	19.5	184.3	62.0	27.0	92.6	54.3
9.3	38.5	19.5	179.5	68.0	104.4	92.6	60.2
9.4	124.7	19.5	246.1	68.6	17.4	93.8	64.5
12.2	61.9	19.5	114.0	69.0	90.5	93.9	44.9
18.2	75.9	19.6	124.5	69.4	44.4	94.7	34.7
18.8	86.6	19.6	196.3	70.9	49.6	96.5	43.7
18.9	133.4	19.6	179.0	73.3	55.8	96.7	51.6
19.1	142.2	19.7	109.8	73.7	32.3	96.8	60.7
21.9	202.9	19.9	221.5	74.8	23.3	96.9	41.4
22.1	59.0	20.2	206.7	76.4	3.7	97.1	38.2
33.9	127.5	20.3	133.4	77.2	66.0	107.3	57.9
37.9	110.6	20.3	71.4	77.3	67.6	110.5	117.2
38.7	84.7	20.4	129.2	77.3	79.1	110.9	31.7
41.7	71.2	21.0	197.1	77.3	10.6	111.3	57.1
58.0	37.5	22.0	82.7	77.3	63.7	116.6	22.9
58.7	41.7	22.4	185.2	77.3	64.5	121.8	52.5
61.6	50.8	25.6	78.0	77.4	97.3	126.3	87.5
73.5	34.8	25.7	93.4	77.4	70.5		
77.8	88.8	27.7	86.8	77.4	29.5		
81.5	49.3	29.6	47.4	77.4	44.4		
82.5	71.2	47.4	71.2	77.5	40.5		
91.4	48.7	47.8	94.7	77.5	50.9		
101.4	38.9	47.9	99.1	77.5	29.5		
104.2	63.8	48.4	44.3	77.9	88.9		

Table 14 (ref. Section 3.6). Particulate Co

Nov. 1999		April 2000		April 2000 (cont.)		April 2000 (cont.)	
Depth (m)	Co (pM)	Depth (m)	Co (pM)	Depth (m)	Co (pM)	Depth (m)	Co (pM)
1.1	274.1	19.4	27.3	48.9	45.3	73.3	14.2
1.3	87.0	19.4	22.8	48.9	19.6	73.7	21.3
1.4	117.5	19.5	80.2	49.0	20.1	74.8	23.5
1.5	21.3	19.5	30.0	49.0	18.9	76.4	13.9
2.1	105.5	19.5	38.2	49.1	51.9	77.2	21.6
8.2	34.8	19.5	71.5	49.1	21.9	77.2	31.2
9.0	57.3	19.5	35.6	49.2	49.3	77.3	11.4
9.2	79.8	19.5	23.9	49.2	27.1	77.3	24.8
9.3	56.6	19.5	21.1	49.2	29.2	77.3	30.4
9.4	33.6	19.5	14.5	49.3	21.4	77.4	23.0
12.2	87.7	19.5	14.8	49.3	19.9	77.4	32.9
18.2	78.9	19.5	14.2	49.4	16.3	77.4	20.8
18.8	45.4	19.5	14.7	49.4	20.2	77.4	28.8
18.9	75.1	19.6	26.3	49.4	17.6	77.5	38.6
19.1	7.7	19.6	17.9	49.8	27.9	77.5	23.7
22.1	49.2	19.6	13.2	50.8	13.0	77.5	27.4
33.9	62.1	19.7	38.8	52.7	51.6	77.9	52.6
37.9	37.4	19.9	17.7	58.0	25.4	78.7	21.3
38.7	86.2	20.2	26.1	62.0	15.5	78.8	37.3
41.7	27.9	20.3	19.6	66.3	22.0	78.9	18.1
58.0	178.2	20.3	37.6	67.0	8.0	80.8	39.8
58.7	43.6	20.4	44.8	67.5	16.4	81.5	34.6
61.6	52.0	21.0	15.8	67.7	12.2	83.4	32.6
73.5	46.1	22.0	37.6	68.0	19.4	87.9	32.1
77.8	18.1	22.4	40.4	68.0	13.8	90.1	3.0
81.5	55.8	25.6	42.0	68.3	18.6	92.6	31.7
82.5	75.3	25.7	38.6	68.5	17.1	92.6	38.5
91.4	53.8	27.7	40.2	68.6	14.2	93.9	32.6
101.4	18.5	29.6	49.1	68.6	12.2	94.7	33.2
104.2	5.4	47.4	37.3	68.9	19.4	96.5	39.6
		47.8	26.0	68.9	18.4	96.7	49.2
		47.9	19.9	69.0	22.8	96.8	38.0
		48.4	14.6	69.0	14.7	96.9	29.7
		48.4	24.6	69.1	18.3	97.1	26.7
		48.4	21.6	69.2	13.8	107.3	1.6
		48.5	12.8	69.2	21.5	110.5	20.5
		48.5	13.4	69.2	17.1	111.3	26.6
		48.7	7.9	69.2	16.6	116.6	1.5
		48.7	5.5	69.3	16.4	121.8	1.6
		48.9	27.3	69.4	14.8	126.3	15.5
		48.9	14.1	70.9	40.2		